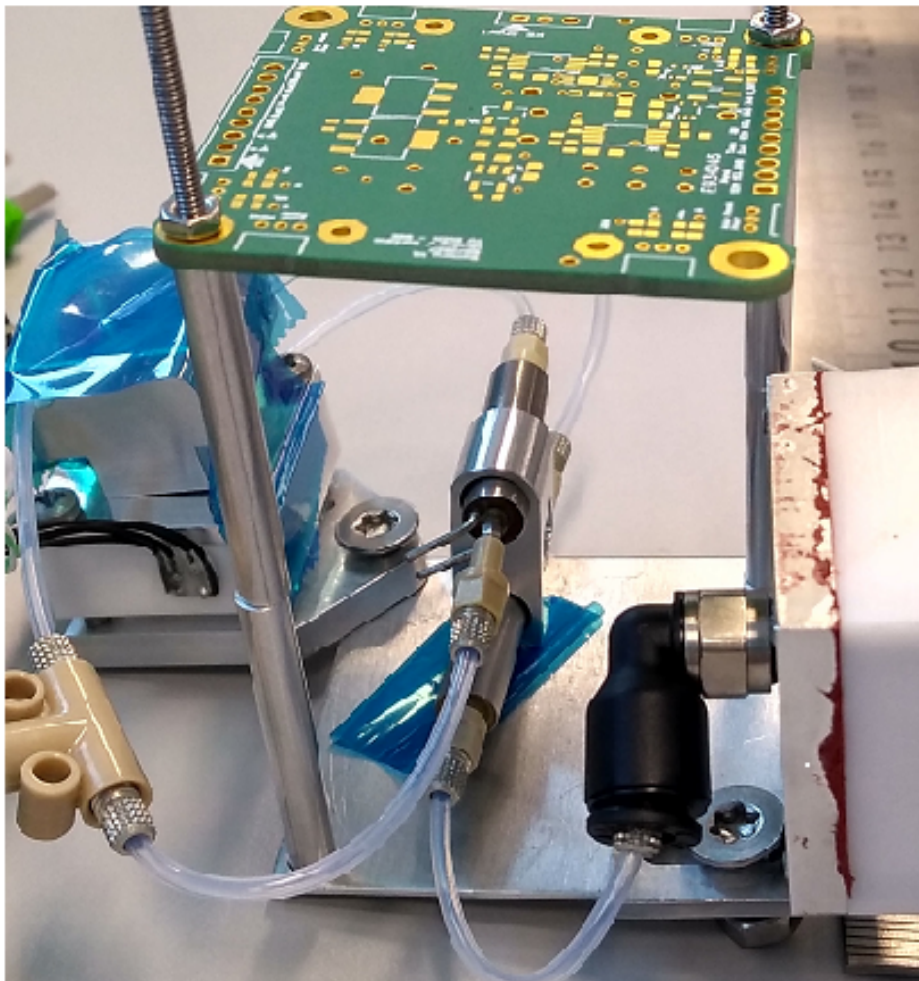


# A technology demonstration payload for micro-resistojet thrusters on Delfi-PQ

L. A. Turmaine

Technische Universiteit Delft





# A technology demonstration payload for micro-resistojet thrusters on Delfi-PQ

by

**L. A. Turmaine**

in partial fulfilment of the requirements for the degree of

**Master of Science**  
in Space Engineering

at the Delft University of Technology,  
to be defended publicly on Wednesday 19th of September, 2018 at 11:00 AM.

Student number: 4139690  
Project duration: February 16, 2018 – September 19, 2018  
Supervisor: Dr. A. Cervone  
Thesis committee: Dr. A. Cervone, TU Delft  
Ir. B. T. C. Zandbergen, TU Delft  
Ir. M.C. Naeije, TU Delft

An electronic version of this thesis is available at <http://repository.tudelft.nl/>.



# Summary

The primary purpose of this thesis is to present the design of a technology demonstrator for VLM (vaporizing liquid microresistojet) and LPM (low pressure microresistojet) technology as a payload on the picosatellite Delfi-PQ. The required technology demonstrator was selected to be a propulsion system which could test two separate thrusting methods in one 42 mm x 42 mm x 30 mm volume payload. What resulted was the selection of a system with a shared propellant tank in the form of a coiled capillary tube between two valves, each of which lead to a thruster. The propellant was determined to be liquid water while the pressurant was determined to be gaseous nitrogen. Thrusting of the VLM occurs first and reduces the pressure over time, until the LPM is activated which benefits from the lower pressure inside the capillary tubing. A functional analysis of the Delfi-PQ mission led to the generation of requirements for the propulsion system of which the killer requirement of the propulsion system design was the restriction set on the volume of the satellite due to Delfi-PQ's PocketQube platform. This meant that the design was centred around efficient use of the volume available and primarily around the placement of the two solenoid valves. The use of 3D-modelling software provided an efficient option to developing different concepts. What resulted was a compact design with two stacked valves placed diagonally within the 42 mm x 42 mm x 30 mm volume. The remaining components were selected and placed to adhere to the generated requirements. Continuous communication with Delfi-PQ team members was required to adhere to the integration requirements of the satellite. Finally, a fit test was successfully completed using 3D printed components to verify whether the propulsion system adhered to the driving volume requirement.

The propellant tank of the system was designed to store 0.51 g of water propellant in a 30 cm 1.57 mm diameter capillary tube. Together with the 4 W restriction on peak power to the propulsion system, this allowed for calculation of the operational envelope which contains the initial pressure and nitrogen volume. What results is an estimation of pressure, mass flow and thrust profiles over time. The initial pressure was set at 1.1 bar based on the peak power and the initial volume of nitrogen at 12 percent of the capillary tube. The expected in-orbit testing time of the VLM thruster is set to be 1200 s, while the expected testing time for the LPM is 200 s.

The final stage of this thesis focused on the development of a test plan and a prototype for the verification of the design. The main risks for the development of the technology demonstration payload are: the redesign of the thruster housings, capillary tubing flexibility (avoiding kinks) and the filling of the system. To mitigate these risks, a test plan at component level, assembly level, prototype level and flight model level is presented. As of August 2018, the prototype of this system is being manufactured and currently, there are no indications that the design presented in this report is unsuitable for flight on Delfi-PQ in 2019.



# Preface

I hereby proudly present my MSc. thesis in the field of Space Engineering conducted at the Technical University of Delft. I decided to work on micropropulsion to challenge myself into designing a new subsystem from scratch. Something that was challenging but also very rewarding and could not have been achieved without the help of professors, researchers and fellow students at TU Delft.

I would like to thank my supervisor Dr. Angelo Cervone for always being available (and patient) when I was in need of help. Special thanks as well to systems engineer Vidhya Pallichadath for providing assistance in a large number of areas. She was one of the main reasons this thesis was a success. To all the other department members in the Space Engineering department, thanks for all the feedback and enjoyable seven months.

Finally, I couldn't have done it without the support and many coffee breaks provided by my good friends Alessandro, Jun and Krishti. Of course, thanks to my family and my girlfriend Sophie who had to put up with me during the final stages of my thesis.



# List of Figures

1.1	Statistics from 1-50 kg satellites launched since the year 2000 [1]	2
1.2	Schematic of a general liquid resistojet with optional cold gas generator	4
1.3	Schematic of a TU Delft LPM concept, taken from Cervone et al. (2015)[2]	5
1.4	Left: Total of 685 launched nanosatellites, only 19 had propulsion. Right: Types of propulsion systems flown on nanosatellites or smaller (<10 kg)	6
1.5	Basic heating chamber design, retrieved from Kundu et al.(2012)[3]	6
1.6	Four chamber channels and four pillar geometries selected for analysis by TU Delft, retrieved from Cervone et al. (2017)[4]	7
1.7	Electrostatic MEMS valve on Ursa Maior[5]	7
1.8	Specific impulse of the most promising resistojet propellants for the VLM [6].	8
1.9	Volumetric Delta V of the most promising resistojet propellants for the VLM [6].	9
1.10	Methodology for answering research questions	10
2.1	Functional flow diagram for the technology demonstrator payload and Delfi-PQ	12
2.2	Sequence diagram between OBC and demonstrator payload	13
2.3	PQ9 interface for the PCB	19
2.4	3D drawing of PCB with mechanical and electrical interface	19
2.5	Schematic of the physical architecture of the system	25
2.6	Design option tree with valve placement set as the driving requirement	26
2.7	Design listed under block C with both diagonal and symmetrical valve placement	27
2.8	Design listed under block C with horizontal valves placed next to each other	27
2.9	Design A1.1	28
2.10	Design A2.2	28
2.11	Design B1.1	29
2.12	Design B2.2	29
2.13	Design A1.1 with all components. Yellow: LPM thruster housing, Dark Blue: VLM thruster housing, Light Blue: Propellant storage location. 3D view	30
2.14	Design A1.1 with all components. Yellow: LPM thruster housing, Dark Blue: VLM thruster housing, Light Blue: Propellant storage location. Top view	30
2.15	Design B1.1 with all components. Orange: LPM thruster housing, Dark Blue: VLM thruster housing, Light Blue: Propellant storage location. 3D view	31
2.16	Design B1.1 with all components. Yellow: LPM thruster housing, Dark Blue: VLM thruster housing, Light Blue: Propellant storage location. Top view	31
2.17	Graphical trade-off for the conceptual design of the propulsion system	33
2.18	The numerical trade-off for the conceptual design	36
2.19	Final conceptual design: 3D view	37
2.20	Final conceptual design: top view	38
3.1	3D-printed mock-up of the design without the PCB and stacking connectors. The one euro coin is presented for scale	39
3.2	1.57 mm diameter tubing from The Lee Company with 0.138-40 UNF interface [7]	40
3.3	Technical drawing of the INKX0514300A solenoid valve [8]	40
3.4	3D mockup model: Inlet of the top valve (A) connects to the propellant storage. Outlet of the top valve (C) connects to the LPM thruster. Inlet of the bottom valve (D) connects to the propellant storage, while Outlet of the bottom valve (B) connects to the VLM thruster.	41
3.5	The old valve support structure	42
3.6	The updated valve support structure	42

3.7	Structural interface with Delfi-PQ, where the large square hole shows the LPM thruster exit, the rectangular hole shows the VLM thruster exit and the circular hole is the fill location for the propellant. . . . .	43
3.8	Location of brackets to connect interface to the propulsion system. . . . .	43
3.9	Comparison of the current VLM thruster housing and the volume of the housing required for the conceptual design. This volume is shown in dark blue. . . . .	44
3.10	Comparison of the current LPM thruster housing and the volume of the housing required for the conceptual design. This volume is shown in yellow. . . . .	44
3.11	MANIFOLD-3-.062 MINSTAC-PEEK from the Lee Company, which is used to fill the propellant prior to operation [9] . . . . .	45
3.12	Location of the manifold within the propulsion system: on the side of the propellant storage box. . . . .	45
3.13	TKLA3201112H check valve from The Lee Company to be used as a back up option for filling the system [10] . . . . .	46
3.14	Location of the check valve shown in red for filling purposes as a backup solution for filling the system. The manifold must be oriented in a different direction to allow for a tube to connect to the check valve and still remain within the designated volume. . . .	46
3.15	The MS5837-30BA pressure sensor [11] . . . . .	47
3.16	Flight model of the propulsion system with all components discussed in this chapter, with the exception of capillary tubing to connect components and PCB electronics. . . . .	48
4.1	Top-level functional flow diagram for the payload demonstrator . . . . .	49
4.2	The flow diagram for system start-up mode of the propulsion system . . . . .	50
4.3	The flow diagram for system idle mode of the propulsion system . . . . .	51
4.4	The flow diagram for abort mode of the propulsion system . . . . .	51
4.5	The flow diagram for VLM testing mode of the propulsion system . . . . .	52
4.6	The flow diagram for LPM testing mode of the propulsion system . . . . .	52
4.7	The flow diagram for the end-of-life mode of the propulsion system . . . . .	53
4.8	An overview of the operations of the system. . . . .	54
4.9	Mass flow of the propulsion system over time at different initial pressures with $V(0) = 0.1 \cdot V_{tube}$ and $T_c = 600K$ . . . . .	56
4.10	Mass flow of the propulsion system over time at different initial volumes of nitrogen with $p(0) = 1.8bar$ and $T_c = 600K$ . . . . .	57
4.11	Pressure of the propulsion system over time at different initial pressures with $V(0) = 0.1 \cdot V_{tube}$ and $T_c = 600K$ . . . . .	57
4.12	Pressure of the propulsion system over time at different initial volumes of nitrogen with $p(0) = 1.8bar$ and $T_c = 600K$ . . . . .	58
4.13	Vaporization temperature to pressure graph using the Clausius-Clapeyron relation . . .	59
4.14	Power transfer required into propellant over time at different initial volumes with $p(0) = 1.8bar$ and $T_c = 600K$ . . . . .	59
4.15	Propellant mass over time at different initial volumes with $p(0) = 1.8bar$ and $T_c = 600K$ . . .	60
4.16	Comparison of mass flows over time using a variable temperature input equal to the vaporization temperature and a constant temperature of $600 K$ . . . . .	61
4.17	Comparison of power transfer required to the propellant over time using a variable temperature input equal to the vaporization temperature and a constant temperature of $600 K$ . . . . .	61
4.18	Mass flow over time with operational envelope inputs as specified in Table 4.4. . . . .	63
4.19	Power required to flow into propellant over time with operational envelope inputs as specified in Table 4.4. . . . .	63
4.20	Pressure over time with operational envelope inputs as specified in Table 4.4. . . . .	64
4.21	Temperature over time with operational envelope inputs as specified in Table 4.4. . . .	64
4.22	Propellant mass over time with operational envelope inputs as specified in Table 4.4. . .	65
4.23	The power required to flow into the propellant at each pressure within the system using the operational envelope inputs as specified in Table 4.4. . . . .	65
4.24	Projected thrust over time with operational envelope inputs as specified in Table 4.4. . .	66

---

5.1 Risk matrix, showing the danger each risk poses to the development and launch of the system . . . . .	71
5.2 CATIAv5 Model showing the locations of the LPM (blue) and VLM (red) thrusters with the current thruster housings. . . . .	72
5.3 Schematic of all the components used in the prototype shown in Figure 5.2 . . . . .	73
5.4 Assembly of the prototype completed in the clean room. Pressure sensors and wiring are not attached. . . . .	74
5.5 Schematic of the test setup for the valve test . . . . .	75
5.6 Schematic of the test setup for the VLM- and LPM-thruster tests . . . . .	76
5.7 Test setup for the heater efficiency test. . . . .	77
5.8 Test setup for fill and leak test by method of overpressurizing and plugging the manifold after inserting the propellant . . . . .	78
5.9 General test setup for the prototype testing phase . . . . .	79



# List of Tables

1.1	General comparison between propulsion types	3
2.1	List of system requirements	14
2.2	List of system requirements	15
2.3	List of performance requirements	15
2.4	List of performance requirements	16
2.5	List of functional requirements	16
2.6	List of functional requirements	17
2.7	List of interface requirements	17
2.8	List of interface requirements	18
2.9	List of safety- and assembly requirements	20
2.10	List of safety- and assembly requirements	21
2.11	List of environment- and launch requirements	21
2.12	List of environment- and launch requirements	22
2.13	A list of all components needed to satisfy the requirements for the propulsion payload	23
2.14	A list of all components needed to satisfy the requirements for the propulsion payload.	24
2.15	Results from the survey completed by eight TU Delft experts to objectively find the weights of the trade-off	34
2.16	Normalized weights with the final average weight of each trade-off criterion	35
3.1	Lengths of tubing (not including valve length or interfaces) for the propulsion system	41
3.2	Operational parameters for the MS5837-30BA pressure and temperature sensor [11]	47
3.3	Operational parameters for the BMX055 IMU [12]	47
3.4	Mass estimation for the propulsion system and comparison with PROP-SYST-100	48
4.1	Various constants required in this chapter	54
4.2	Inputs for the calculations on the operational envelope	54
4.3	Inputs for the Clausius-Clapeyron relation	58
4.4	Final values for the operational envelope of the propulsion system	62
5.1	Verification methods of requirements	67
5.2	Verification methods of requirements	68
5.3	Verification methods of requirements	69
5.4	Identified risks associated with the further development and manufacturing of the propulsion system (before testing)	70
5.5	Table of in-orbit measurements to be made	83



# Nomenclature

$d$	Inner diameter of tubing [ $m$ ]
$l$	Length of propellant storage tubing [ $m$ ]
$A_t$	Nozzle throat area VLM thruster [ $m^2$ ]
$R$	Gas constant for water vapour [ $J/kgK$ ]
$\Gamma$	Van der Kerckhoven constant water vapour [-]
$\rho$	Density of liquid water [ $kg/m^3$ ]
$T_0$	Ambient temperature [ $K$ ]
$h_{vap}$	Heat of vaporization for liquid water [ $J/kg$ ]
$V_{tube}$	Total volume of the propellant storage tubing [ $m^3$ ]
$c_p$	Specific heat of water [ $J/K/kg$ ]
$p(0)$	Initial pressure of propulsion system at $t = 0s$ [ $Pa$ ]
$V(0)$	Initial volume of nitrogen at $t = 0s$ [ $m^3$ ]
$T_c$	Temperature within the VLM thruster [ $K$ ]
$p(t)$	Pressure within the propulsion system over time [ $Pa$ ]
$V(t)$	Volume of the nitrogen within the propulsion system over time [ $m^3$ ]
$m_{exit}$	Water mass to have left the system at a time $t$ [ $kg$ ]
$\dot{m}$	Mass flow into the VLM thruster [ $kg/$ ]
$c^*$	Characteristic exhaust velocity [ $m/s$ ]
$\Delta t$	Timestep used for calculations [ $s$ ]
$\dot{Q}$	Power transferred into the propellant [ $W$ ]
$\Delta T$	Difference in temperature [ $K$ ]
$m_w$	Mass of remaining propellant [ $kg$ ]
$V_w$	Volume of remaining propellant [ $K$ ]
$t_{VLM}$	Total testing time for VLM [ $kg$ ]
$I_{sp}$	Specific impulse [ $s$ ]
$g_0$	Gravitational acceleration [ $m/s^2$ ]
VLM	Vaporizing Liquid Microresistojet
LPM	Low Pressure Microresistojet
EOL	End-of-life
OBC	On-board computer
PQ	PocketQube
COTS	Commercial-off-the-shelf
PCB	Printed Circuit Board
MEMS	Micro-electro Mechanical Systems



# Contents

<b>Summary</b>	<b>iii</b>
<b>Preface</b>	<b>v</b>
<b>List of Figures</b>	<b>vii</b>
<b>List of Tables</b>	<b>xi</b>
<b>List of Symbols</b>	<b>xiii</b>
<b>1 Introduction</b>	<b>1</b>
1.1 Background Information . . . . .	1
1.2 Literature Study . . . . .	2
1.2.1 Vaporizing Liquid Micro-resistojet (VLM) . . . . .	3
1.2.2 Low Pressure Micro-resistojet (LPM). . . . .	4
1.2.3 Review of Micropropulsion on Nanosatellites . . . . .	4
1.2.4 Microresistojet Components . . . . .	4
1.2.5 The Delfi-PQ PocketQube . . . . .	8
1.3 Problem, Objective and Method . . . . .	9
1.4 Thesis Scope and Structure . . . . .	10
<b>2 Conceptual Design</b>	<b>11</b>
2.1 Functional Analysis - Mission . . . . .	11
2.2 Sequence Diagram . . . . .	13
2.3 Propulsion Payload Demonstrator Requirements . . . . .	14
2.3.1 System Requirements . . . . .	14
2.3.2 Performance Requirements . . . . .	15
2.3.3 Functional Requirements . . . . .	16
2.3.4 Interface Requirements . . . . .	17
2.3.5 Safety- and Assembly Requirements . . . . .	20
2.3.6 Environment- and launch requirements . . . . .	21
2.4 Physical System Architecture. . . . .	23
2.5 Design Options . . . . .	26
2.6 Concept Trade-off . . . . .	32
2.6.1 Trade-off Criteria . . . . .	32
2.6.2 Graphical Trade-off . . . . .	32
2.6.3 Numerical Trade-off . . . . .	34
2.7 Final Concept . . . . .	37
<b>3 Detailed Design</b>	<b>39</b>
3.1 Fit Test . . . . .	39
3.2 Propellant Tubing and Valves . . . . .	40
3.3 Propellant Storage . . . . .	41
3.4 Valve Support Structure . . . . .	42
3.5 Structural Interface with Delfi-PQ . . . . .	42
3.6 Thruster Chip Housings. . . . .	43
3.7 Propellant Manifold and Fill Valve. . . . .	44
3.8 Sensors . . . . .	46
3.9 Flight model design . . . . .	47

<b>4</b>	<b>Operational Envelope</b>	<b>49</b>
4.1	Functional Flow Diagram - Payload . . . . .	49
4.1.1	Start-up Mode. . . . .	50
4.1.2	Idle Mode . . . . .	50
4.1.3	Abort Mode . . . . .	50
4.1.4	Testing Mode . . . . .	50
4.1.5	End-of-life Mode . . . . .	52
4.2	VLM Thruster: Initial Nitrogen Pressure and Volume . . . . .	53
4.2.1	Option 1: Constant Thruster Temperature. . . . .	55
4.2.2	Option 2: Provide Minimum Vaporization Temperature . . . . .	59
4.3	Final Operational Envelope . . . . .	62
<b>5</b>	<b>Design Verification and Testing</b>	<b>67</b>
5.1	Verification of Design . . . . .	67
5.2	Risk Analysis . . . . .	69
5.3	Prototype Design . . . . .	72
5.4	Proposed Test Campaign . . . . .	73
5.4.1	Component Testing . . . . .	74
5.4.2	Assembly and Integration Testing . . . . .	76
5.4.3	Prototype Testing. . . . .	78
5.4.4	Flight Model Testing . . . . .	81
5.5	Validation . . . . .	83
<b>6</b>	<b>Conclusion</b>	<b>85</b>
	<b>Bibliography</b>	<b>87</b>
<b>A</b>	<b>Concept Trade-off Survey</b>	<b>89</b>
<b>B</b>	<b>Matlab Code: Operational Envelope</b>	<b>91</b>
B.1	Operational Envelope: Constant Temperature and Multiple Initial Pressures . . . . .	91
B.2	Operational Envelope: Constant Temperature and Multiple Initial Nitrogen Volumes . . . . .	93
B.3	Operational Envelope: Variable Temperature and Final Values . . . . .	94

# 1

## Introduction

This document is a design-related thesis for the department of Space Engineering at TU Delft. It contains an initial design for a technology demonstrator payload capable of testing VLM (vaporizing liquid microresistojet) and LPM (low pressure microresistojet) micropropulsion technologies under development at TU Delft. This chapter will provide the background information and literature study preceding the design phase conducted in this report. The setup for the research proposal will also be provided in Section 1.3.

### 1.1. Background Information

Space has, until about 18 years ago, only been attainable by entities with enormously high budgets. The industry started to change in 2000 when the Aerospace Corporation successfully launched six 1 kg satellites into space. The Aerospace Corporation project showed other companies and universities that it was indeed possible for such low budget nano-satellites to survive the harsh conditions in space and by 2008 there had already been 60 nano-satellite launches [13]. In 2014 alone there were 80 launches and the number continues to increase rapidly: by August 2016 there were 471 recorded launches of CubeSats (10 cm x 10 cm x 10 cm platform) [14]. The overall growth of small satellites is projected to accelerate over the coming three years[1]. A diagram of (projected) growth of 1 to 50 kg satellites can be seen in Figure 1.1 and shown by the blocks in each year. The red-dotted line specifically shows the number of CubeSats launched while the black line refers to the number of scientific publications on satellites between 1-50 kg. Finally, the hollow black line shows the number of scientific articles dedicated to small satellites [1].

Nano- and pico-satellites have the distinct advantage of being low cost, flexible and also have a very low development time, which makes them ideal for university research. In the pursuit of even lower-cost methods of space research, TU Delft is looking at the PocketQube platform (5 cm x 5 cm x 5 cm) as a possibility. As of March 2017, only four PocketQube satellites have been launched to space on the Dnepr launch of 21/11/2013 [15]. The PocketQube's volume constraint is eight times lower than the CubeSat and its mass range puts it in the pico-satellite (100 g - 1 kg) category, requiring state-of-the-art MEMS (Micro-electromechanical systems) devices. Although MEMS devices provide a low cost, low mass and low power alternative to optical and mechanical devices, they currently do not have their accuracy or resilience. MEMS devices for use on nano- and pico-satellites are currently a hot topic of research in the space sector [16].

An especially difficult challenge in the miniaturisation of satellites lies in the propulsion department. Generally, propulsion systems can be used for drag correction, active attitude control, reaction wheel desaturation and interplanetary missions [17]. Giving the nano- and pico-satellite these capabilities is key to increasing its application in space missions. One thing becomes clear though, the smaller the satellite, the more difficult the inclusion of a propulsion system. So far only one PocketQube used any kind of propulsion system: the Wren. This propulsion system used pulsed plasma micro-thrusters (PPTs) which work by ablating a solid material and accelerating it using an electronic charge [18]. Re-

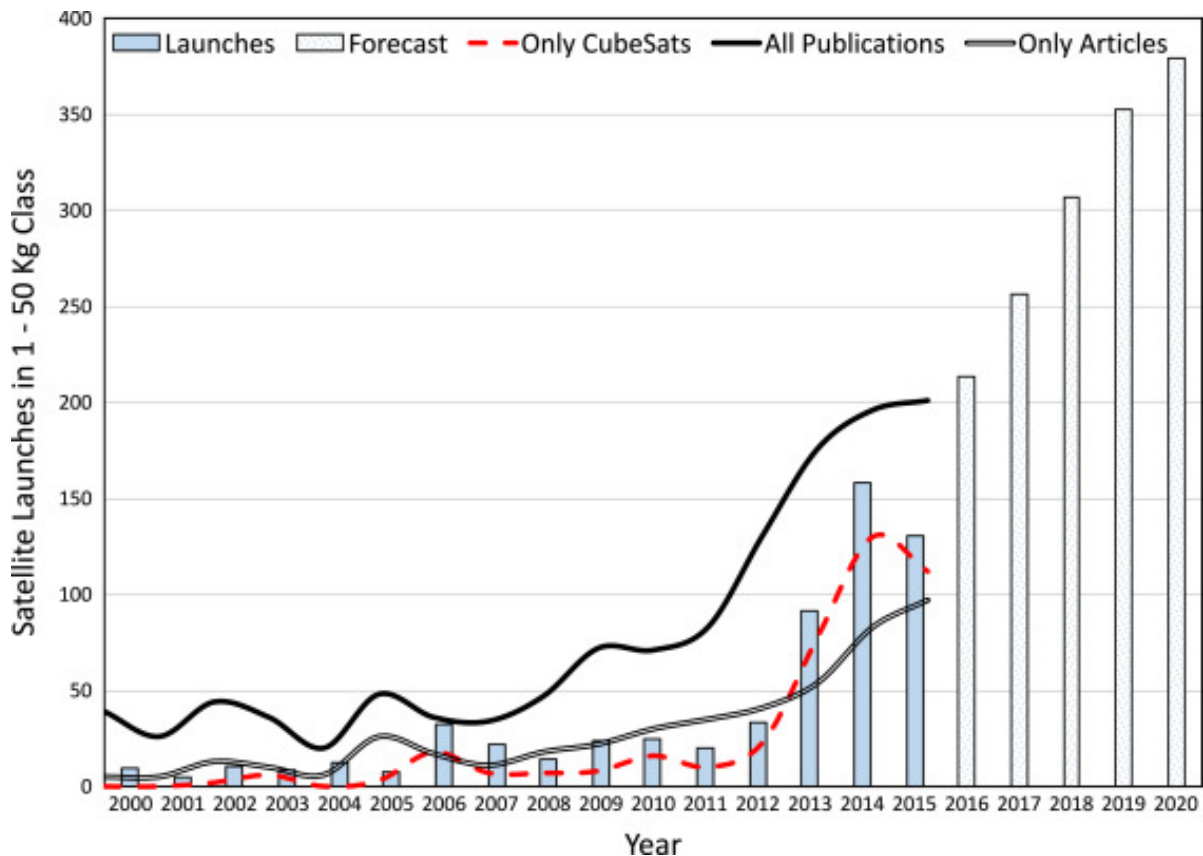


Figure 1.1: Statistics from 1-50 kg satellites launched since the year 2000 [1]

sults from the Wren 1P propulsion system are unknown, however the satellite is still transmitting. Due to the gap in the market for highly miniaturized propulsion systems, TU Delft is currently researching a different type of propulsion system called the micro-resistojet. Two types of resistojets are being analysed for use on nano- and pico-satellites. The first resistojets-based MEMS propulsion unit works by heating water stored in liquid form. Pressurized water is expelled through a nozzles printed on a tiny silicon wafer to produce thrust. This type of propulsion system is called the Vaporising Liquid Micro-resistojet (VLM). To solve the limitations of the need for a pressurised tank, researchers at TU Delft have revisited a concept by Ketsdever et al. (2005) called the free molecular micro-resistojet, also called the low pressure micro-resistojet (LPM). This type of propulsion can operate at extremely low ( $< 1000$  Pa) pressures by heating individual propellant particles through heated expansion slots in the side of the spacecraft [4]. These types of propulsion systems are better suited for use on a PocketQube, because their volume and power specifications are very low [19]. However, current micro-resistojet designs in the industry are all sized for the CubeSat standard and take up at least 1 unit (10 cm x 10 cm) of volume, which would be 8 units in the PocketQube [4] [20].

Although both VLM and LPM-concepts have been proven in the clean room, there now comes a need to prove the technology in space. With the development of the Delfi-PQ PocketQube at TU Delft, there is a unique opportunity to design a technology demonstrator as a payload on the Delfi-PQ satellite. This technology demonstrator will be the first of its kind to fly both VLM and LPM technology on a PocketQube platform and be the first step to implementing miniaturized propulsion technology to allow for formation flying missions.

## 1.2. Literature Study

This section will cover the most critical parts of the literature study that preceded this thesis. This literature study was written by the author of this document to fully understand the background of micropropulsion and acquire sufficient knowledge of micropropulsion technology to write this thesis.

The literature study contained:

- An in-depth analysis on the different types of micropropulsion technologies
- Statistics on current nanosatellites and their propulsion systems
- An in-depth analysis of all past and current micropropulsion systems
- A breakdown of VLM- and LPM- propulsion systems at component level
- Information on MEMS manufacturing techniques
- Background information on the PocketQube platform

A general comparison for different types of micropropulsion can be seen in Table 1.1. The cold gas thrusters are by far the most common type of propulsion for small satellites. They are simple and have good flight heritage, however, the low specific impulse and use of gas results in bulky propulsion systems that become even less attractive when implemented on a PocketQube platform (5 cm x 5 cm x 5 cm). The next thruster type is of a chemical thruster and is the mono-propellant micro thruster, this type of thruster has only been successfully flown once on the LithuanicaSAT-2 QB50 Project [21]. The mono-propellant thruster's advantage is that it has a much higher specific impulse (200-300 s) compared to cold gas thrusters and electrothermal thrusters. However, minimum operational thrust ranges are often on the scale of 1 N, making it difficult to implement mono-propellant thrusters for precise attitude control purposes. The complexity of the system due to the high temperatures and ignition of propellant make it difficult to implement on small satellites. Electric propulsion is a promising method of propulsion based on ionizing solid or liquid propellants to expel them from the satellite using electric fields. The specific impulse for electric propulsion is very high compared to the other propulsion types but the thrust levels are generally much lower due to low mass flow rates. Electric propulsion systems have the capability for high levels of miniaturization but the technology readiness levels are still low. Finally, the thermo-electric thrusters use a combination of pressurized propellant and heaters to raise the specific impulse of the system. By using liquid propellants and vaporizing them, the amount of propellant which can be stored increases dramatically.

Table 1.1: General comparison between propulsion types

	Cold Gas	Chemical	Thermoelectric	Electric
Specific Impulse	30 - 100 s	150 - 350 s	80 - 180 s	300 - 3000 s
Thrust	0.1 - 10 mN	0.1- 1 N	0.1 - 10 mN	0.1 - 1 $\mu$ N
Optimal App.	Station Keeping, Attitude Control	Orbit Transfers	Station Keeping, Attitude Control	Station Keeping, Attitude Control, Orbit Transfers
Ref.	[22]	[23]	[4]	[23]

### 1.2.1. Vaporizing Liquid Micro-resistojet (VLM)

The first type of micro-resistojet that TU Delft is testing is a micro-resistojet which uses liquid water stored under pressure as a propellant. The feed system sends the propellant into the reaction chamber which has a MEMS heating unit. This raises the temperature of the gas and expels it out of the MEMS nozzle to provide thrust. The reaction chamber is fully made out of MEMS components and can therefore easily be altered in manufacturing. For example, different heating unit geometries and nozzles are possible for application on to the system. The major disadvantage for this system is that the propellant needs to be pressurised, which either needs to be done either before launch or in flight by use of cool gas generators, both of which increase mass and reduce system efficiency [4]. A general outline of such a VLM can be seen in Figure 1.2.

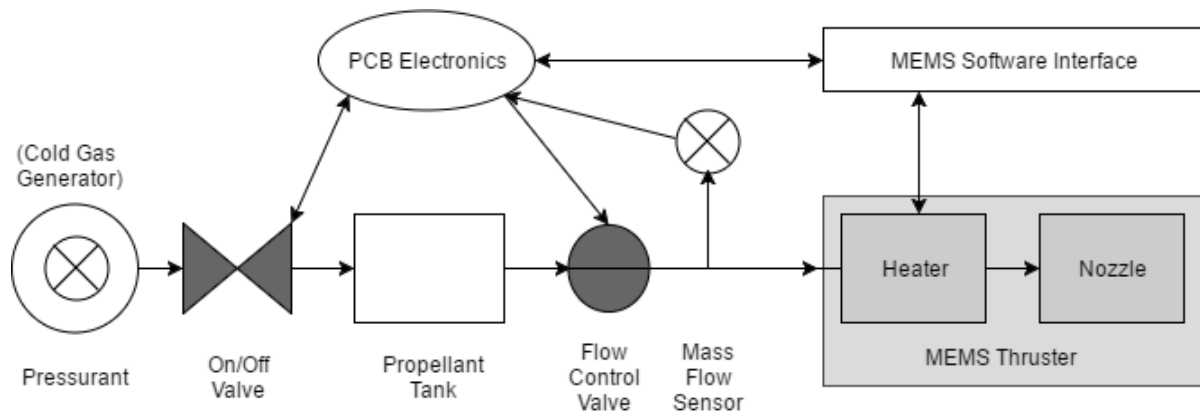


Figure 1.2: Schematic of a general liquid resistojet with optional cold gas generator

### 1.2.2. Low Pressure Micro-resistojet (LPM)

The Low Pressure Microresistojet (LPM) is the other type of thruster under development at TU Delft. It operates at extremely low pressures ( $<1000$  Pa) and uses a different method to generate thrust. Several slots are engraved into a chip, the walls of which are heated to high temperatures. When particles hit these walls, a portion of them get accelerated out of the spacecraft to generate thrust. However, a certain amount can also bounce back into the chamber resulting in 'lost' thrust. This type of thruster also has the problem of storing low pressure gaseous propellants. To solve this problem, a concept of using sublimating ice was proposed to continuously provide the low pressures required for thruster operation. However, freezing water before launch causes large difficulties in logistics and is unrealistic because PocketQube launches are almost always piggy-back launches. At this moment, the most promising method is to freeze liquid water in space using a Peltier device, but has the down side of increasing power consumption [4] [2]. The concept using ice as a propellant can be seen in Figure 1.3.

### 1.2.3. Review of Micropropulsion on Nanosatellites

Of the 685 nanosatellites launched until June 2017, only 19 satellites had a propulsion system onboard. This translates to just three percent of the satellites. Conclusions to be taken from the review of previous nanosatellites with propulsion systems show that cold gas thrusters are the most thoroughly tested method of propulsion for small satellites. However, more recent satellites seem to prefer electric methods of propulsion. Although the technological readiness level is low, electric propulsion systems are more efficient in terms of volume and Delta V. A statistical representation of micropropulsion systems within the industry can be seen in Figure 1.4. It is important to note that some scientific articles define their propulsion systems as cold gas thrusters, but still use heaters, which makes them quite similar to resistojets.

### 1.2.4. Microresistojet Components

The components required to operate a system with a microresistojet thruster consist of the following:

- Thruster
- Heater
- Valve
- Propellant Tank
- PCB & Software Interface

The thruster for the VLM micro-resistojet is etched into a silicon chip. This includes channels for the propellant to flow through, an inlet for the thruster, a convergent-divergent nozzle and a nozzle outlet. This nozzle can have different geometries, which are often created by the DRIE (deep reactive ion etching) method. DRIE etching of nozzles allows deep extruded geometries and high aspect ratios,

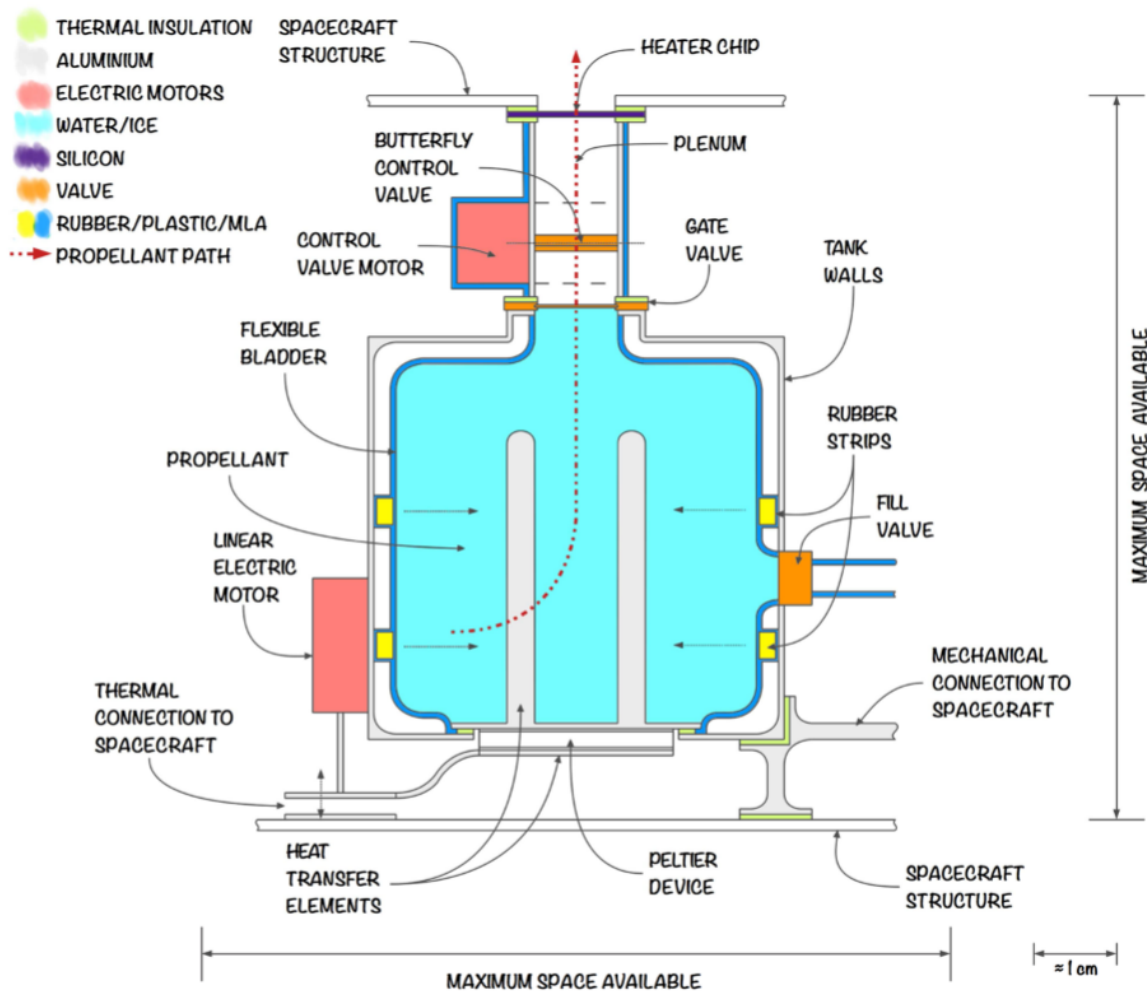


Figure 1.3: Schematic of a TU Delft LPM concept, taken from Cervone et al. (2015)[2]

which can help avoid separation, shock formation and premature transition to turbulence. However, these grooves are often designed to be rectangular for manufacturing simplicity, which results in a 2D nozzle. To get an axisymmetric (3D) nozzle, which is necessary for maximum efficiency, anisotropic etching of silicon or even better laser processing techniques are required.

The function of the heater is to convert electrical power into heat and vaporise the propellant. A high exhaust velocity increases the performance of the thruster. This high exhaust velocity is achieved by increasing the temperature and pressure of the propellant. The desired temperature increase provided by the heater must be sufficient to fully vaporise the liquid in order to avoid major losses in specific impulse. This can be done using many different types of heater geometries. Pillars can be located within the heating chamber to increase heat transfer and mixing, which aids propellant vaporisation. Here, the heating elements would be located in between the pillars. Another option is to split the heater chamber into multiple flow channels, where the heating elements are located in between each channel. The question then arises which geometries should be used. Manufacturability, pressure drops and heat transfer over the heating chamber should all be accounted for in the choice. The design by P. Kundu et al. (2012) uses a rectangular single flow chamber with heating elements mounted on the top and bottom of the heating chamber. This basic design, which can be seen in Figure 1.5, is very common among resistojet designs. Heat flows from the heating element to the wafer through conduction and then via convection to the propellant in the wafer channel[3].

The choice by Kundu et al. (2012) was done out of simplicity and decided that further optimisation was not necessary due to the high voltage supplied to the heater [3]. For the heater on the VLM

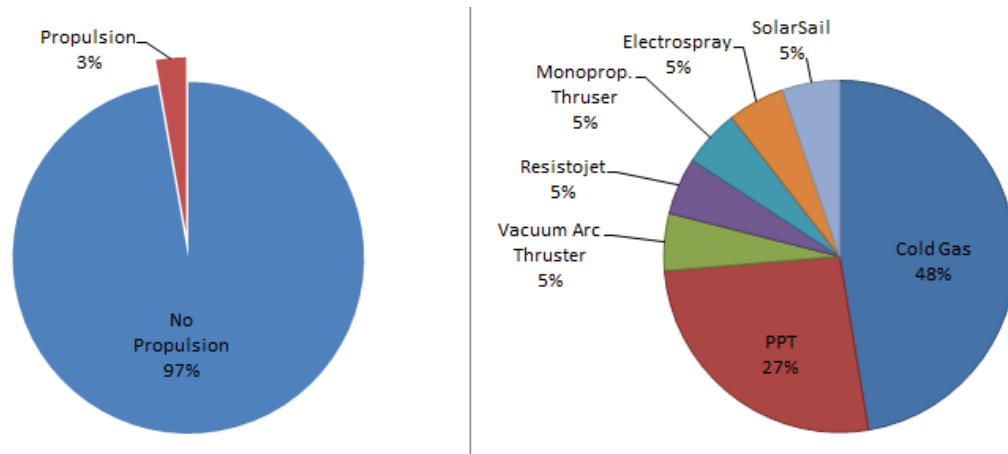


Figure 1.4: Left: Total of 685 launched nanosatellites, only 19 had propulsion. Right: Types of propulsion systems flown on nanosatellites or smaller (<10 kg)

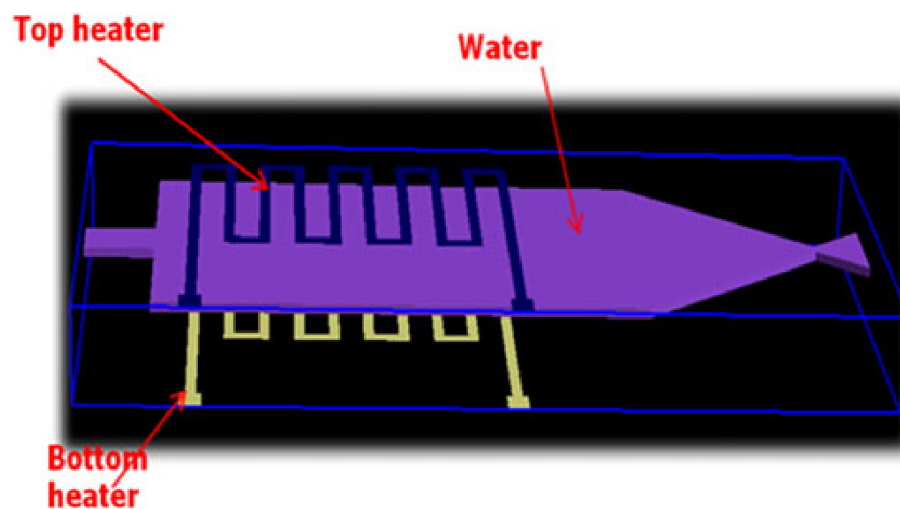


Figure 1.5: Basic heating chamber design, retrieved from Kundu et al.(2012)[3]

at TU Delft, low power and voltage input is paramount. Which means that some kind of additional geometry such as pillars would probably be needed to fully vaporise the fluid. Options are shown in Figure 1.6. Testing has shown that the serpentine geometries are probably the most advantageous and are currently the number one design choice [24].

All components need to be connected to one another which gives the need for a feed system. Most early propulsion systems all used rigid piping as a feed system with the propellant stored at pressure to provide propellant feed. A review of recent micropropulsion systems showed that capillary tubing is most commonly used as a method of feeding propellant from the valve to the silicon thruster wafer. Connections between the propellant tank, valves and thruster need to be carefully bonded to avoid excessive leakage. This requires a physical interface which funnels the flow from the capillary tubing to the MEMS thruster opening, which may need to be house made to connect two COTS components. It is also common for micropropulsion systems to have an ON/OFF valve and a thrust regulation valve.

Another design choice for the VLM is the type of valves to use. The key considerations for the valves within a micro-resistojet system are: power consumption, operating voltage, volume, mass, pressure capabilities and response time. Of these, specifically the operating voltage will be of importance as it must comply with the power subsystem design of the satellite. Considering the small volume requirement of the VLM, the main COTS option would be solenoid valves, which also allow for throttling and generally have a sufficient response time. Another option would be the use of a MEMS valve. Of

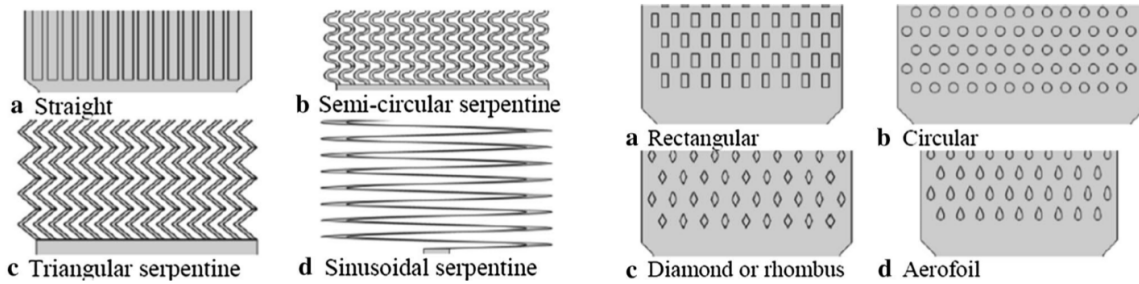


Figure 1.6: Four chamber channels and four pillar geometries selected for analysis by TU Delft, retrieved from Cervone et al. (2017)[4]

the many types, the electrostatic MEMS valve has a fast response time and is fairly simple in use. Its disadvantage is that it requires a high operational voltage, which could be a problem depending on the satellite bus design [25]. Furthermore, it only allows for on/off control and no proportional thrust control. Although the use of capacitors may be possible, this would take up additional volume. The satellite Ursa Maior used such an electrostatic MEMS valve in their subsystem design. A schematic of this valve can be seen in Figure 1.7 [5].

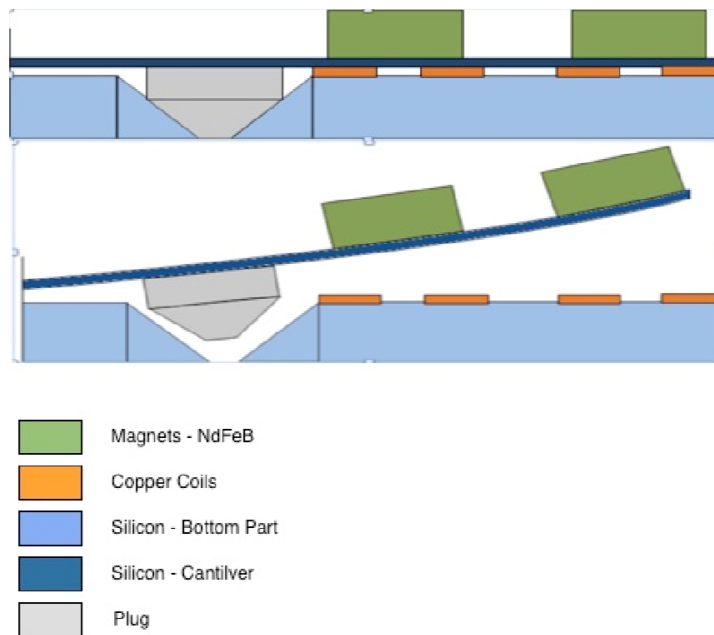


Figure 1.7: Electrostatic MEMS valve on Ursa Maior[5]

One of the opportunities for simplifying the integration of the micro-resistojet lies in the development of a MEMS valve. Although an in-house design would be costly, the reduction in complexity and volume would benefit the integration of the system enormously. Current COTS options such as the solenoid valve are cheap and simple, but take up more volume. If using a COTS valve, the length of the valve might need modifying or might need be mounted diagonally on a PCB.

For the propellant selection, water is very promising when it comes to its low molecular mass. However, it has a very high heat of vaporisation compared to other resistojet propellants, which may result in high power requirements for the heater or loss of specific impulse due to insufficient vaporisation. However, further research by Guerreri et al. (2017) does indeed show that the most promising liquid propellant at ambient temperature and less than 10 bar for a resistojet is water, alongside ammonia [6]. This is because the article takes into account both volume and power and the Delta V and power, respectively. Figures 1.8 and 1.9 give the specific impulses and volumetric Delta V at different power levels.

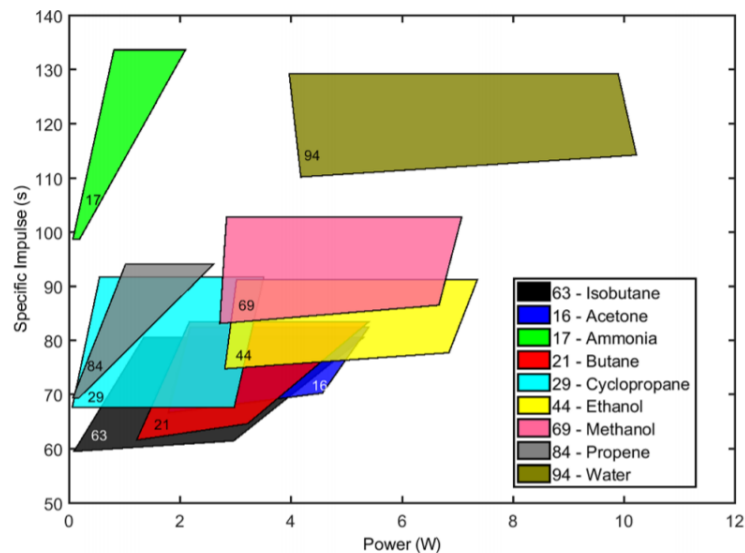


Figure 1.8: Specific impulse of the most promising resistojet propellants for the VLM [6].

The propellant tank shape is also of importance. Cylindrical or spherical tanks allow for the highest storage pressure in the tank, which increases Delta V. However, in a square volume such as the PocketQube, circular shapes are inefficient as there will be irregular shaped spaces left over for other systems. A rectangular shaped tank would store the largest amount of propellant and could be reinforced at corners to provide enough strength for the necessary pressure in the storage tank.

The VLM system would be designed for the PocketQube platform, therefore there will be a stack of 5 cm x 5 cm PCBs for the propulsion system to be mounted on. The electrical power interface will be RS485 with a 9-bit connector, as determined by the current satellite bus of Delfi-PQ. Furthermore, the micro-resistojet propulsion system could either have its own microcontroller or use the onboard computer of the satellite. By having its own microcontroller, physical connections would be short, resulting in fewer wires running through the satellite. This is most likely the best option and would lead to use of the MSP432 microcontroller by TI, which was selected by researchers at TU Delft because of its high accuracy signal processing and low power usage.

The most challenging part in the design of a micro-resistojet propulsion system will be the integration of all previously mentioned components into a 4.2 cm x 4.2 cm x 3.0 cm volume. Integration will therefore be mainly focused on space-saving design options. The two most volume consuming elements in the system will probably be the valve and the fuel storage. Therefore, integration would be centred around these two components. Furthermore, a software interface for communication with the rest of the satellite will be required as there will be multiple flight modes necessary. Also, a physical interface (housing for the thruster chip) will be needed between the inlet of the MEMS thruster and the feed system. The current interface used at TU Delft for testing purposes is unnecessarily bulky and could probably be reduced to a fraction of its size. MEMS pressure sensors for the supply lines and propellant tank would also be needed to provide data during in-orbit testing and required input values for power to the heater.

### 1.2.5. The Delfi-PQ PocketQube

The Delfi-PQ is a PocketQube currently under development by TU Delft with launch planned in 2019. It is a 3-unit (3P) PocketQube designed with a total mass of approximately 500 grams and a maximum power level of 4.5 W. The concept is based on using a core platform that will reliably provide a structure, communication, power and data transfer with one advanced payload for technology demonstration purposes. For this payload, a micropropulsion system is the most likely candidate for the technology demonstration payload. Central to the development of this satellite is an iterative approach

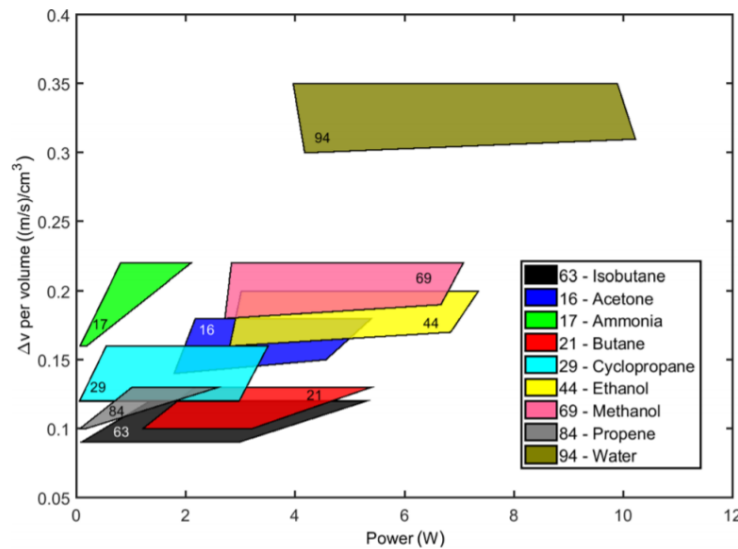


Figure 1.9: Volumetric Delta V of the most promising resistojet propellants for the VLM [6].

to design as apposed to the widely used waterfall model.

### 1.3. Problem, Objective and Method

TU Delft is currently developing and testing components for two types of microresistojet: a vaporizing micro-resistojet (VLM) and a low pressure micro-resistojet (LPM). Both of which have shown to provide thrust through MEMS nozzles. In order to prove the design of the TU Delft microresistojet thrusters in space, a technology demonstrator is required. This demonstrator should be able to test both the VLM and the LPM in a single payload and is likely to be flown on a PocketQube platform, requiring a high level of integration and miniaturization. It is important to note that the thrusters only require technology demonstration and are not required for mission critical systems, which translates in the following research objective for an MSc. thesis conducted at the space engineering department within TU Delft:

*To design a single-payload in-orbit technology demonstrator for VLM and LPM thrusters on a PocketQube satellite within 7 months.*

The objective is then split into two research questions with multiple sub-questions. These sub-questions are to be answered before the end of this report.

- **Q1:** How can VLM and LPM technology be successfully demonstrated in future TU Delft satellite missions?
  - **Q1.1:** Which components are required for the design of a VLM and LPM technology demonstrator?
  - **Q1.2:** How can the technology demonstrator fit into the designated payload volume?
  - **Q1.3:** What is the operational envelope of the propulsion system?

Questions 1.1 will be answered with the use of systems engineering tools such as: a functional analysis of the system, a sequence diagram and requirement generation. Information gathered during the literature study will also be of importance in answering this question. Question 1.2 will be completed using CAD modelling of components and the generation of concepts. Two trade-offs will be completed to find a final conceptual design which adheres to all the requirements generated during Question

1.1. Question 1.3 will be answered by creating a Matlab model of the selected concept to analyse its behaviour. By comparing results from this Matlab model with the requirements, operational parameters can be set for initial testing.

- **Q2:** How can the completed VLM and LPM technology demonstrator design be verified?

Question 2 is answered by setting up a verification plan for each requirement. This results in a test plan and prototype design for future researchers at TU Delft.

An overview of the methodology for answering these research questions is given in Figure 1.10 and also shows the structure of this report. Information collected in the literature study provides a basic understanding of the system that is required after which the distinct tasks run in parallel to finish with a test plan as the final step of this thesis report. 3D-modelling of concepts will be one of the first steps to be completed and will be done using CATIA software. After concept selection, a model will be created for the system in Matlab to make important design choices. These will both be continuously updated after discussions with department members, after which the final versions will translate into a prototype and test plan.

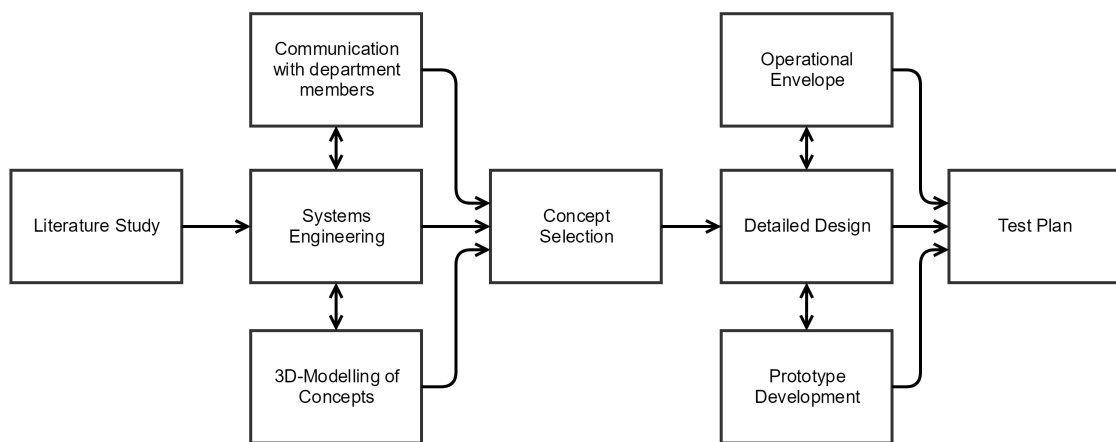


Figure 1.10: Methodology for answering research questions

## 1.4. Thesis Scope and Structure

The scope of this report is determined to be the design of a propulsion system, the setup of an initial verification plan for the design and the manufacturing of a prototype for the technology demonstrator. An initial test plan is accompanied with the prototype to provide a starting point for future students to continue the development of the technology demonstration payload.

This report contains four main chapters. Chapter 2 covers the systems engineering and conceptual design of a technology demonstrator capable of testing both VLM- and LPM-technology. This includes a functional analysis, requirements generation, concept generation, trade-offs and the final concept generated by 3D CATIA modelling. Following this, Chapter 3 discusses detailed design choices as well as presenting a 3D-printed mock up to give an indication of scale and verify the selected final design using a fit test. Chapter 3 also discusses component level choices which result in a complete design of the system. Chapter 4 uses the design choices from the detailed design to create the operational envelope of the system such as thrust times, mass flow, power inputs and pressure changes. Functional diagrams of all necessary modes for the system are also included in this chapter. Finally, Chapter 5 provides an initial verification plan for the design and shows the prototype model for testing. An initial test plan is also provided in this Chapter as a starting point for future students.

# 2

## Conceptual Design

As the goal of this thesis is to design a technology demonstration payload for use on future TU Delft PocketQube satellites, a systematic approach to concept design will be followed to minimise design flaws and provide reproducibility for future work. This chapter will follow a series of systems engineering steps to come up with a final conceptual design for a dual VLM-LPM technology demonstration payload. The first step is the creation of a functional analysis of the technology demonstration mission including its integration into a TU Delft PocketQube satellite. This functional analysis can be used to ensure that no requirements were missed during earlier requirement generation. After creating a finalised list of requirements, design parameters and component selection are addressed in coming up with multiple concepts for use in a trade-off. Trade-off methods will be applied using killer requirements and trade-off criteria. This chapter concludes with the final conceptual design for the dual VLM-LPM technology demonstration payload on a PocketQube platform.

### 2.1. Functional Analysis - Mission

The first step to developing a concept for the demonstrator payload is the use of a functional flow diagram. By mapping each of the stages in the development and operation of the demonstrator payload, the designer can make sure that the final list of requirements is comprehensive. For this reason, the entire mission including the development, manufacturing, launch and end-of-life stages are considered. Figure 2.1 shows the final version of this functional flow diagram, stages of which will be referred to in the future by the numbering system in the bottom right corner of each block.

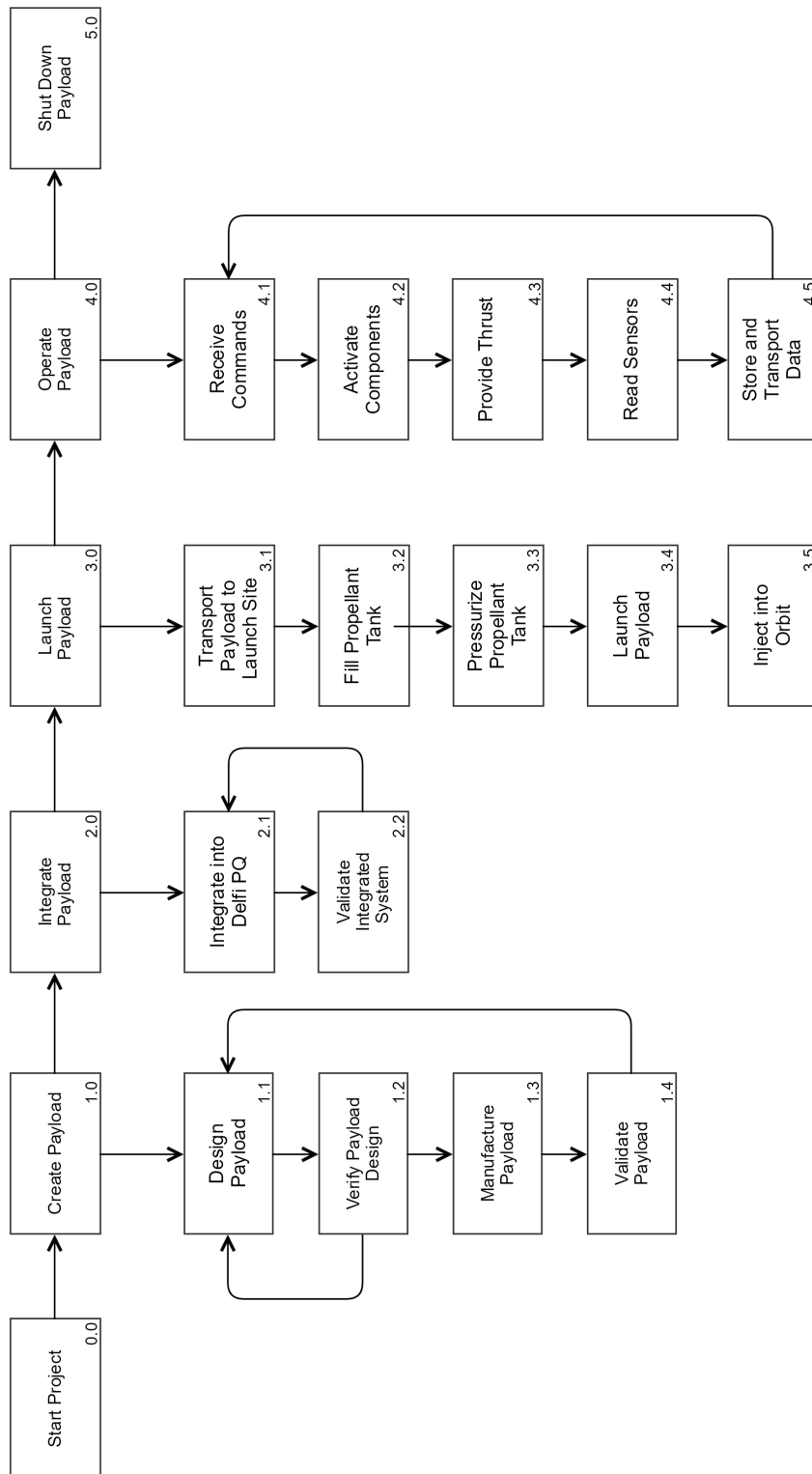


Figure 2.1: Functional flow diagram for the technology demonstrator payload and Delfi-PQ

## 2.2. Sequence Diagram

The use case scenario will be used as an additional method to show the functions of the payload operations, especially in a software interface framework. Figure 2.2 shows the necessary communication capabilities with the onboard computer (OBC) and the payload. Effectively, Figure 2.2 'zooms in' on the payload operation block (4.0) of Figure 2.1.

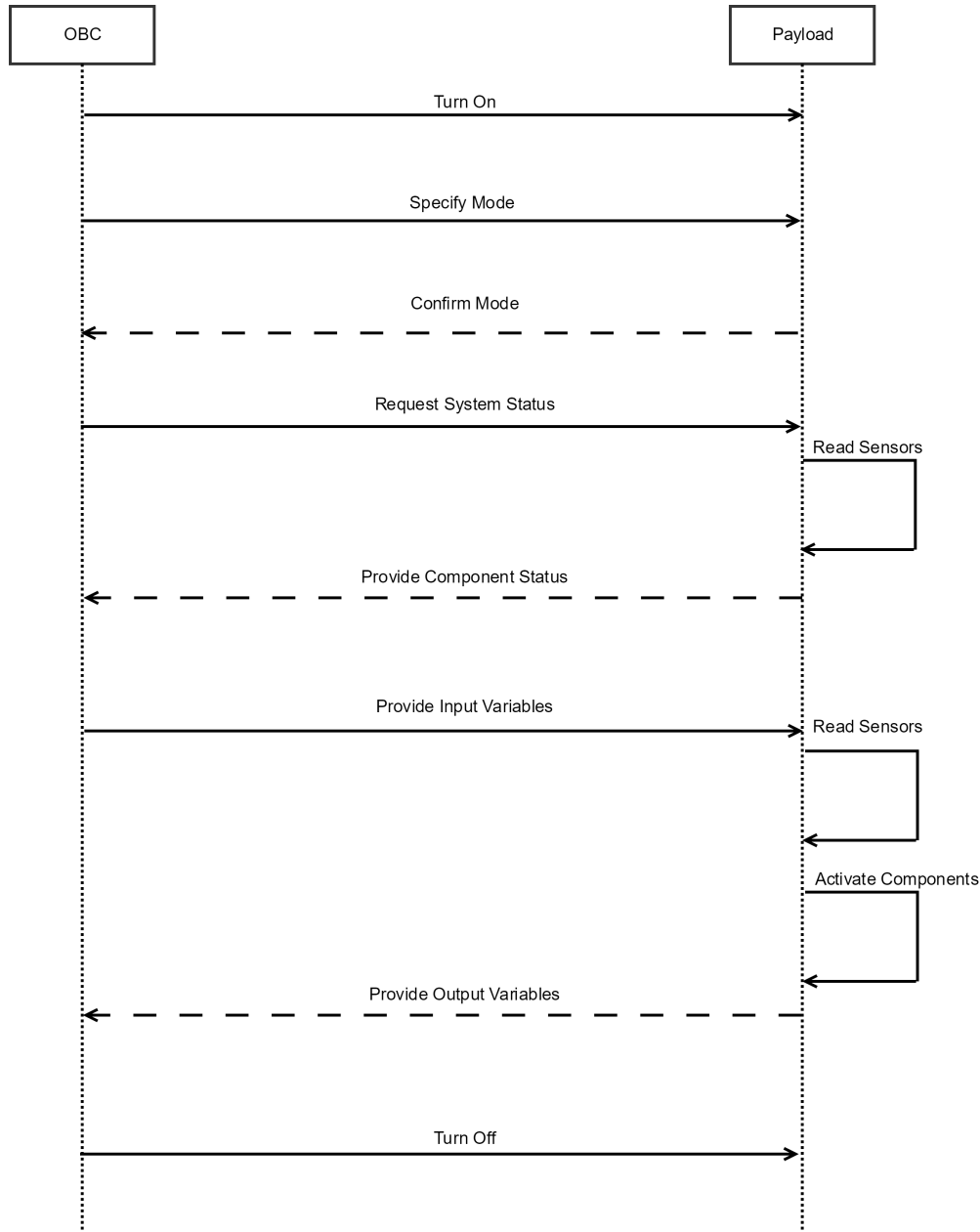


Figure 2.2: Sequence diagram between OBC and demonstrator payload

## 2.3. Propulsion Payload Demonstrator Requirements

An initial list of requirements for the propulsion payload subsystem was already set up prior to writing this report and can be seen in an internal final requirements document for the propulsion payload on Delfi-PQ [26]. To ensure that this final list is complete, each requirement will be traced back to the functional flow diagram and sequence diagram. If any of the blocks in the functional flow diagram (Figure 2.1) are not accounted for in the requirements, then the final list of requirements will be deemed incomplete. It is also possible for multiple requirements to fall under one functional flow block.

The most important part of this section is located in the third column of each requirements table, which provides the influence of the requirement on the conceptual design phase. During concept generation this column will be revisited many times.

### 2.3.1. System Requirements

The first requirements are those set by the Delfi-PQ satellite. These are denominated by the **SYST**-identifier and can be seen in Table 2.1. Most of these requirements relate to the integration of the payload demonstrator with Delfi-PQ. For this reason, the final column in Table 2.1 mostly refers to block 2.1 in the functional flow diagram.

Table 2.1: List of system requirements

Identifier	Requirement	Influence on conceptual design	FFD Block
<b>PROP-SYST</b>			
PROP-SYST-100	The total wet mass of the propulsion system at launch shall not be higher than 75 g.	Directly influences total component mass and specifically limits the propellant mass.	2.1
PROP-SYST-200	The total size of the propulsion system shall be within 42 mm x 42 mm x 30 mm (including thrusters, valves, electronics board, harness, connectors & propellant storage tube).	<b>Driving requirement.</b> Severely limits the placement of components in the design phase. Especially when using solenoid valves, the smallest of which are 40 mm in length. <b>Note: After consultation with Delfi-PQ team, there is a 2.4 mm overhang allowed on all sides of the PCB board.</b>	2.1
PROP-SYST-210	The system shall adhere to the following distance specifications: Maximum component height above: PCB 4 mm Maximum component height below PCB: 27-28 mm Board spacing distance: 32 – 33mm Pin insert depth: 4.6–5mm 3.6–5mm Total stacking height: 33.6 – 34.6mm.	Limits the height of components to allow for placement of electronics on the PCB together with the spacers and brackets.	2.1
PROP-SYST-300	The peak power consumption of the propulsion system during ignition or heating shall be not higher than 4 W and duration shall not be longer than <b>&lt;TBD&gt;</b> s per day.	One of the driving requirements in selecting components. Limits the power which can be supplied to the VLM and LPM thrusters and will influence the maximum operating pressure of the system. Higher operating pressures require higher input powers.	2.1

Table 2.2: List of system requirements

Identifier	Requirement	Influence on conceptual design	FFD
<b>PROP-SYST</b>			
PROP-SYST-400	The maximum amount of propulsion system data that can be stored in the memory storage unit on board the satellite is <TBD> GB.	Influences the selection of electronics and measuring frequency during in-orbit testing. Raises question whether a microcontroller is required.	2.1, 4.5
PROP-SYST-500	The critical mission lifetime of the propulsion system shall be equal to at least 3 months.	Main influence will be on the leakage of the propellant tubing storage and corresponding tubing interfaces. Another influence on the choice of components will be the amount of on/off cycles that the valves can support.	1.0
PROP-SYST-600	The time available for the development of the propulsion system is <TBD> months	This requirement will have direct influence on the design process and testing of the propulsion system. Time-saving design choices may be required.	1.0, 2.0

### 2.3.2. Performance Requirements

The performance requirements give the minimum and maximum values for typical propulsion system characteristics such as delta V and thrust levels. However, because this propulsion system is designed to be a technology demonstrator, there is no fixed delta V requirement. The most important requirement and the main goal of the propulsion system is to demonstrate and measure the provision of in-orbit thrust using VLM and LPM thrusters. The list of performance requirements can be seen in Table 2.4.

Table 2.3: List of performance requirements

Identifier	Requirement	Influence on conceptual design	FFD Block
<b>PROP-PERF</b>			
PROP-PERF-100	The first prototype shall be a technology demonstration.	No minimum delta V requirement is required. Only proof of thrust from both the VLM and LPM thrusters is required.	4.3
PROP-PERF-200	The thrust provided by the propulsion system shall be 3 mN as a maximum.	This maximum thrust requirement is necessary to avoid excessive rotation of Delfi-PQ in the worst case scenario. Limits the maximum operating pressure of the system.	4.3
PROP-PERF-210	The thrust provided by the propulsion system shall be at least 0.12 mN	The minimum thrust requirement is set to demonstrate that VLM and LPM thrusters can be used to maintain altitude whilst in orbit. This will set a minimum power and pressure under which the two thrusters should operate.	4.3

Table 2.4: List of performance requirements

Identifier	Requirement	Influence on conceptual design	FFD Block
<b>PROP-PERF</b>			
PROP-PERF-300	The maximum leak rate shall be <b>&lt;TBD&gt;</b> at maximum operating pressure.	This requirement will require thorough testing of connections and the tubing storage system. Furthermore, no leakage should damage the rest of Delfi-PQ, which will likely require additional insulation for majority of the propellant tubing in the payload.	1.1, 1.3, 2.1
PROP-PERF-400	The micro-propulsion system shall operate on a single unregulated supply voltage of 3 [VDC] to 4.1 [VDC].	This requirement results in the necessity of having DC-DC converters to provide the correct voltages for components.	1.0

### 2.3.3. Functional Requirements

This section covers the requirements on how the system should function. Many of these requirements can be seen directly from the sequence diagram shown in Figure 2.2. These requirements will have a large influence on the software design of the propulsion system. The full list of functional requirements can be seen in Table 2.5.

Table 2.5: List of functional requirements

Identifier	Requirement	Influence on conceptual design	FFD Block
<b>PROP-FUN</b>			
PROP-FUN-100	The micro-propulsion system shall have at least two modes: idle mode with a maximum power consumption of 15 mW and a full thrust mode with a maximum power consumption of 4 W.	This requirement is of importance the software design of the payload. Especially the software interface between the OBC and the payload. Also means an additional microcontroller should perhaps be used for the payload.	4.2, Fig. 2.2
PROP-FUN-200	The thruster shall be able to operate on gaseous $N_2$ , as well as on liquid $H_2O$ .	$N_2(g)$ will be used as a pressurant and $H_2O(l)$ will be used as the propellant for the propulsion system. Component materials must be compatible with these compounds.	3.2, 3.3, 4.3
PROP-FUN-300	The feed system shall operate in a normally closed configuration.	The valves must be designed such that they fail in a closed state or when there the system is in idle mode.	4.2
PROP-FUN-400	The micro-propulsion payload will be turned off if the system is not undergoing any type of demonstration/operations and also when the propellant storage tank is empty.	Requires the software design to include multiple modes, in which the payload is turned off and uses very little power. See requirement PROP-FUN-100	4.2, Fig. 2.2

Table 2.6: List of functional requirements

Identifier	Requirement	Influence on conceptual design	FFD Block
<b>PROP-FUN</b>			
PROP-FUN-500	The propellant storage shall be left empty when the micro-propulsion payload demonstration is completed.	This requirement shows that there should be an end-of-life mode which can be activated to empty propellant tubing.	5.0
PROP-FUN-600	The control electronics shall have a Spike and Hold circuit, voltage & current monitoring circuit, resistor heater circuit, microcontroller, sensor interfacing and overcurrent protection circuit.	This requirement sets some of the electronic components required for the payload. This will also give an indication towards the amount of space required electronic components on the PCB.	4.0
PROP-FUN-700	The micro-propulsion system shall allow for the mounting of electronic sensing devices for the measurements of propellant temperature and pressure inside the tank, temperature and pressure measurements, IMU measurements (accelerometers & gyroscopes), voltage monitoring/current monitoring/temperature monitoring.	An IMU will be required in the design, together with pressure and temperature sensors located in the propellant tubing and thrusters. A voltage and current monitoring circuit will also be required.	4.4

#### 2.3.4. Interface Requirements

The interface requirements show the required physical and software interfaces between both the Delfi-PQ platform and the propulsion system. The choice for the Delfi-PQ is the use of the PQ9 standard connector on the PocketQube platform with a software interface using RS-485. The resulting list of interface requirements can be seen in Table 2.7.

Table 2.7: List of interface requirements

Identifier	Requirement	Influence on conceptual design	FFD Block
<b>PROP-INT</b>			
PROP-INT-100	The mechanical interface between the propulsion system and the satellite shall be compliant with option 7 from the PQ9 standard connector stacking and shall respect the PQ9 standard in PCB selection and sizing. For more information see [27].	The PQ9 connector determines the minimum height on one side of the PCB, which is 4 mm. The physical interface between PCBs along the satellite provides another limitation on component placement. Each corner of the PCB has spacers of 3 mm in radius where no components may be placed. Exact dimensions of the fixed limitations of the PCB can be seen in Figure 2.3.	1.1, 2.1

Table 2.8: List of interface requirements

Identifier	Requirement	Influence on conceptual design	FFD Block
<b>PROP-INT</b>			
PROP-INT-200	The thermal interface between the propulsion system and the satellite shall allow for the propulsion system components to stay in a temperature range between +5 ° C and +85 ° C during all the mission phases when propulsion system operations are required.	To avoid the propellant freezing and ensure satisfactory performance of the system, there may be some form of insulation required for the propellant tubing storage. Furthermore, locating components such as the storage tank close to heat sources should be included in design considerations.	4.3
PROP-INT-300	The propulsion system shall be electrically connected to the satellite power subsystem through the standard RS-485 interface and shall respect the mechanical and electrical interface of connector stacking option 7 from the PQ9 standard document [27].	This requirement determines how much space the connector for the electrical interface is taking up on the PCB and is therefore of direct influence to the placement of components. See Figure 2.3 for a detailed representation of the PCB. Furthermore, the data transmission from the propulsion system microcontroller to the Delfi-PQ OBC needs to be compatible with the RS-485 platform.	1.1, 2.1
PROP-INT-400	The data exchange interface between the propulsion system and the satellite shall be RS-485 with a data transfer rate of <TBD> bit/s.	This requirement determines the amount of measurements per second the propulsion system can make during operation and will thus limit the quality of the in-orbit test data or limit the number of sensors to be used.	4.2, 4.4, 4.5
PROP-INT-500	The propellant storage system shall allow for filling and draining the propellants at any time when the fully assembled satellite is still accessible to human operators.	This requirement is important for the location of the propellant tubing storage within the propulsion system. Some part of the propellant tubing must be close to the edge of the PCB to allow access for both filling of propellant and pressurant.	3.2, 3.3



### 2.3.5. Safety- and Assembly Requirements

This section covers all requirements concerning manufacturing, testing, assembly and safety which are of importance to the propulsion system. The full list can be seen in Table 2.9.

Table 2.9: List of safety- and assembly requirements

Identifier	Requirement	Influence on conceptual design	FFD Block
<b>PROP-RAMS</b>			
PROP-RAMS-100	The propulsion system shall be installed in the middle unit of the PocketQube. The two thrusters shall be placed on the same side of the PQ or on two opposite sides.	<i>Note:</i> This requirement has been relaxed by the Delfi-PQ team. The thrusters can be placed on any available side of the PCB. The propulsion payload will be placed in the centre of Delfi-PQ.	2.1
PROP-RAMS-200	The internal pressure of all propulsion system components shall not be higher than 10 bar.	This is a high upper limit, which likely will not be reached by the propulsion payload. The power levels required to operate at this pressure is too high for the Delfi-PQ power requirements. Furthermore, there may be more stringent requirements set by the launch provider, which are unknown as of August 2018.	3.3, 3.4
PROP-RAMS-300	The propulsion system shall not include any pyrotechnic devices.	No designs with pyrotechnic devices can be considered. This will not be a problem for this micro-resistojet system.	1.1, 1.3
PROP-RAMS-310	Materials used in the thruster shall be compatible with liquid demineralised water in both liquid and vapour state, nitrogen gas and air.	Important for the selection of components and material selection during manufacturing phase of the project.	1.3
PROP-RAMS-320	Materials used in the propulsion system shall not be toxic, flammable, or in any way potentially hazardous for the operators or the other satellite sub-systems.	Once again, important for the selection of components and manufacturing phase of the project.	1.3
PROP-RAMS-400	A thermal vacuum bake-out of the propulsion system shall be carried out before launch to ensure a proper outgassing of all the components.	Components need to be able to withstand a bakeout process, something to keep in mind during component selection.	1.3
PROP-RAMS-500	All external parts of the thruster shall be electrically grounded.	This requirement influences the design of the PCB electronics.	1.1

Table 2.10: List of safety- and assembly requirements

Identifier	Requirement	Influence on conceptual design	FFD Block
<b>PROP-RAMS</b>			
PROP-RAMS-600	The propulsion system shall have a design factor of safety higher than 1.6 for yield load.	Supporting structures for the components in the propulsion payload design will need structural analysis to ensure they adhere to this requirement. This may require a detailed design of supporting structures for the valves.	1.1, 1.2
PROP-RAMS-700	The propulsion system shall have a design factor of safety higher than 2.0 for the ultimate load.	Supporting structures for the components in the propulsion payload design will need structural analysis to ensure they adhere to this requirement. This may require a detailed design of supporting structures for the valves.	1.1, 1.2

### 2.3.6. Environment- and launch requirements

This section will focus on launch loads which are specified for the Soyuz, Vega, ASLV/SLV/PSLV, Falcon and Electron launchers in the a reference document by M. Boerci (2017) [28]. The full list of environment- and launch requirements can be seen in Table 2.11.

Table 2.11: List of environment- and launch requirements

Identifier	Requirement	Influence on conceptual design	FFD Block
<b>PROP-ERL</b>			
PROP-ERL-100	The payload shall be compatible with a large range of launch opportunities as described in M. Boerci (2017) [28].	This requirement states that the following launchers will be taken into consideration: Soyuz, Vega, ASLV/SLV/PSLV, Falcon and Electron. Depending on the launch provider, there may be a limit to maximum pressure for the system. Maximum delta-V is unlikely to be a problem for this project as it is a technology demonstrator.	3.0
PROP-ERL-200	The maximum axial and lateral accelerations that the propulsion system shall withstand during the launch are as specified in the reference document by M. Boerci (2017) [28].	PROP-ERL-200 requires that there by a vibration and shock test for the propulsion system to ensure that the payload can survive launch loads present on the launchers shown in PROP-ERL-100.	1.4, 2.2
PROP-ERL-300	The maximum vibration levels at the point of attachment of the satellite during the launch are as specified in the reference document by M. Boerci (2017) [28].	A vibration test is required for the Delfi-PQ satellite and its interface with the launcher. The propulsion payload needs to be designed such that it withstands the launch vibrations.	1.4, 2.2

Table 2.12: List of environment- and launch requirements

Identifier	Requirement	Influence on conceptual design	FFD Block
<b>PROP-ERL</b>			
PROP-ERL-400	The maximum acoustic pressures and loads that the propulsion system shall withstand during the launch are as specified in the reference document by M. Boerci (2017) [28].	See explanation at PROP-ERL-100.	1.4, 2.2
PROP-ERL-500	The maximum flight shocks that the propulsion system shall withstand during the launch are as specified in the reference document by M. Boerci (2017) [28].	See explanation at PROP-ERL-200.	1.4, 2.2
PROP-ERL-600	The pre-launch thermal environment within the launcher fairing is as specified in the reference document by M. Boerci (2017) [28].	Selection of components needs to take into account the operational temperatures of components and ensure that the launch temperature is within these limits.	1.1
PROP-ERL-700	The maximum heating of the nose fairing during the launch is as specified in the reference document by M. Boerci (2017) [28].	Selection of components needs to take in to account the operational temperatures of the components and ensure that the maximum in flight temperature is within the limits of the components.	1.1
PROP-ERL-800	The maximum pressure changes inside the fairing that the propulsion system shall withstand during the launch are specified within the reference document by M. Boerci (2017) [28].	Components selection must comply with this requirement in order to ensure nothing breaks during launch or during ascent of the launcher.	1.1, 1.4
PROP-ERL-900	The micro-propulsion subsystem shall be compatible with the vacuum and temperature levels of the space environment in Low Earth Orbit.	All components shall be able to operate under vacuum and typical temperatures in LEO. Therefore space-qualified COTS components shall be used as much as possible.	1.1, 1.3

## 2.4. Physical System Architecture

This section will translate requirements from the previous sections into the required components and the hardware architecture for the system. The simplest valves which have been thoroughly tested at TU Delft are solenoid valves. Although bulky, the simplicity of use and their performance outweigh the development cost and time of an in-house MEMS valve. For this reason, two solenoid valves were determined to be used for the system. With this in mind, efficient use of volume is paramount, therefore a concept for 'sharing' a propellant tank between the two thrusters was decided to be the most advantageous. To avoid designing connectors between the propellant tank and the feed system and to avoid excessive leakage, capillary tubing is chosen to be the 'propellant tank' for the system. A coiled capillary tube is to be connected with valves at each end. This tubing acts as the propellant tank and contains the propellant together with the pressurant. The valves are then connected to the VLM- and LPM-thrusters using additional capillary tubing as a feed system. During operation, the valve to the VLM-thruster is opened first, which allows for testing of the VLM. As the propellant drains from the capillary tubing, the pressure within the tubing drops. When the pressure is determined to have dropped sufficiently for inefficient VLM operation, the VLM valve is closed and the LPM valve is opened. The LPM thruster operates until all propellant is depleted, thereby having tested both types of thrusters in a single payload. For operation of such a system, the components mentioned in Table 2.13 are deemed necessary to comply with the requirements set in this chapter. Mass flow sensors were omitted from this list, because no mass flow sensors could adhere to the volume requirement. Thrust measurements will be completed using accelerations measured by an IMU instead.

Table 2.13: A list of all components needed to satisfy the requirements for the propulsion payload

Component	Requirement(s)	Note
PCB	<b>PROP-INT-100</b>	PCB is required for the mechanical and electrical interface with Delfi-PQ.
VLM & LPM thrusters	<b>PROP-PERF-100</b>	Propulsion system will be a technology demonstrator for VLM- and LPM-technology.
Pressure/Temperature Sensors (x3)	<b>PROP-FUN-700</b>	Requires temperature monitoring and pressure monitoring within the propellant tubing and within the thrusters. Pressure has direct influence on the thrust and temperature must be monitored at all time to ensure the temperature in the tubing does not drop below zero during operation. The temperature within the thrusters also needs to be sufficient to vaporize the propellant.
Solenoid Valves (INK0514300A) (x2)	<b>PROP-FUN-300</b>	System must be able to provide thrust but also operate in a closed position, which requires valves. INK0514300A from The Lee Company has already been tested at TU Delft and will be used for the initial design [8].

Table 2.14: A list of all components needed to satisfy the requirements for the propulsion payload.

Compatible Tubing	-	Required to connect other components.
Mass Flow Sensors (x2)	<b>PROP-FUN-700</b>	No sufficient small mass flow sensors could be found.
MSP432 Microcontroller	<b>PROP-FUN-600</b>	The propulsion system should be able to autonomously read sensors and communicate these readings to the OBC of Delfi-PQ. This requires the use of a microcontroller.
Spike- and Hold Circuit	<b>PROP-FUN-600, PROP-SYST-300</b>	Direct requirement which is required for valve operation at the maximum payload input power of 4 W.
Current Monitoring Circuit	<b>PROP-FUN-600</b>	-
IMU	<b>PROP-PERF-100</b>	Necessary to show thrusting capabilities of the thrusters by measuring acceleration and rotation of the satellite.
Insulation Tape	<b>PROP-INT-200</b>	Required to keep the propellant storage tubing above zero degrees and avoid freezing of the propellant, which would result in the system no longer being able to provide thrust.
Propellant (Demineralized Water)	<b>PROP-FUN-200</b>	-
Pressurising Gas (Nitrogen)	<b>PROP-FUN-200</b>	-
Wiring	-	Required to connect other components.

This list of components translates to the physical architecture seen in Figure 2.5.

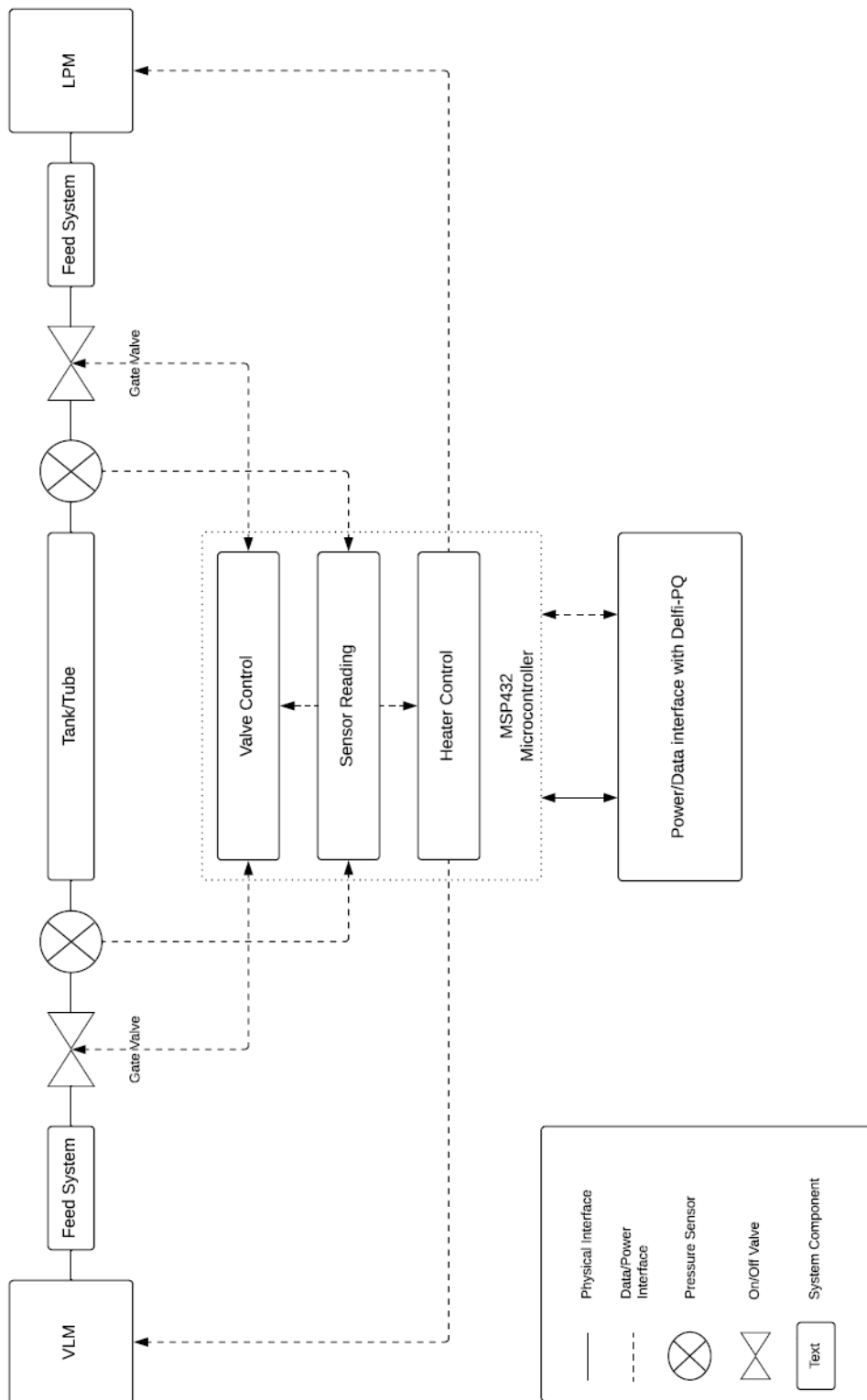


Figure 2.5: Schematic of the physical architecture of the system

## 2.5. Design Options

In order to achieve a design which has all components mentioned in Section 2.4 and adheres to all previously mentioned requirements, all possible design options were listed in the design option tree in Figure 2.6. The driving requirement for finding design options was **PROP-SYST-200** which is a constraint on the amount of volume available to the propulsion system. This constraint is especially of importance when considering valve placement as these are the largest of the required components. Design options were found by modelling components into a 42 mm x 42 mm x 30 mm volume together with all PCB connections dictated in **PROP-INT-100**. This was done using 3D-modelling software, whilst still keeping in mind all previously mentioned requirements. For simplicity, the connecting capillary tubing was omitted from this design process and replacement volumes were used for propellant storage locations and thruster housings.

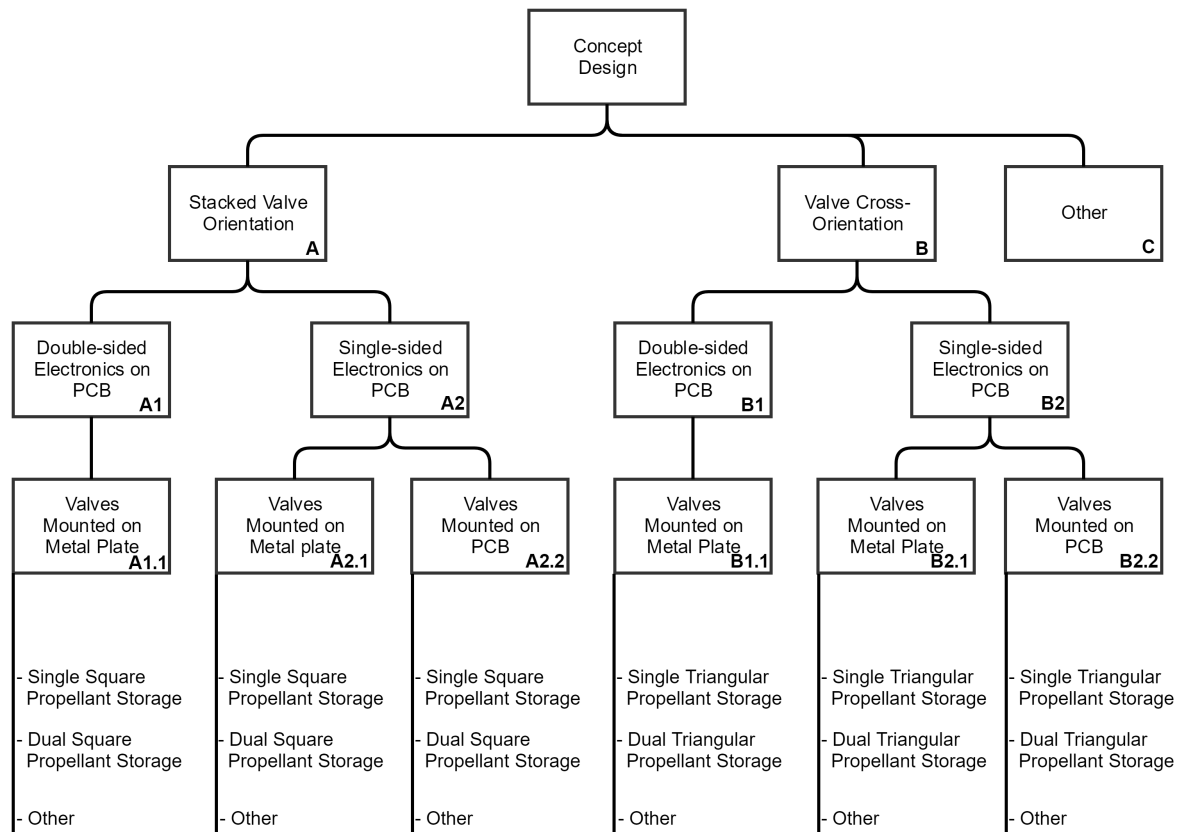


Figure 2.6: Design option tree with valve placement set as the driving requirement

Designs in block A from Figure 2.6 all have valves oriented in an X-shape with respect to the top view of the propulsion system. Block B consists of designs in which the valves are stacked on top of one another. To provide sufficient space for valve connectors, the inlets of these valves need to point in opposite directions. Designs listed under block C cover all other possibilities. Two examples of designs under block C can be seen in Figures 2.7 and 2.8. These were quickly dismissed due to the inefficient use of volume.

Now that designs in block C have been ruled out, the next stage in the design option tree is to determine whether the PCB should have both of its sides available for electronics. For the availability of electronics on both sides to the PCB, an additional plate is required for mounting the valves. The main advantage of two-sided electronics on the PCB is the additional flexibility in placing electrical components and connectors. Furthermore, integration of the propulsion system into Delfi-PQ will be easier if components are not directly installed onto the PCB which contains the electrical and mechanical interfaces. The disadvantage of using two-sided electronics on the PCB is a 16 percent loss of propellant

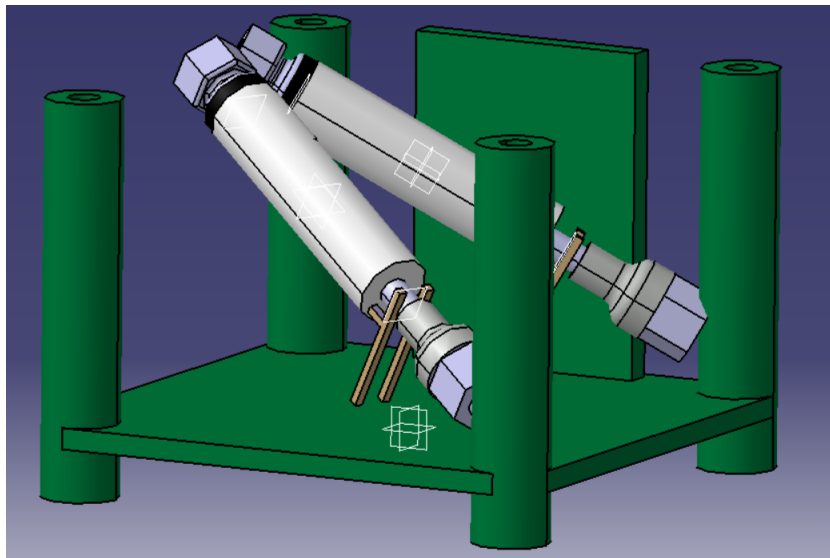


Figure 2.7: Design listed under block C with both diagonal and symmetrical valve placement

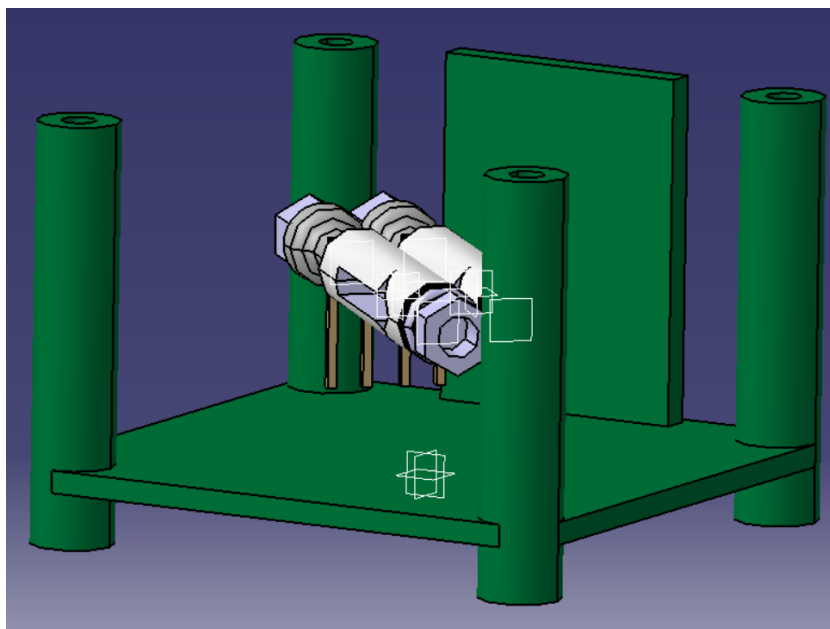


Figure 2.8: Design listed under block C with horizontal valves placed next to each other

tank volume and the additional mass of the metal plate. The 16 percent loss of volume occurs due to the loss of 4 mm of height for the propellant storage location which is required for double sided electronics. For a 42 mm x 42 mm x 1 mm aluminium plate the additional mass is equal to 4 g. Design option A1.1 can be seen in Figure 2.9 and design option A2.2 can be seen in Figure 2.10.

The same trade-off between single- and double-sided electronics is considered for the cross-orientation designs of block B. In these designs one of the valves will be mounted on top of the VLM thruster (shown in blue in Figure 2.11). Once again the difference in designs is whether the valves be placed on an additional metal plate or directly on to the PCB. These design options are shown in Figures 2.11 and 2.12.

The simplicity and flexibility of designs A1.1 and B1.1 which have the advantage of two sided PCB electronics allow for less complications during the design phase of the PCB, which will be a challenging part of the system. This consideration outweighed the 16 percent decrease in propellant tank volume and additional mass as compared to the single sided electronics designs. Therefore designs A1.1 and

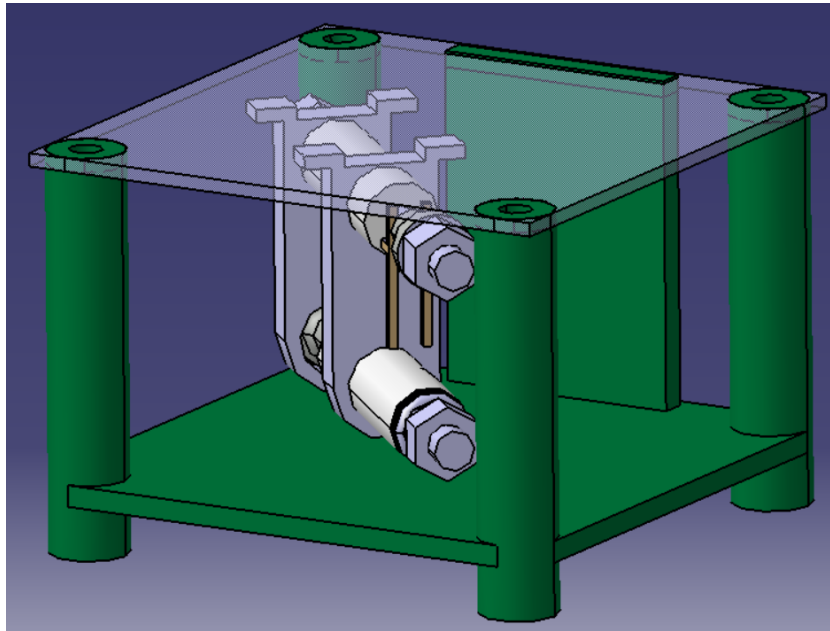


Figure 2.9: Design A1.1

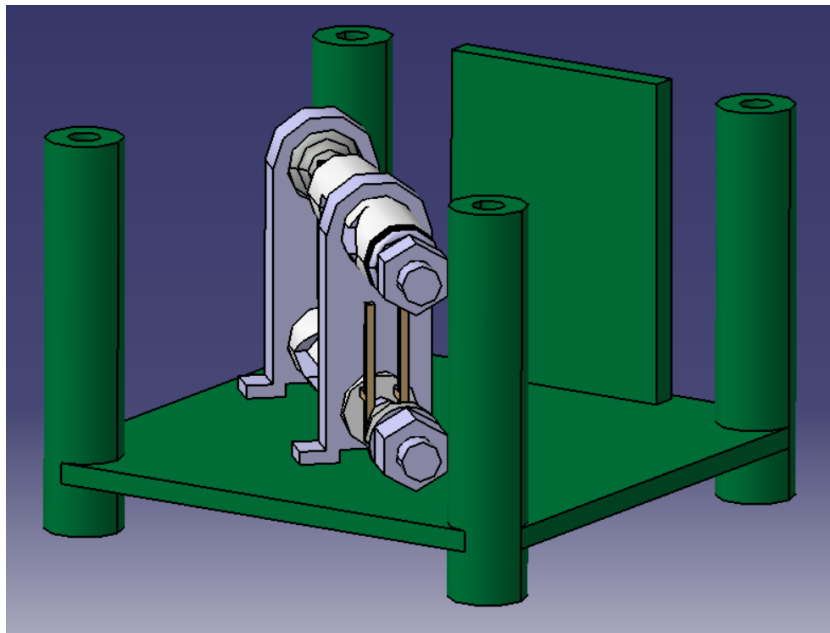


Figure 2.10: Design A2.2

B1.1 were selected for the concept trade-off in the following section. Both have multiple options for propellant storage locations, both in shape and in number. However, the most simple version of the A1.1 design with one square propellant volume which will hold a coiled capillary tube and can be seen in Figures 2.13 and 2.14.

Similarly, the cross-oriented valve design option which is mounted on an additional metal plate (B1.1) can be seen in Figure 2.15.

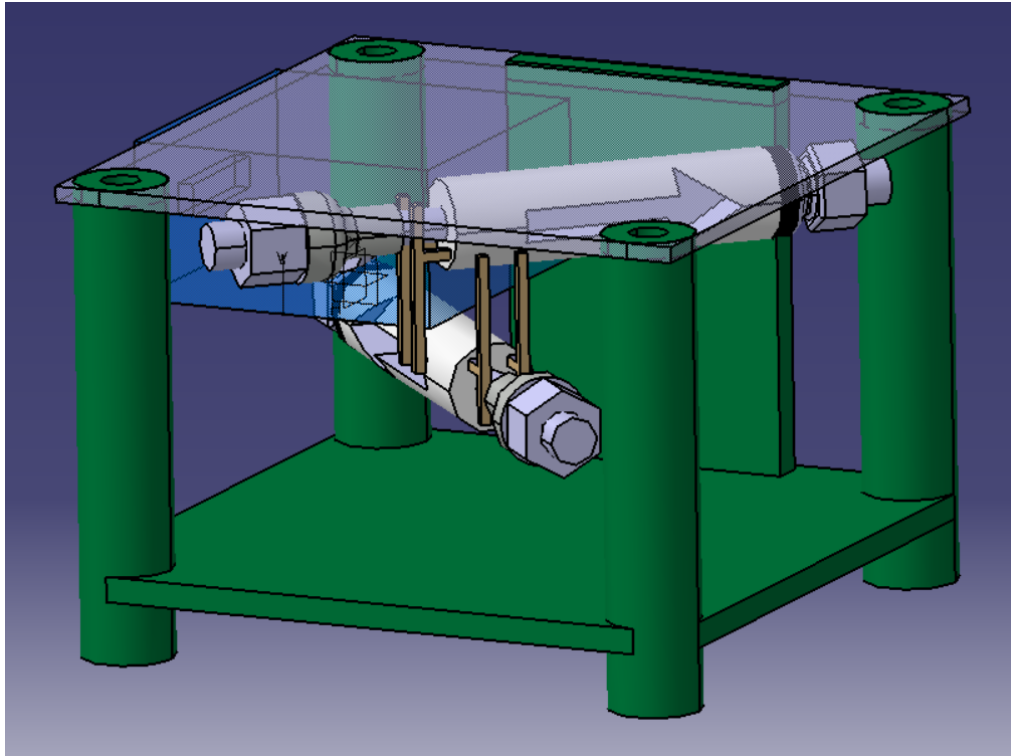


Figure 2.11: Design B1.1

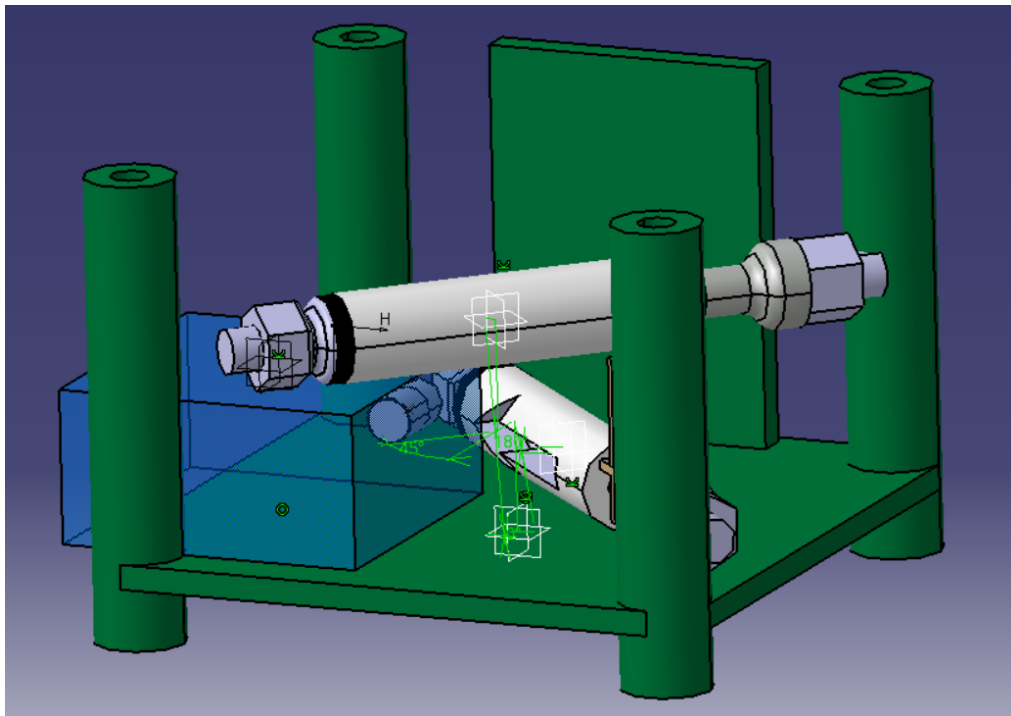


Figure 2.12: Design B2.2

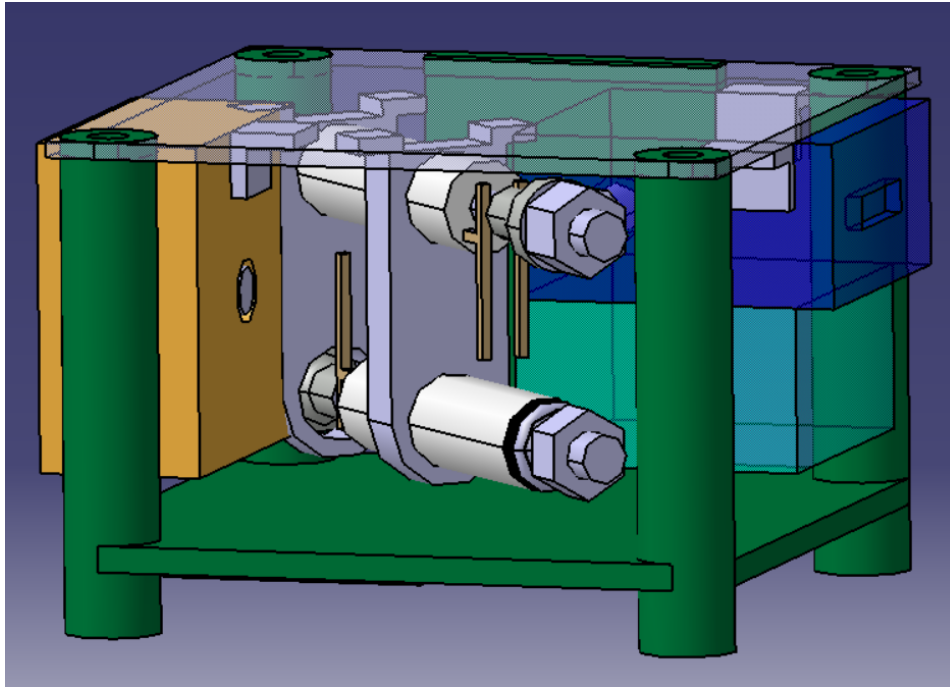


Figure 2.13: Design A1.1 with all components. Yellow: LPM thruster housing, Dark Blue: VLM thruster housing, Light Blue: Propellant storage location. 3D view

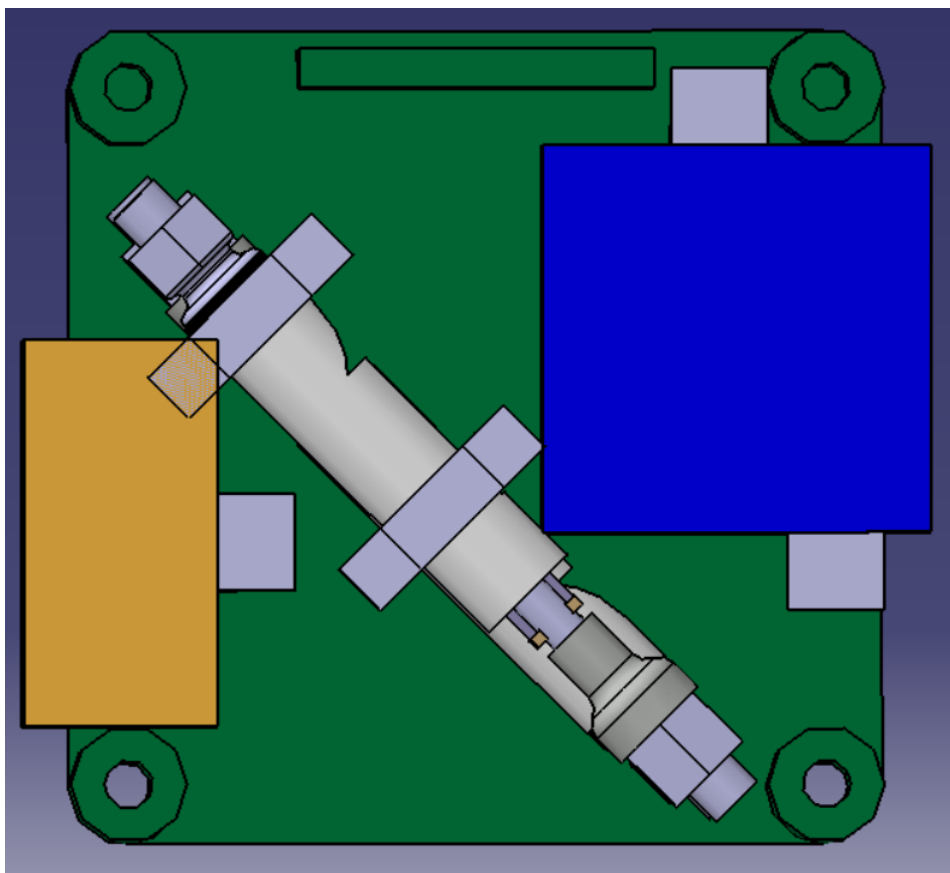


Figure 2.14: Design A1.1 with all components. Yellow: LPM thruster housing, Dark Blue: VLM thruster housing, Light Blue: Propellant storage location. Top view

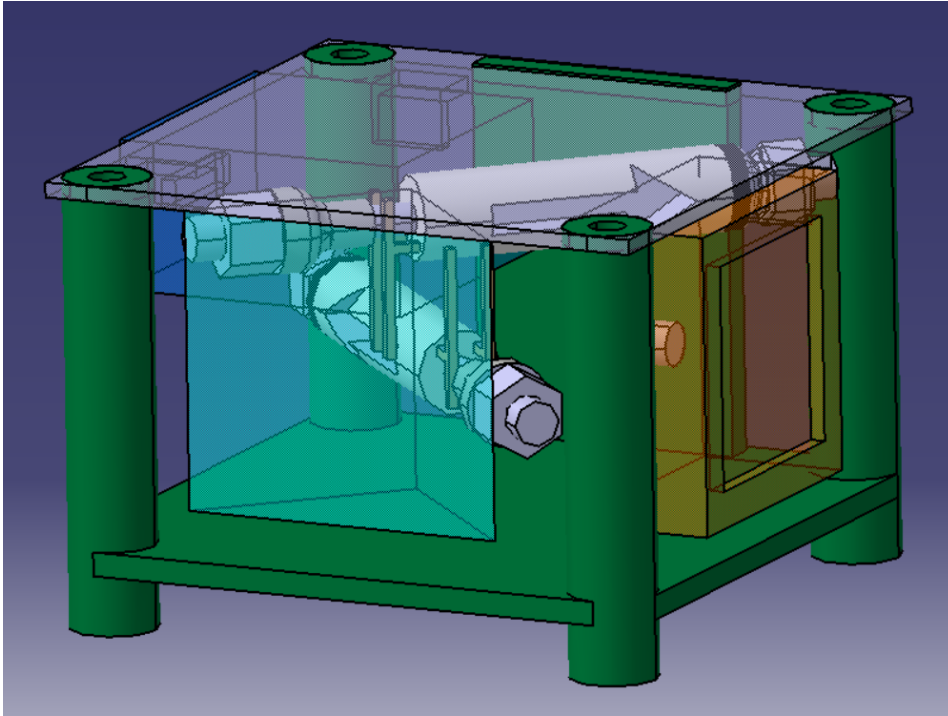


Figure 2.15: Design B1.1 with all components. Orange: LPM thruster housing, Dark Blue: VLM thruster housing, Light Blue: Propellant storage location. 3D view

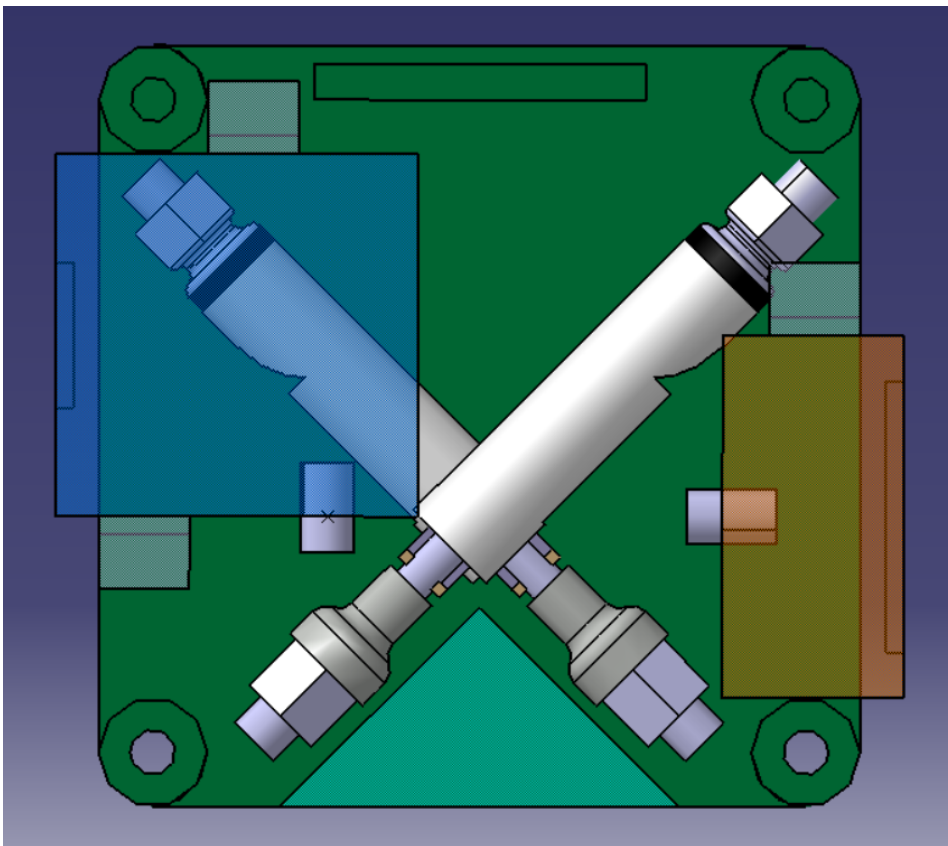


Figure 2.16: Design B1.1 with all components. Yellow: LPM thruster housing, Dark Blue: VLM thruster housing, Light Blue: Propellant storage location. Top view

## 2.6. Concept Trade-off

This section will generate two trade-offs to select either design A1.1 with single or double propellant storage or design B1.1 with single or double propellant storage for further detailed design. These dual-propellant storage designs are the same design but use any additional space within the design for an additional propellant storage location. This would allow for additional propellant storage but possibly cause a hindrance for connections to components. To select a final concept, both a graphical trade-off and a numerical trade-off will be completed. Weights for the trade-off criteria will be generated with the help of faculty members within the TU Delft micropropulsion team.

### 2.6.1. Trade-off Criteria

The trade-off criteria are set up to show all pros and cons of the designs to select the best design which fits the requirements. Weighting for the criteria will be done by use of a survey conducted within the micropropulsion team at TU Delft. This will help give an element of objectivity to the weighting procedure and the numerical trade-off. A copy of the survey can be seen in Appendix A. This method is similar to an AHP (Analytical Hierarchy Process). The AHP method decomposes a complex decision into multiple sub-decisions or in this case trade-off criteria. After this, a pair-wise comparison is made between the trade-off criteria by multiple decision makers to determine the trade-off weights. The decision makers then identify the performance of each of the trade-off candidates to the trade-off criteria according to a predefined AHP scale. Multiplying by the weights of the trade-off criteria gives the final decision for the AHP. The process for the numerical trade-off in this report differs because the AHP method in this report is only applied to generating trade-off criteria and not to the final trade-off decision. This was due to the fact that conducting an AHP trade-off with eight faculty members was deemed impractical and unfeasible at the time.

The trade-off criteria are chosen to be the following four characteristics of the designs:

- Proximity of thermal components near valve
- Volume of propellant storage
- Proximity of thermal components near propellant storage
- Simplicity of design, manufacturing and testing

The proximity of the thermal components near the valves is of importance to avoid problems with the operational temperature of the valves. Placement of valves away from thermal components will reduce the thermal considerations required in the design and testing phase. The volume of propellant storage is directly linked to the testing time for the VLM and LPM thrusters, higher available volume is advantageous. The proximity of thermal components to the propellant is included because the propellant runs the risk of freezing in-orbit. However, if the propellant tubing is located near heat sources, this will reduce the risk of this occurring. Finally, the simplicity of the design, manufacturing and testing is taken as an important trade-off criteria. To adhere to the time line for the completion of design and testing for the demonstrator payload micropropulsion system by 2019 requires simplifying the system wherever possible.

### 2.6.2. Graphical Trade-off

The graphical trade-off done for concept design is shown in Figure 2.17. The four trade-off criteria are noted at the top of each column and the design options are noted on the left at the start of each row. Green is selected to be the most favourable design within that trade-off criteria in comparison to the other design options, while yellow is the average compared to the most favourable design and orange is the least favourable with respect to the best design. Rationale for scoring of the designs can be seen within each block of the graphical trade-off. Of these rationale, only the propellant storage volume can be found quantitatively.

Although not fully conclusive, the graphical trade-off shows that design A1.1 and design A1.1-dual (with dual propellant locations) are likely to be the best fit according to the trade-off criteria.

Option/ Criterion	Simplicity	Valve Proximity to Heat Sources	Propellant Storage Volume	Propellant Proximity to Heat Sources
<b>A1.1</b>	Easiest to test & more space for wiring and tubing.	No direct contact with heat sources.	3.52 $cm^3$	Propellant storage located on top of VLM thruster. May prevent propellant freezing.
<b>B1.1</b>	Complex propellant storage shape, possible difficulty in valve support.	One of valves located directly on top of VLM thruster.	2.42 $cm^3$	No direct contact of propellant with heat sources.
<b>A1.1-dual</b>	Two propellant storages to be placed. Reduced space for wiring & tubing.	No direct contact with heat sources.	5.92 $cm^3$	Only one tank located on top of VLM thruster.
<b>B1.1-dual</b>	Two propellant storages to be placed. Reduced space for wiring & tubing. Complex shape.	One of valves located directly on top of VLM thruster.	4.84 $cm^3$	No direct contact of propellant with heat sources.

Figure 2.17: Graphical trade-off for the conceptual design of the propulsion system

### 2.6.3. Numerical Trade-off

With the trade-off criteria set, the weighting of each criterion needs to be done. In order to keep this process as objective as possible, eight experts within the micropropulsion team at TU Delft were asked to complete a survey on the weights for the trade-off criteria, which can be seen in Appendix A. The experts were asked to complete the survey using weights scored from one to ten. The concepts were not shown during the completion of this survey in order to keep the process as objective as possible. The raw results from this survey can be seen in Table 2.15.

Table 2.15: Results from the survey completed by eight TU Delft experts to objectively find the weights of the trade-off

Criterion \ Expert	#1	#2	#3	#4	#5	#6	#7	#8
<b>Simplicity</b>	4	10	6	7	9	9	7	7
<b>Thermal Proximity to Valves</b>	2	1	2	4	7	7	3	4
<b>Volume of Propellant Storage</b>	10	1	10	2	10	7	6	6
<b>Proximity of Thermal Components near Propellant</b>	6	1	8	7	7	8	7	5

The results from Table 2.15 are then normalized with respect to the full range of the weighting scale which was set from one to ten for each expert. After normalization the weights are converted to scores between zero and one. The equation used for this is given in Equation 2.1. Here  $W_n$  is the weight of the criteria, while  $x_n$  is the score for that criteria,  $MIN(x_n)$  and  $MAX(x_n)$  are the minimum and maximum scores of all the criteria. The final weights used in the trade-off can be seen in the last column of Table 2.16.

$$W_n = \frac{x_n - MIN(x_n)}{MAX(x_n) - MIN(x_n)} \quad (2.1)$$

An example using the simplicity criterion by expert number 1 is shown in Equation 2.2. Because the experts did not use the full spectrum of weights available, this method of normalization allows the most important trade-off criteria per expert to have a value of 1, while the least important criteria per expert has a value of 0. This was preferred over other normalization methods because the experts used different ranges for their highest and lowest weights compared to one another.

$$W_1 = \frac{x_1 - MIN(x_n)}{MAX(x_n) - MIN(x_n)} = \frac{4 - 2}{10 - 2} = 0.25 \quad (2.2)$$

Now that the weights have been established, the numerical trade-off can be done. Scores for each concept are based on the same rationale seen in the graphical trade-off in Table 2.17 with further explanation provided below. The final scores for the numerical trade-off are found by simply taking an average of the individual scores and weights to give a score out of 100, which can be seen in Equation 2.3. The final trade-off and result can be seen in Figure 2.18.

$$Finalscore = \frac{\sum(x_n \cdot w_n)}{10 \cdot \sum(w_n)} \cdot 100 \quad (2.3)$$

#### Criterion: Simplicity

The scores for simplicity were determined as follows. A score of 10 is given to the simplest design, while a score of 0 is determined to be too complex to consider for further development. A score of 5 is determined to be acceptable, but with probable delays caused by the design. The scoring of simplicity is mainly to do with the contingency concerning the available volume for wiring and tubing connections. Due to the largest amount of space left over for wiring and tubing, design A1.1 is selected to have a scoring of 10. Design B1.1 is determined to be more complex because the placement of the valves results in a triangular storage shape to be filled by tubing, furthermore, the valve support structure will be more complex. These two elements reduce the score rating to 8. Both dual-storage designs result

Table 2.16: Normalized weights with the final average weight of each trade-off criterion

Criterion \ Expert	#1	#2	#3	#4	#5	#6	#7	#8	Av.
<b>Simplicity</b>	0.25	1	0.5	1	0.67	1	1	1	<b>0.80</b>
<b>Thermal Proximity to Valves</b>	0	0	0	0.4	0	0	0	0	<b>0.05</b>
<b>Volume of Propellant Storage</b>	1	0	1	0	1	0	0.75	0.67	<b>0.55</b>
<b>Proximity of Thermal Components near Propellant</b>	0.5	0	0.75	1	0	0.5	1	0.33	<b>0.51</b>

in very limited space and possible difficulties for connecting all components. This lowers the scores of the A1.1-dual and B1.1-dual designs by 4, which results in scores of 4 and 6 respectively.

#### **Criterion: Thermal Proximity Valves**

The scores for the thermal proximity to the valves are determined as follows. A score of 10 is given if both valves are not in direct contact with heat sources such as the thrusters. A score of 5 is given if one of the valves is in contact with a heat source. Finally a score of 0 is given if both of the valves are in contact with heat sources. For this reason designs A1.1 and A1.1-dual both have scores of 10. Designs B1.1 and B1.1-dual both have scores of 5.

#### **Criterion: Propellant Volume**

The scores for the propellant volume are determined as follows. A score of 10 is given to the design with the highest propellant volume, design A1.1-dual. Propellant storage volumes for each of the designs are divided by the propellant volume of A1.1-dual to give scores for each design. After rounding the results this gives design B1.1 a score of 4, design A1.1 an 6 and design B1.1-dual a score of 8.

#### **Criterion: Proximity of thermal components near propellant**

The scores for the proximity of thermal components near propellant are determined as follows. A score of 10 is given if the entire propellant storage location is in contact with a heat source, which is the case for design A1.1. For designs B1.1 and B1.1-dual the propellant storage is not located near the thrusters and will not benefit from any heat. These designs therefore get scores of zero. A1.1-dual only has half of the propellant storage locations in contact with a heat source. Therefore design A1.1-dual is determined to have a score of 5.

Concept/ Criterion	Simplicity	$w$	Thermal Proximity Valves	$w$	Propellant Volume	$w$	Thermal Proximity Propellant	$w$	Final Score
<b>A1.1</b>	<b>10</b>	<b>0.80</b>	<b>10</b>	<b>0.05</b>	<b>6</b>	<b>0.55</b>	<b>10</b>	<b>0.51</b>	<b>88/100</b>
<b>B1.1</b>	<b>8</b>	<b>0.80</b>	<b>5</b>	<b>0.05</b>	<b>4</b>	<b>0.55</b>	<b>0</b>	<b>0.51</b>	<b>46/100</b>
<b>A1.1-dual</b>	<b>6</b>	<b>0.80</b>	<b>10</b>	<b>0.05</b>	<b>10</b>	<b>0.55</b>	<b>5</b>	<b>0.51</b>	<b>70/100</b>
<b>B1.1-dual</b>	<b>4</b>	<b>0.80</b>	<b>5</b>	<b>0.05</b>	<b>8</b>	<b>0.55</b>	<b>0</b>	<b>0.51</b>	<b>41/100</b>

Figure 2.18: The numerical trade-off for the conceptual design

## 2.7. Final Concept

The conceptual design which was chosen for the propulsion system based on Table 2.18 is design A1.1, which has a single location for propellant storage and uses a stacked orientation for valves. The system operates using flexible capillary tubing within a storage box as the method of propellant storage. The propellant will consist of liquid demineralised water which is pressurised by nitrogen gas. This tubing is connected to the a valve with VLM thruster at one end and a valve with the LPM thruster at the other end. At the start of operation, the valve connected to the VLM thruster will be opened to provide thrust. As the propulsion system is used, the pressure in the tubing will decrease until a yet to be determined point. Once this point has been reached, the valve to the VLM will close and the valve to the LPM will open, allowing for firing of the low-pressure micro-resistojet for the second part of the technology demonstration. The orientation of components according to the requirements can be seen in Figures 2.19 and 2.20. The colour dark blue shows the VLM thruster, orange shows the LPM thruster, green shows the PCB with spacers and connectors and light blue shows the propellant storage location. This design adheres to the volume requirement **PROP-SYST-300** and the interface requirement **PROP-INT-100**. The propellant volume is decided to be a physical box of the same shape in which the capillary tubing is coiled. This way, most of the propellant leakage should be contained within the box which was required by **PROP-PERF-300**.

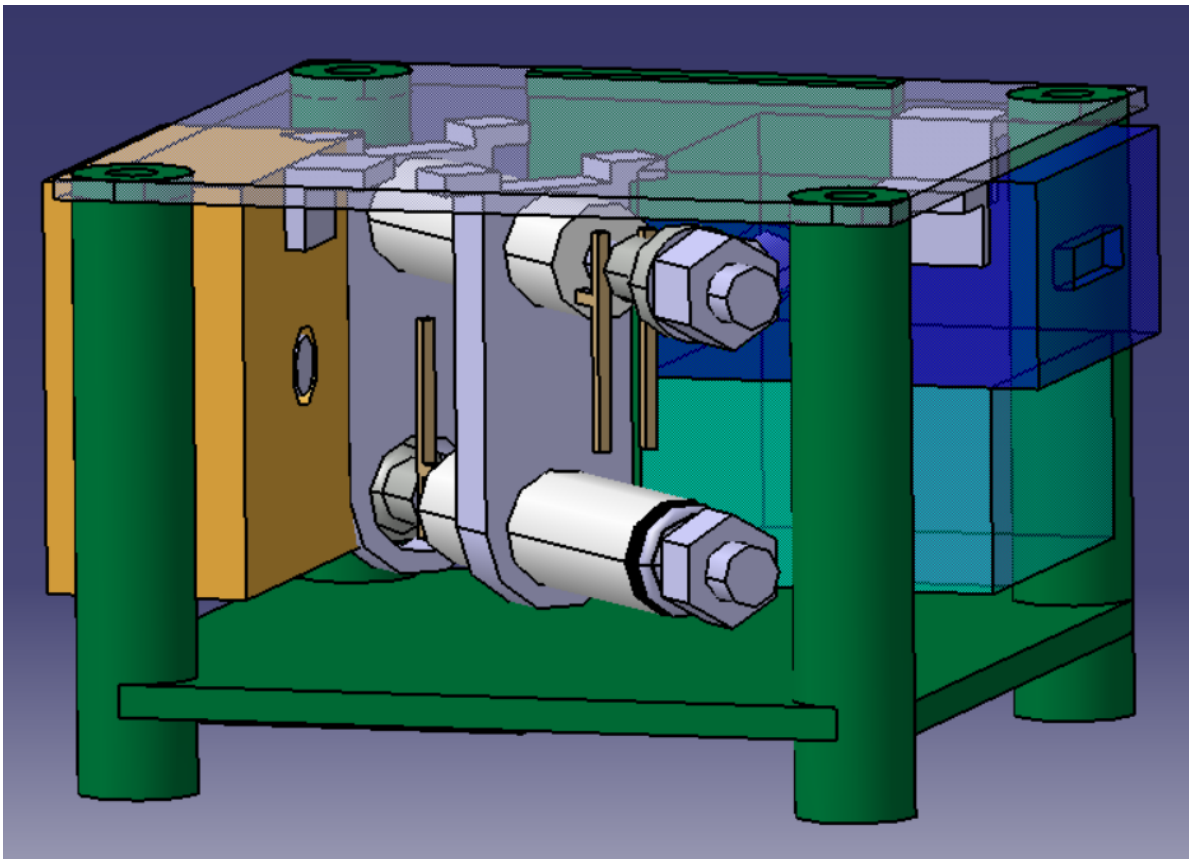


Figure 2.19: Final conceptual design: 3D view

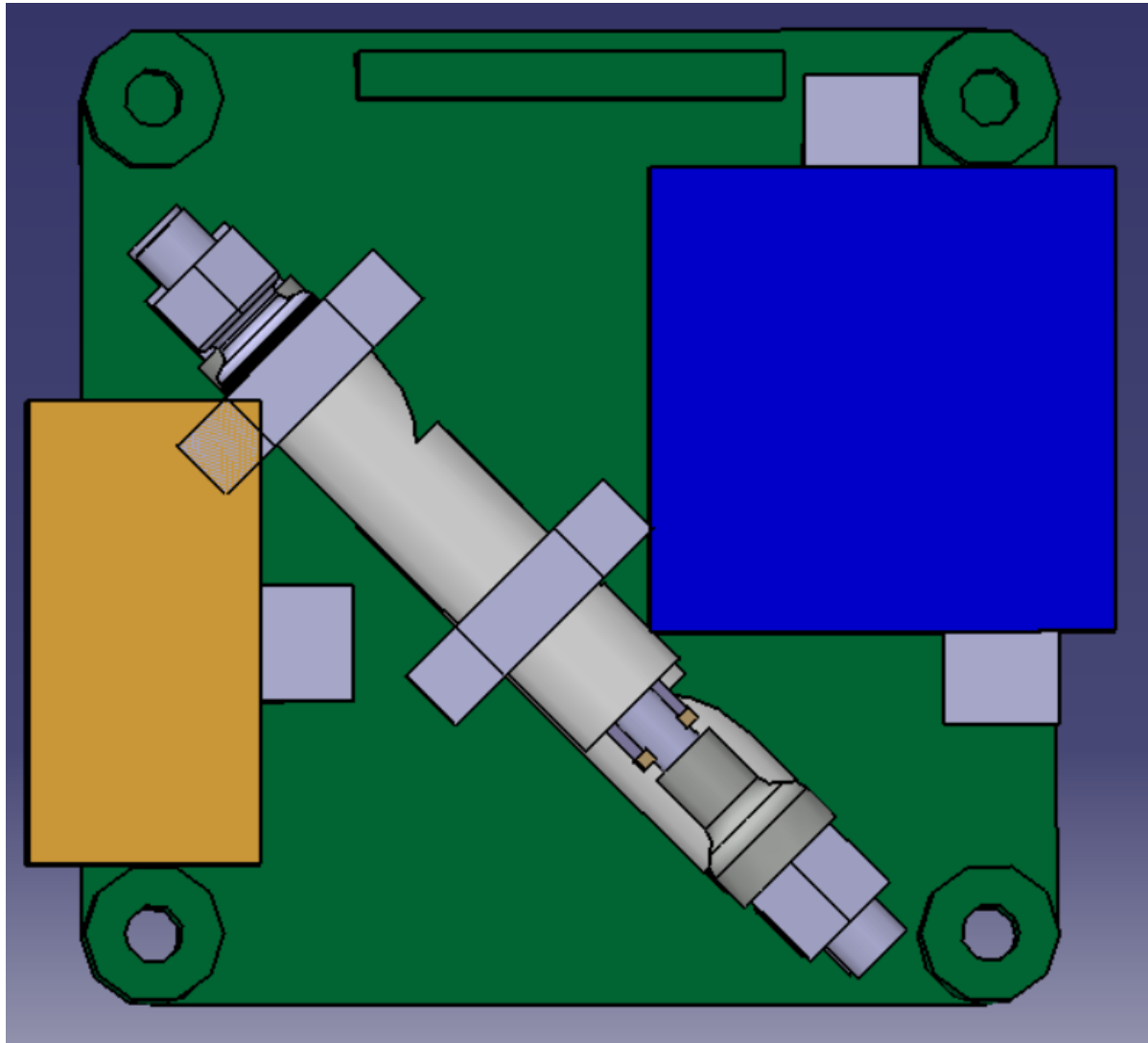


Figure 2.20: Final conceptual design: top view

# 3

## Detailed Design

Now that a concept for the layout of the propulsion system has been chosen, a detailed design at component level is to be completed. This detailed design consists of the following tasks: the designated propellant volume will be filled, tubing will be selected, interfaces between components will be chosen and integrated into Delfi-PQ. Furthermore, the valve support structure will be updated based on a fit test of the system using a mock-up model. The 3D-printed mock-up of the conceptual design can be seen in Figure 3.1 and successfully showed that the concept fitted within the designated volume. Interface components between the tubing, valves and thrusters were unavailable for this fit test.

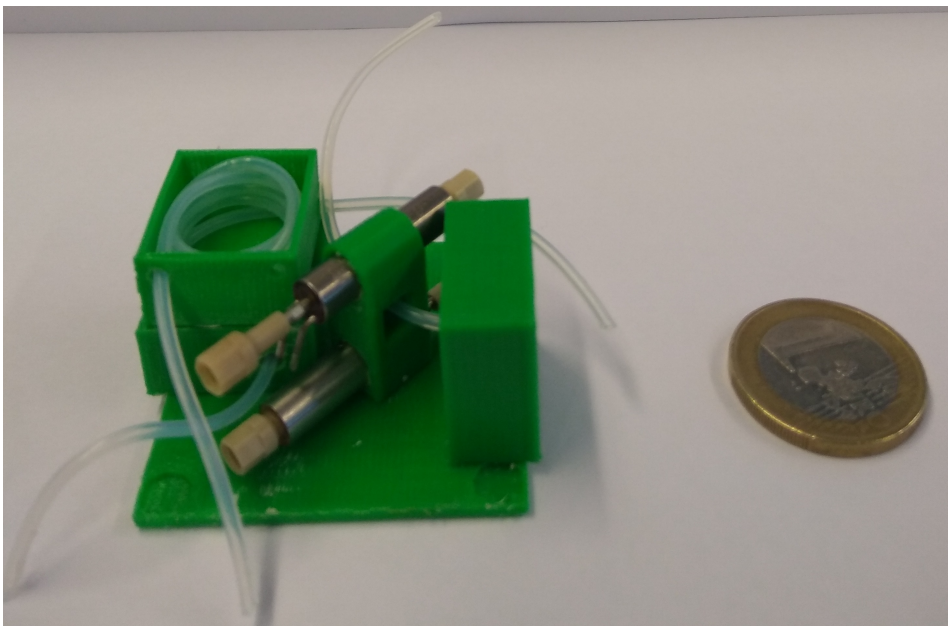


Figure 3.1: 3D-printed mock-up of the design without the PCB and stacking connectors. The one euro coin is presented for scale

### 3.1. Fit Test

In order to check whether design A1.1 fit in the desired volume and in order to get a more tangible feel for the system, a mock-up model is created for the conceptual design. The 3D-modelled parts for the VLM thruster, LPM thruster, metal plate, valve support structure and propellant storage location are 3D-printed and glued in place. Two solenoid INKX0514300A valves are temporarily placed to show that the design meets the volume requirements of PROP-SYST-200 and PROP-SYST-210. Once this is complete, capillary tubing is coiled within the propellant storage box in the 3D-mock-up to show the length of tubing which can be coiled within the propellant storage volume without causing kinks. The

result of this fit test showed that the conceptual design of A1.1 was indeed feasible and adhered to the requirements of PROP-SYST-200 and PROP-SYST-210. Furthermore, other practical conclusions came to light after this fit test which will be discussed in other sections of this chapter. The 3D-printed mock-up model with tubing can be seen in Figure 3.1.

### 3.2. Propellant Tubing and Valves

The choice of valves was already made by the micropropulsion team as the solenoid valves are already determined to be supplied by the Lee Company. These valves have been previously used by TU Delft in testing VLM and LPM thrusters. Furthermore, the tubing needs to have the same interface as the valves. What results is the choice to use tubing supplied by the Lee Company to reduce the risk of leakage from the valve-tube interfaces. The Lee Company provides tube diameters of 3.96 mm, 3.18 mm and 1.57 mm. During the fit test, only the 1.57 mm diameter tubing proved to have the flexibility required to fit the design. The 1.57 mm diameter tubing was the only tubing able to connect components within the required volume without causing kinks in the tubing. This was concluded following the fit test mentioned in Section 3.1. The interface located at the end of the tubing will be the 0.138-40 UNF fitting end, which is the smallest and most reliable leak proof interface at the Lee Company and can be seen in Figure 3.2. There are multiple COTS tubing lengths available: 5 cm, 25 cm, 75 cm and 100 cm. The design will require the use of three pieces of 5 cm tubing and one piece of 25 cm tubing.

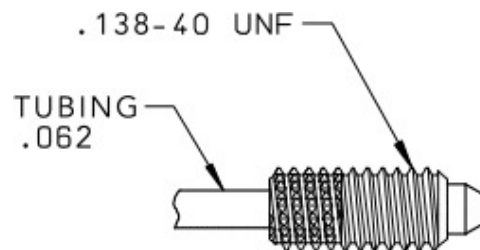


Figure 3.2: 1.57 mm diameter tubing from The Lee Company with 0.138-40 UNF interface [7]

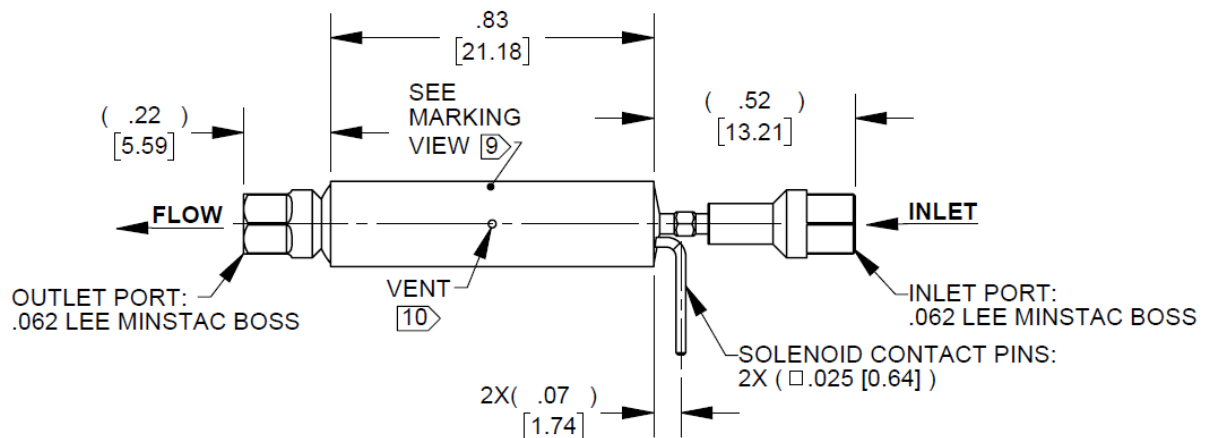


Figure 3.3: Technical drawing of the INKX0514300A solenoid valve [8]

The next design choice was to determine which valve is to be connected to which thruster. Also the location of the inlet and outlet of the bottom valve is to be determined based on the simplicity of connecting the thrusters, valves and tubing to one another. During the fit test mentioned in Section 3.1, all combinations of connections between valves and thrusters were attempted. What followed was that the connections shown in Figure 3.4 required the least amount of effort to stay within the designated volume. The result is that the bottom valve is chosen to be connected to the VLM and the top valve is used for controlling flow to the LPM thruster. A lettering system to identify the connections is shown in Figure 3.4.

The tubing lengths for each piece of tubing were then measured which results in the lengths seen in Table 3.1. The result of this means that COTS tubing of 5 cm would be sufficient for the connections

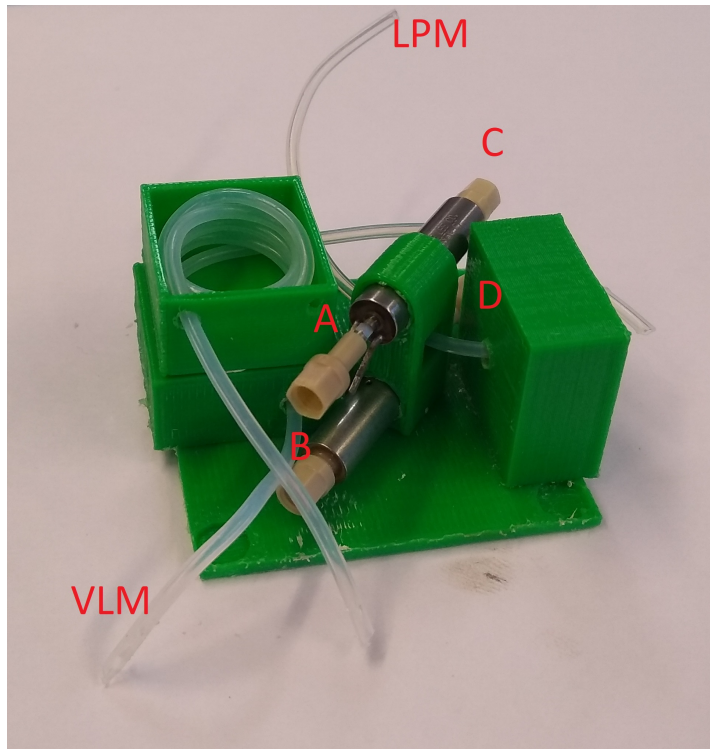


Figure 3.4: 3D mockup model: Inlet of the top valve (A) connects to the propellant storage. Outlet of the top valve (C) connects to the LPM thruster. Inlet of the bottom valve (D) connects to the propellant storage, while Outlet of the bottom valve (B) connects to the VLM thruster.

of the valves to the thrusters. A combination of a COTS tube of 5 cm and 25 cm accounts for the 30 cm of tubing required for the propellant tubing.

Table 3.1: Lengths of tubing (not including valve length or interfaces) for the propulsion system

Tube	Length
VLM-to-VLM valve	3.8 cm
Propellant	30 cm
LPM-to-LPM valve	5.5 cm

### 3.3. Propellant Storage

Although the chosen concept shows a volume for the propellant storage, precisely how the tubing fills the system is not yet defined. In order to avoid leakage and to keep the propellant tubing contained to the designated volume, coiled capillary tubing is used within a box structure. The total length of the tubing within the propellant storage area directly influences the thrusting time for the payload demonstrator. Therefore the main objective of this section is to efficiently fill the available volume without compromising the performance of the system. The main restriction for this problem is avoiding kinks within the tubing. However, during the fit test it was possible to coil the tubing within the propellant storage volume without causing kinks. What resulted was a circular coiled tube within a square box with the length of tubing between the inlets of the two valves of 30 cm, which can be used to determine the volume for the liquid propellant & pressurising gas. This simple calculation can be seen in Equation 3.1, where  $d$  is the inner diameter of the tubing and  $l$  is the length of the tubing from one valve inlet to the other valve inlet.

$$V_{tube} = \frac{\pi \cdot d^2 \cdot l}{4} = \frac{\pi \cdot 0.00157^2 \cdot 0.30}{4} = 0.581 \text{ cm}^3 \quad (3.1)$$

As can be seen in Figure 3.4, two holes were made in the propellant storage box. Using holes which are precisely the diameter of the tubing helps keep the tubing coiled up within the propellant storage box.

### 3.4. Valve Support Structure

Originally the valve support structure was designed to be two separate structures spaced approximately 8 mm apart as can be seen in Figure 3.5. However, during the creation of the mock-up model, it became apparent that a single extended structural support would provide the same stability with simpler assembly. The reason for this was that the pins for the valves which connect the wiring need sufficient space, which means that the two support structures need to be located close to one another. What results is that the support structure becomes less stable, especially as the valves are not glued in place. The design of a single structure gives the pins sufficient space and still provides sufficient stability. However, with the change to a single structure, there was little space for the tubing connection to the VLM thruster. Therefore a pocket is created which allows the tubing to go through the support structure and also reduces mass. The updated valve support structure can be seen in both Figure 3.4 and Figure 3.6. In the flight model of the propulsion system, the valve support structure will be made out of aluminium, which requires soldering to the metal plate.

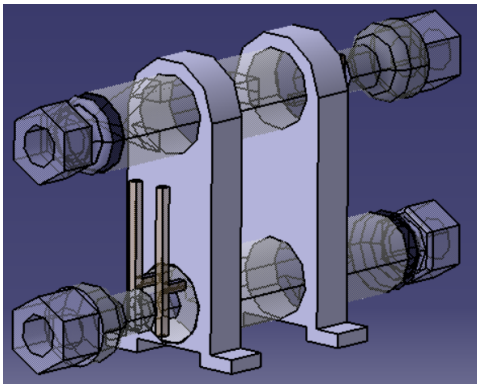


Figure 3.5: The old valve support structure

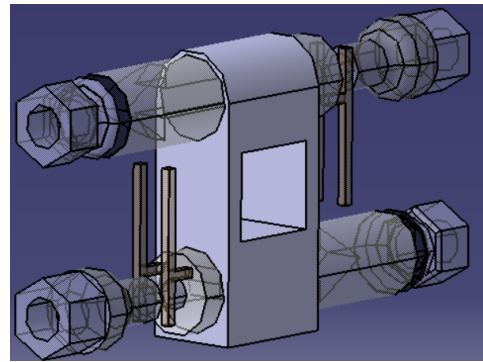


Figure 3.6: The updated valve support structure

### 3.5. Structural Interface with Delfi-PQ

Due to its small size, the Delfi-PQ satellite requires maximum coverage by solar panels on the satellite surface. This results in the fact that there are only certain locations where the demonstrator payload can be connected to the satellite, because there cannot be any screws through solar panels. This results in the need of an additional structure for the demonstrator to ensure that holes for thrusters are aligned at the correct location. This section will show the design of a structure which will allow for use of both thrusters, while still securing the payload to the satellite with a low mass. The locations of the connection points to the satellite shell are shown by red crosses in Figure 3.7. An important consideration for the design of the structure is that the corners are free so that tubing has the maximum amount of space to connect to the valves. Furthermore, it is important to note that the structure must be contained within the 30 mm height designated for the payload.

The sides of the structure with the thrusters are covered in more material as these will be the locations where the system is mounted onto the satellite. The other sides are cut out in triangular shapes to save mass but continue to provide structural support. The filling location is just above and to the right of the VLM-thruster so that it is easily accessible for pre-launch filling of propellant and pressurant.

Finally, the structure is connected by brackets to the metal plate and PCB where the rest of the propulsion system are located. This was chosen so that there is flexibility possible in the design in terms of PCB height if testing shows this to be required. This way, the structure and the rest of the propulsion system can be developed in parallel. Location of the brackets can be seen in Figure 3.8. The brackets connect to the metal plate and the PCB and can be welded onto the structure. The mass of the aluminium structure as shown in this section is equal to 5 grams.

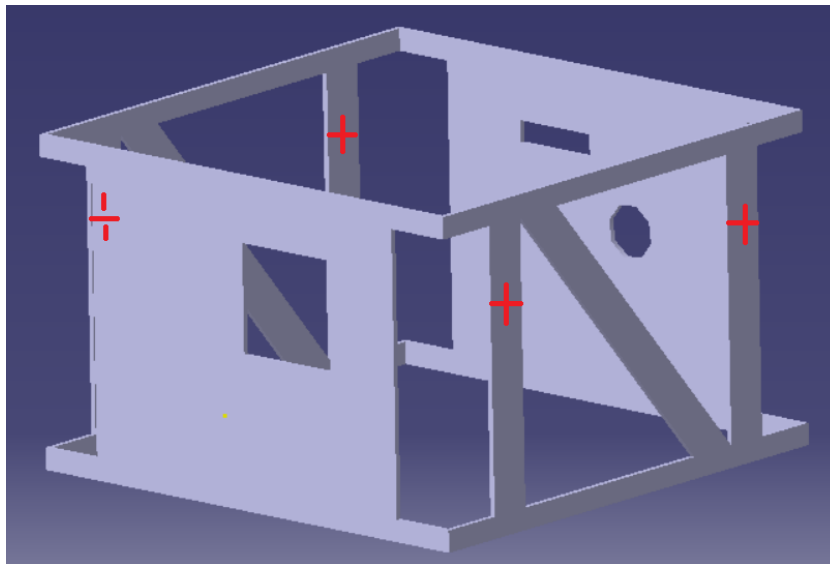


Figure 3.7: Structural interface with Delfi-PQ, where the large square hole shows the LPM thruster exit, the rectangular hole shows the VLM thruster exit and the circular hole is the fill location for the propellant.

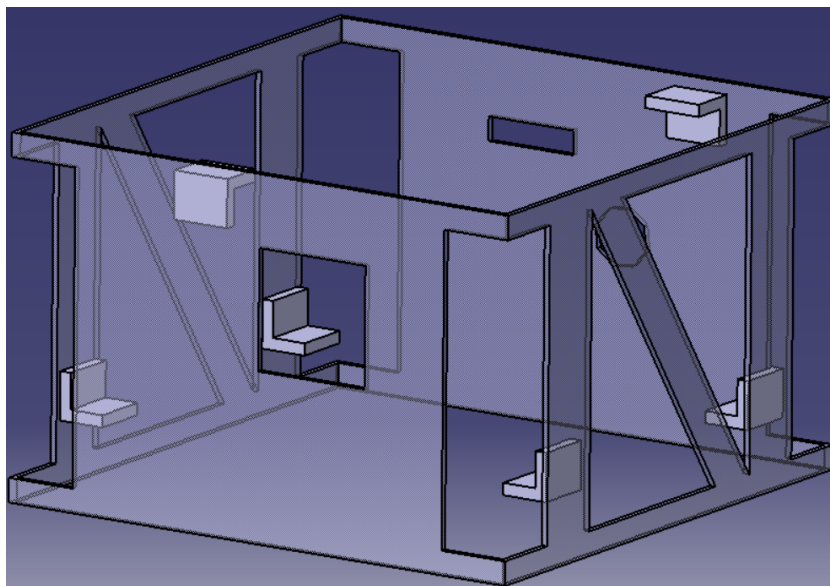


Figure 3.8: Location of brackets to connect interface to the propulsion system.

### 3.6. Thruster Chip Housings

The current thruster housings used at TU Delft for both the VLM- and LPM-thrusters exceed the volume set for the requirements of this payload demonstrator. Therefore, they need to be redesigned to fit into the final design developed in this report. These housings provide the structural interface connecting the thruster chips and propellant tubing. They also allow for an electrical interface between the heater and the power system/onboard computer. The pressure and temperature sensors are also connected to the thruster housings. A comparison between the current VLM- and LPM-thruster housings and the current thrusters used during testing can be seen in Figures 3.9 and 3.10. The redesign and manufacturing of the thruster housings do not fall within the scope of this thesis report.

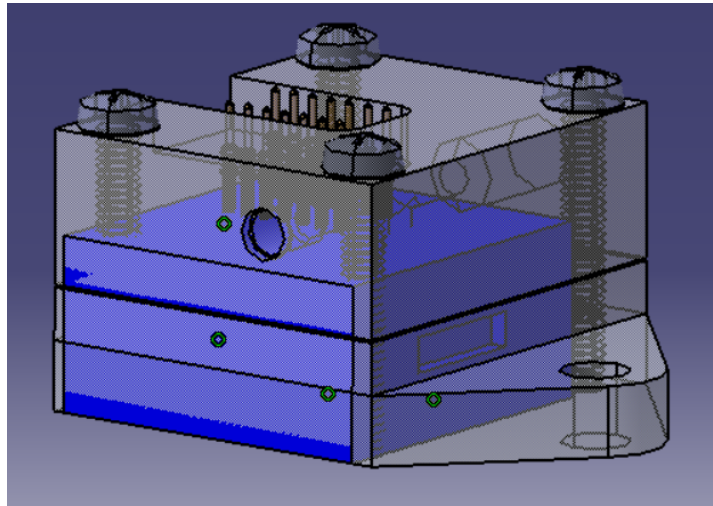


Figure 3.9: Comparison of the current VLM thruster housing and the volume of the housing required for the conceptual design. This volume is shown in dark blue.

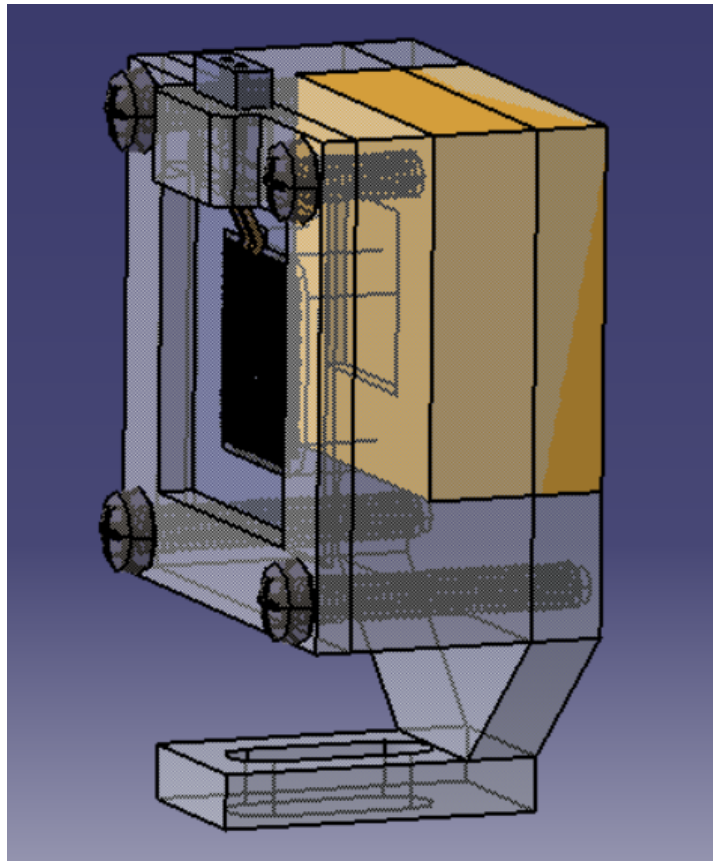


Figure 3.10: Comparison of the current LPM thruster housing and the volume of the housing required for the conceptual design. This volume is shown in yellow.

### 3.7. Propellant Manifold and Fill Valve

In order to fill the system with propellant and pressurize the system with nitrogen, an access point to the propellant storage system is required. This means a T-shape manifold is required within the 30 cm propellant capillary tube, which provides a location to be used for filling. Once the system is filled, it needs to stay pressurized with limited leakage. There are two options identified to fill the system. The

first is simply to directly attach the propellant filling system to the manifold. The propulsion system is then pressurized to slightly over the required initial pressure and nitrogen volume. The propellant filling system is disconnected and a plug is inserted in the manifold. Due to the thin orifice in the manifold and the low pressure difference at sealevel (approximately 0.1 bar, see Chapter 4.2), the loss of pressure and mass will be minimal. The integration of the manifold into the propulsion system can be seen in Figure 3.12 where the filling orifice of the manifold is located towards the outside of the satellite, which will be easily accessible for filling. The plug to be used is the LINE SEAL CAP-062 MINSTAC PEEK [29], which is small and has negligible mass.

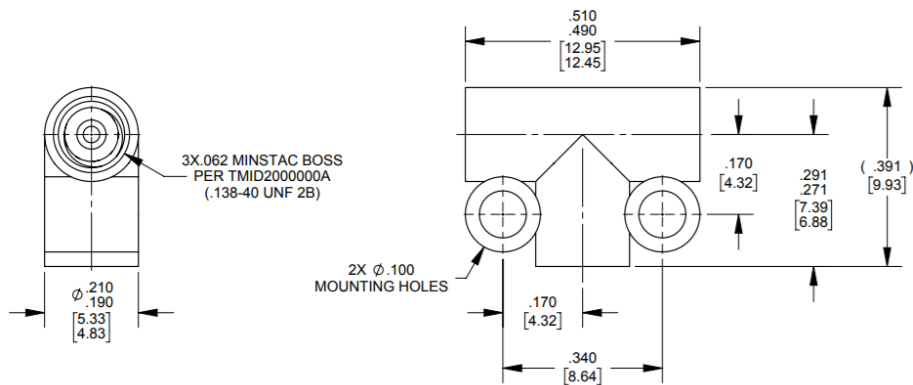


Figure 3.11: MANIFOLD-3-.062 MINSTAC-PEEK from the Lee Company, which is used to fill the propellant prior to operation [9]

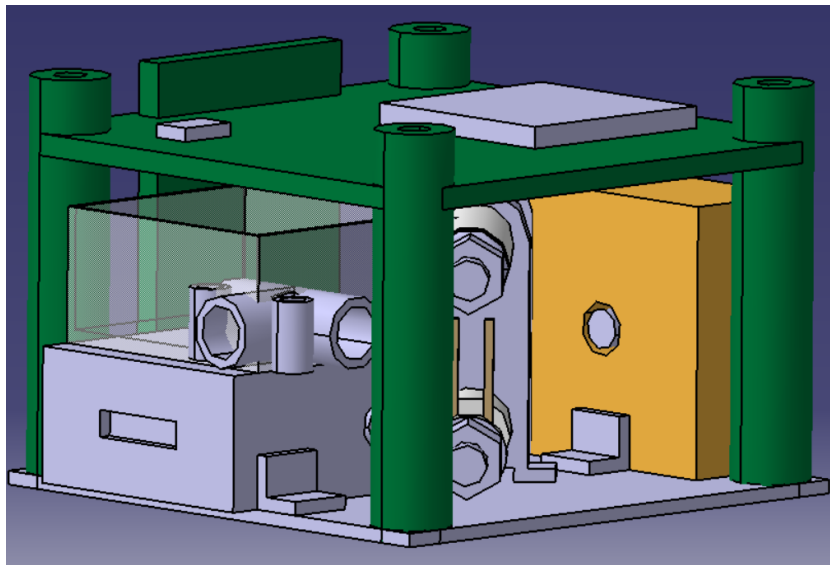


Figure 3.12: Location of the manifold within the propulsion system: on the side of the propellant storage box.

The second option is the use of a one way valve called a check valve. However, the smallest available check valve by the Lee Company which integrates nicely with their 1.57 mm tubing is still quite bulky and can be seen in Figure 3.13. Although this check valve could potentially fit in the volume available, it decreases the simplicity of the system and is therefore only to be used as a back-up solution if the plugging of the manifold is deemed unfeasible during the testing phase. If needed, the integration of the check valve into the propulsion system could be done similarly to Figure 3.14. The check valve could hang away from the propulsion system during filling, after which it is pushed into its the system just before launch. This allows for the check valve to be placed anywhere within the system without having to take into account tubing on both sides of the check valve.

However, avoiding the use of check valve all together would be most beneficial, as remaining volume for tubing and wiring after placing a check valve is very limited when using a check valve as can be seen in Figure 3.14.

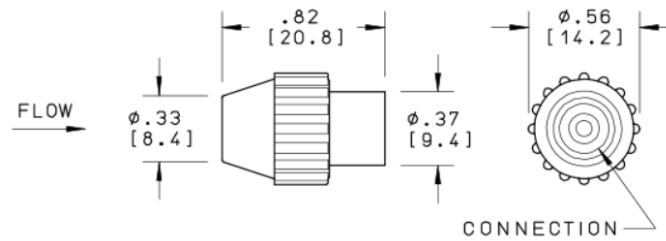


Figure 3.13: TKLA3201112H check valve from The Lee Company to be used as a back up option for filling the system [10]

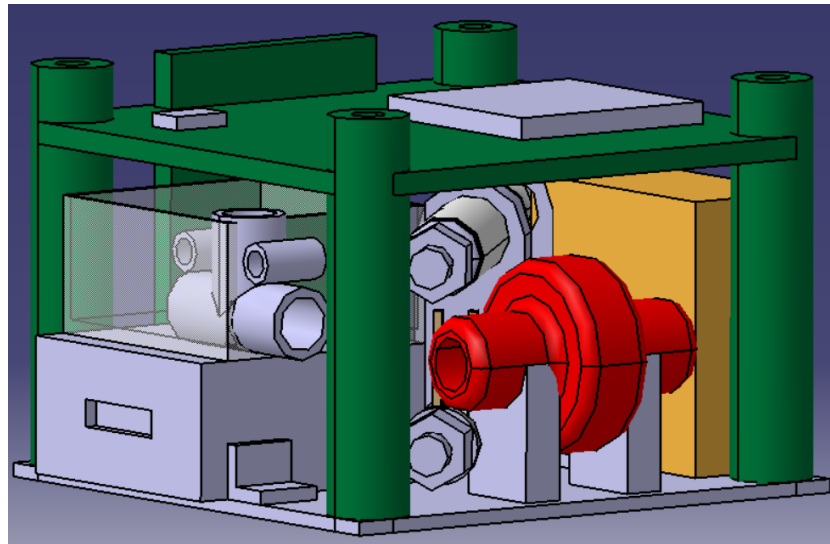


Figure 3.14: Location of the check valve shown in red for filling purposes as a backup solution for filling the system. The manifold must be oriented in a different direction to allow for a tube to connect to the check valve and still remain within the designated volume.

The check valve has the component name of TKLA3201112H in the Lee Company catalogue and can be seen in Figure 3.13. The manifold has the name of MANIFOLD-3-.062 MINSTAC-PEEK and can be seen in Figure 3.11. Furthermore, the use of T-junction manifold results in the propellant tubing being split into two parts, because two tubing parts will be connected to the manifold. As the tubing has a total length of 30 cm and the Lee Company provides COTS tubing lengths of 25 cm and 5 cm, these were chosen to be the lengths of tubing for the propulsion system.

### 3.8. Sensors

The sensors used to measure the pressure in the thrusters and the propellant tank are MS5837-30BA pressure-temperature sensors. There will be one located at the plenum for each thruster and one located at the manifold of the propellant tubing. The sensors themselves are not included in the drawings as they will be attached to the PCB, with wires connecting them to the desired locations. A drawing of the MS587-30BA sensor can be seen in Figure 3.15. Important parameters can be seen in Table 3.2.

The chosen IMU to measure the acceleration provided by the propulsion system is the BMX055 IMU by Bosch. The BMX055 is a 9-axis IMU of movements, rotation and magnetic heading. Within it are three different sensors: a gyroscope, accelerometer and magnetometer. It comes in a housing of the dimensions 3.0 mm x 4.5 mm x 0.95 mm and has 20 pins making it suitable for the propulsion system [12]. By reading the angular acceleration and the forwards acceleration before and after thruster operation, a calculation of the thrust level can be found using the moment of inertia of the Delfi-PQ satellite. However, when doing this calculation one must take into account both rotation and translation caused by thrusting of the propulsion system. This calculation is not within the scope of this report. The IMU will be fixed to the PCB, which should have sufficient available space since both sides of the

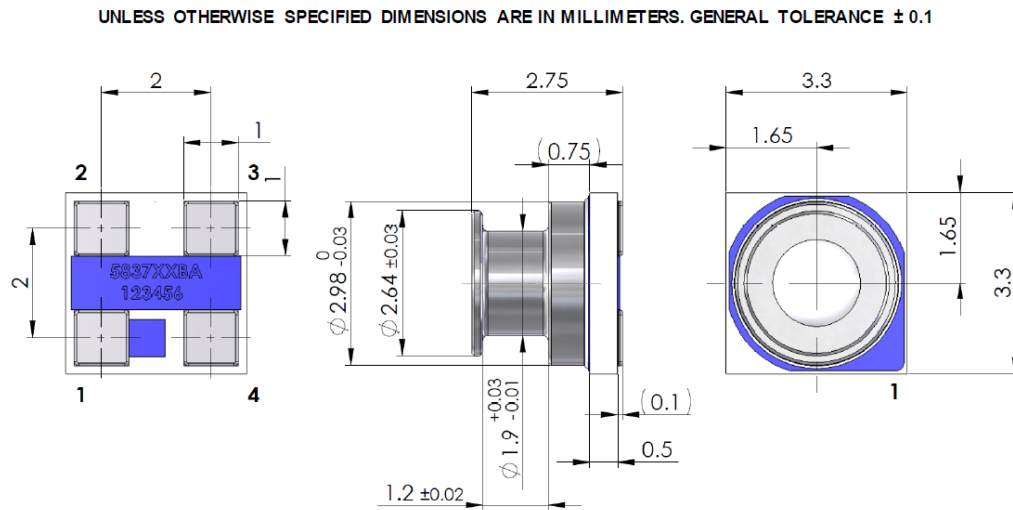


Figure 3.15: The MS5837-30BA pressure sensor [11]

Table 3.2: Operational parameters for the MS5837-30BA pressure and temperature sensor [11]

Parameter	Specification
Volume	3.3 mm x 3.3 mm x 2.75 mm
Resolution	0.2 mbar
Supply voltage	1.5 V - 3.6 V
Operating Pressure	0 bar - 30 bar
Operating Temperature	-20 °C - 85 °C
Interface Type	I <sup>2</sup> C

PCB will be used for electronics. The IMU is shown by the small rectangular block on the top side of the PCB shown in Figure 3.16.

Table 3.3: Operational parameters for the BMX055 IMU [12]

Parameter	Specification
Volume	3.0 mm x 4.5 mm x 0.95 mm
Resolution	See data sheet for resolutions of each sensor [12]
Supply voltage	2.4 V - 3.6 V
Operating Temperature	-40 °C - 85 °C
Interface Type	Digital bidirectional SPI and I <sup>2</sup> C

### 3.9. Flight model design

The complete payload design which would be able to ‘slot’ into the Delfi-PQ satellite is shown in Figure 3.16. This would be the flight model design of the propulsion system. All parts are included in this except the finished PCB design, which would include the pressure sensors, IMU, microcontroller and wiring. The design of the PCB is complex and falls outside the scope of this report. The tubing used as a feed system is also not shown in Figure 3.16, but has sufficient space to connect to each component as shown in the fit test at the start of this chapter.

Finally, a breakdown of the mass estimation for the propulsion system and the components can be seen in Table 3.4. The mass estimation is then compared to the requirement for the total mass of the system given by requirement PROP-SYST-100.

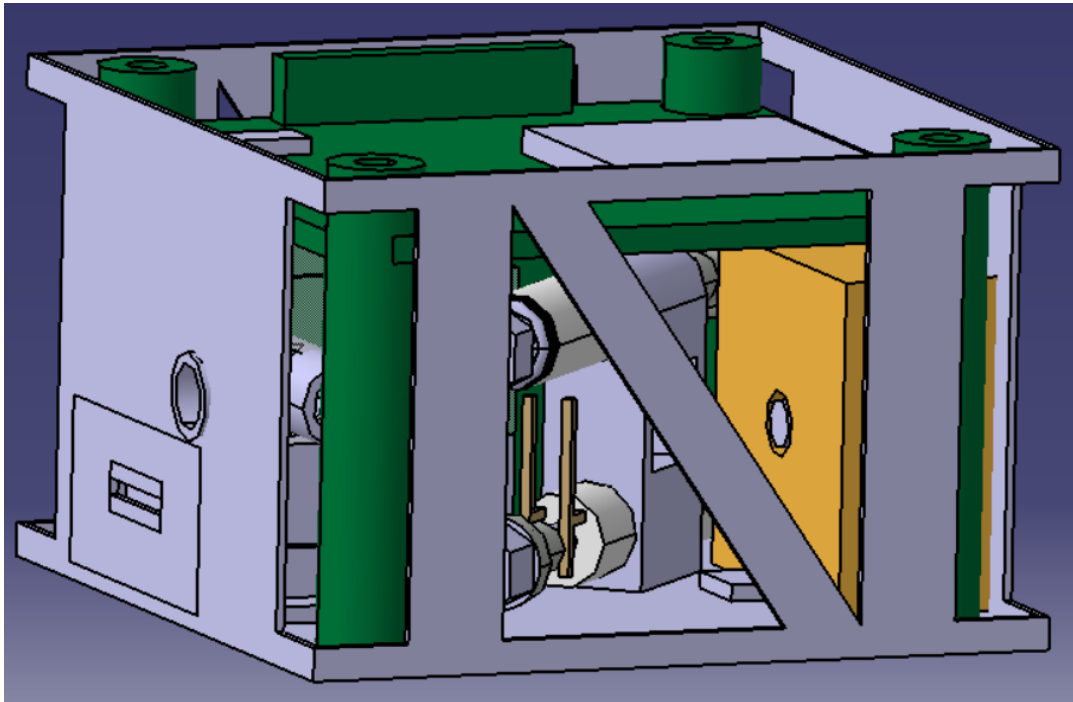


Figure 3.16: Flight model of the propulsion system with all components discussed in this chapter, with the exception of capillary tubing to connect components and PCB electronics.

Table 3.4: Mass estimation for the propulsion system and comparison with PROP-SYST-100

Component	Mass	Comment
Aluminium metal plate	4 g	Estimated using CATIA model
Sensors, PCB & electronics	15 g	From Pallichadath (2018) [30]
VLM & LPM Thrusters	20 g	From Pallichadath (2018)[30]
Valves x2	3.6 g	From Micro-Fluidic Handbook (2013) [31]
Tubing	1 g	For 0.5 m of tubing (weighed 21/3/2018)
Wiring	5 g	Conservative estimate
PEEK Manifold	1 g	Estimated using CATIA model
PEEK Check valve	1.5 g	Estimated using CATIA model
Propellant	0.5 g	See Section 4.2
Delfi-PQ interface structure	5 g	Estimated using CATIA model
Valve support structure	1 g	Estimated using CATIA model
Propellant storage	2 g	Estimated using CATIA model
Contingency	6.4 g	10 percent contingency
<b>Total</b>	<b>69 g</b>	Falls within the 75 g budget

# 4

## Operational Envelope

Now that the physical system has been designed, a performance analysis can be made for the system to select initial operating conditions for the system. This chapter contains the flow diagrams for in-orbit operation of the payload including the definition of the flight modes. Specifically for the VLM testing mode, the switching point between VLM testing phase and the LPM testing phase is required. Now that the initial length of the propellant tubing is determined to be 30 cm in length, calculations can be made on the volume of nitrogen gas used as a pressurant. Furthermore, the initial pressure at which the propellant is stored also needs to be set. The chosen combination of these two variables results in the selection of the switching point between the VLM thruster testing phase and the LPM testing phase. The LPM testing section will be relatively straightforward, as the system will simply open the LPM valve and heat the thruster to the highest possible temperature to provide thrust with the remaining propellant and does therefore not require the same amount of detail in this chapter. The output for this chapter will be the approximations to the change in pressure, mass flow and power required over time. A rough estimate of the thrust over time is also provided at the end of this chapter.

### 4.1. Functional Flow Diagram - Payload

This section breaks down the various functions that need to be performed by the payload to successfully test the VLM and LPM thrusters. Figure 4.1 shows the highest level functional flow diagram which relies on the onboard computer for Delfi-PQ sending signals to the MSP432 microcontroller on the payload to change modes which will be specified in this section.

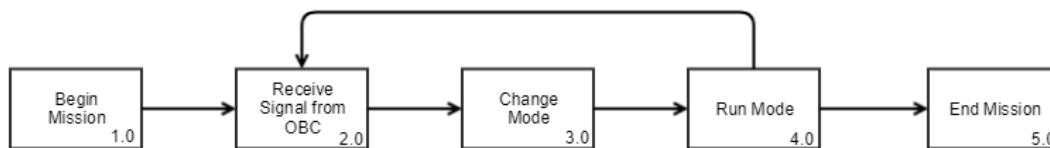


Figure 4.1: Top-level functional flow diagram for the payload demonstrator

The required modes are selected to be the following list of modes, which are to account for any eventuality.

- Start-up Mode
- Idle Mode
- Abort Mode
- Testing Mode

- VLM Testing Mode
- LPM Testing mode
- End-of-life Mode

#### 4.1.1.1. Start-up Mode

The first required mode is the start-up mode, which is the initial starting point for the payload. The system receives a signal from the OBC to initiate microcontroller functions and provide a full system check on both components and sensors. To avoid erroneous readings of the sensors this will be conducted for 1 second at measurement intervals of 10 ms. After this is complete, the system will automatically go into idle mode. The flow diagram for the start-up mode is seen in Figure 4.2.

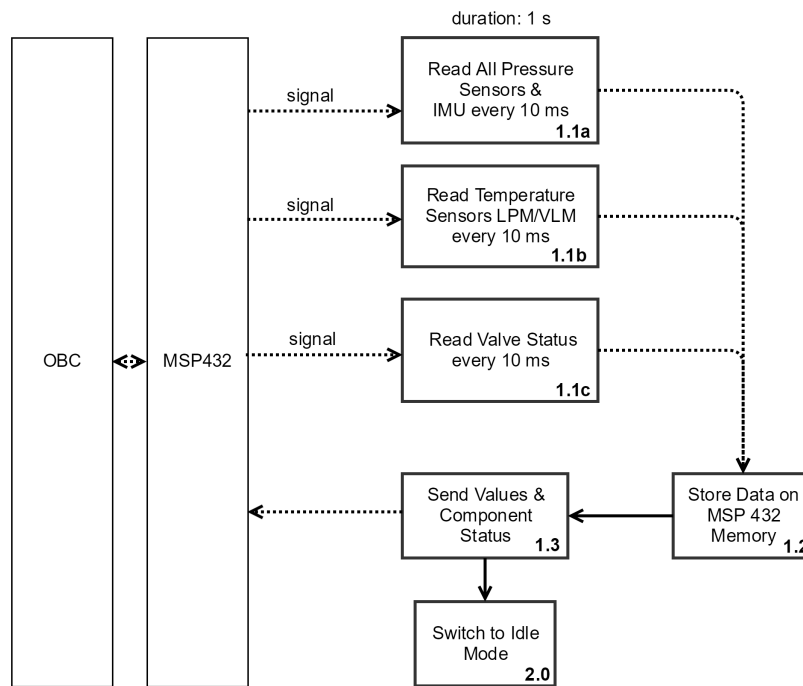


Figure 4.2: The flow diagram for system start-up mode of the propulsion system

#### 4.1.1.2. Idle Mode

The idle mode is used when the system is not actively being used by the satellite. The primary reason for this would be to conserve power on the spacecraft and is also directly asked for in the requirement **PROP-FUN-100**. Only basic information on system welfare is needed. By analysing pressure changes within the tubing in idle mode, the leakage of the system can be measured in this mode. The flow diagram for the idle mode can be seen in Figure 4.3.

#### 4.1.1.3. Abort Mode

Switching to the abort mode could be done in the middle of testing to avoid damage to the propulsion system or spacecraft. Effectively it ends all activities by stopping heating and closing all valves. At the end of this mode, the system is automatically switched to idle mode. The flow diagram for this mode can be seen in Figure 4.4.

#### 4.1.1.4. Testing Mode

The most complex of the modes is the testing mode. This mode will comprise of the VLM and LPM testing modes, which are defined as two different modes. The first is the VLM testing mode which will

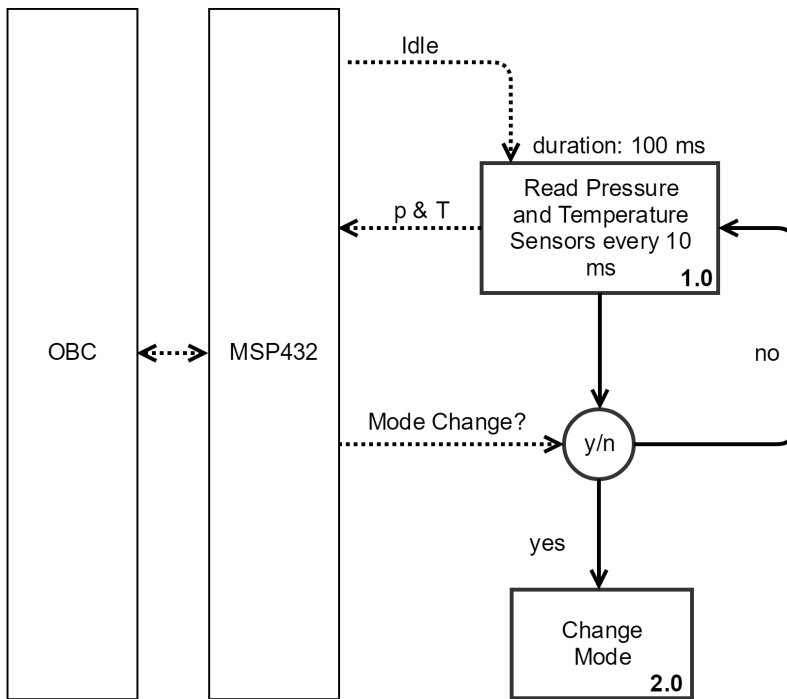


Figure 4.3: The flow diagram for system idle mode of the propulsion system

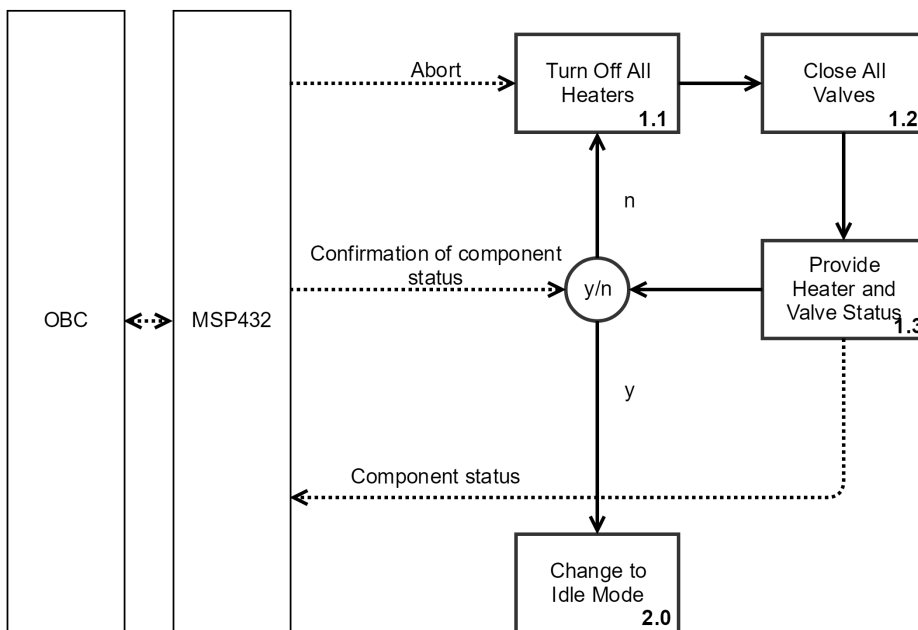


Figure 4.4: The flow diagram for abort mode of the propulsion system

be the first to be initiated by the OBC. Once the pressure has dropped sufficiently, the OBC will send a signal to the MSP432 microcontroller to initialize the LPM thruster. This will be confirmed by the OBC based on the pressure sensors readings on the propulsion system. The VLM testing flow diagram can

be seen in Figure 4.5.

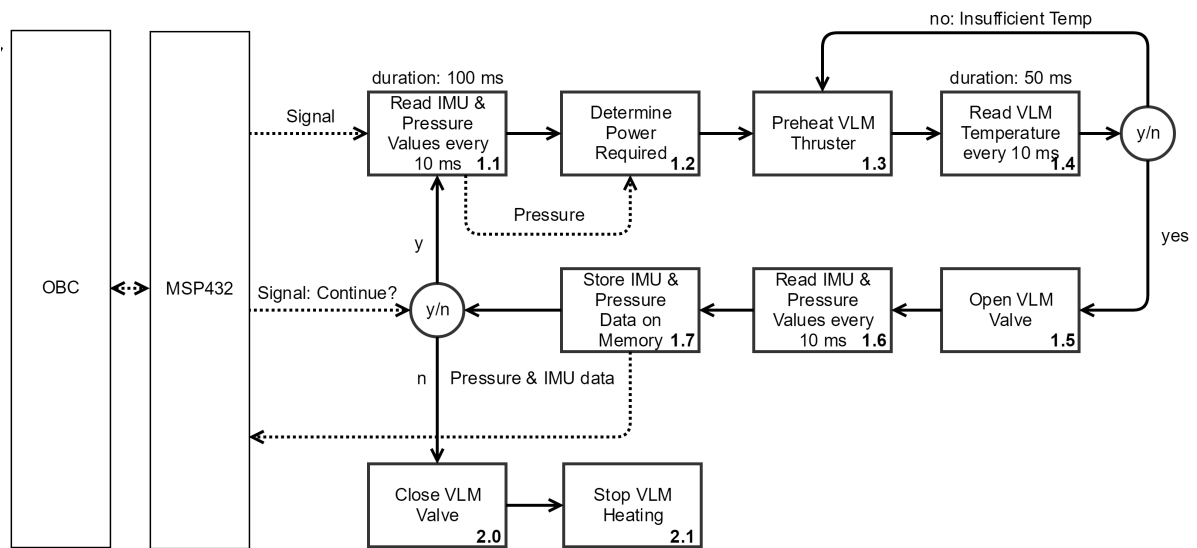


Figure 4.5: The flow diagram for VLM testing mode of the propulsion system

The flow diagram for the LPM testing mode can be seen in Figure 4.6. The main difference for the LPM mode is that the required power for the heaters is not influenced by the pressure readings on the sensor.

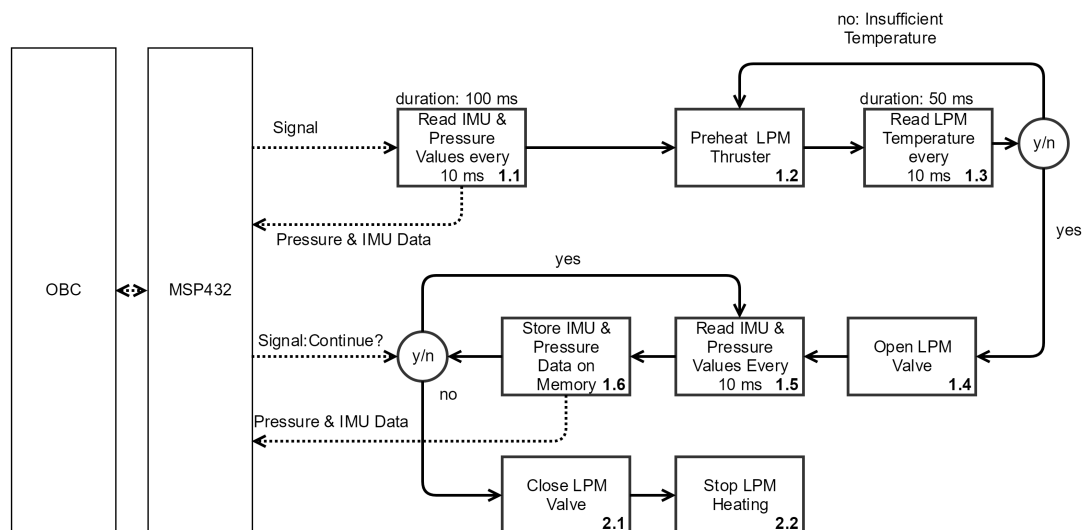


Figure 4.6: The flow diagram for LPM testing mode of the propulsion system

#### 4.1.5. End-of-life Mode

The final mode is the end-of-life mode, which is required to ensure that the system is fully empty and cannot leak into the rest of the satellite. The flow diagram for the EOL mode can be seen in Figure 4.7.

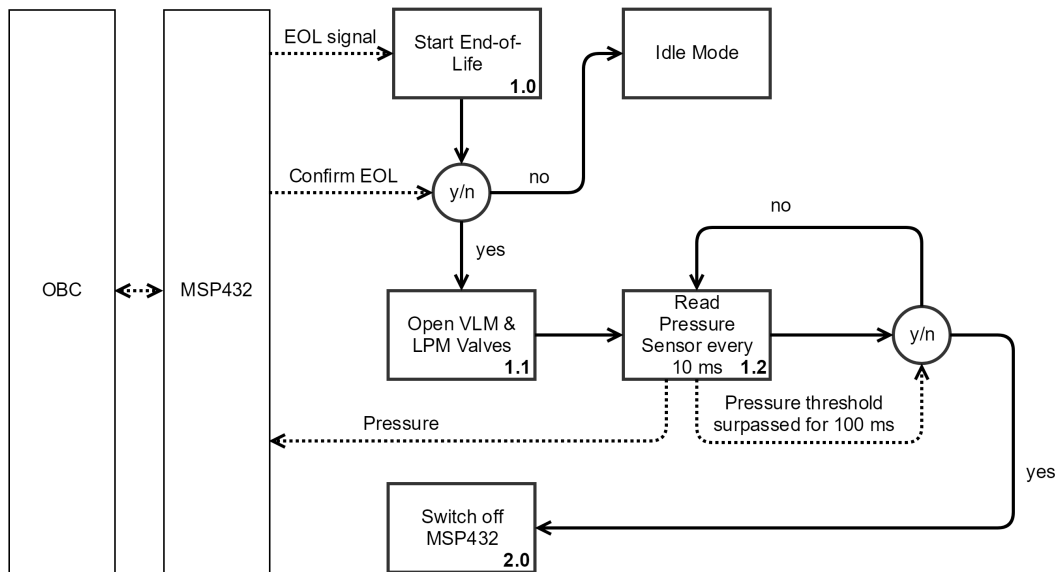


Figure 4.7: The flow diagram for the end-of-life mode of the propulsion system

## 4.2. VLM Thruster: Initial Nitrogen Pressure and Volume

This section will explore the initial conditions for the propulsion system that adhere to the thrust and power requirements. For example, the initial pressure and volume of nitrogen influence the mass flow of the propellant within the tubing over time, but also the power input required, thrust time and pressure over time. The propellant (water) is in liquid phase and therefore is assumed to be fully incompressible, which means that the pressure of the liquid water is deemed to be equal to the pressure of the nitrogen. Isothermal expansion of the gas within the propellant tubing is deemed an acceptable assumption because the expansion of nitrogen volume occurs slowly within a larger system (Delfi-PQ) which has a thermal control system. Changes in temperature within the tubing adjust continuously to the satellite temperature. The other assumptions made in this section are:

- The pressure in the tubing is equal to the pressure in the thruster (blowdown mode for the thruster)
- No mixing between propellant and pressurant
- Propellant is expelled before the pressurant during operation of the propulsion system
- Ideal gas law assumption of no friction between pressurant molecules
- No boundary layer effects accounted for which is especially of importance for the nozzle throat area
- Liquid propellant is fully incompressible
- Isothermal expansion of the gas within the propellant tubing
- Constant values for specific heats

Using these assumptions, the pressure, mass flow and propellant mass over time within the propellant tubing are calculated first. The constants for this calculation are given in Table 4.1.

The total volume of the propellant storage tube is easily calculated using Equation 4.1. The input for the initial volume of nitrogen will be given in percentage of the total volume of the propellant storage tube. A table for the inputs to this calculation can be seen in Table 4.2.

$$V_{tube} = \frac{l \cdot \pi \cdot d^2}{4} = 5.81 \cdot 10^{-7} m^3 \quad (4.1)$$

Table 4.1: Various constants required in this chapter

Variable	Value	Unit	
$A_t$	$4.5 \cdot 10^{-9}$	$m^2$	Nozzle throat area
$l$	0.30	$m$	Propellant tubing length
$R_{water}$	461.67	$J/(kgK)$	Gas constant water vapour
$\Gamma_{water}$	0.67	–	Van der Kerckhoven constant water vapour
$\rho_{water}$	997	$kg/m^3$	Density liquid water
$d$	$1.57 \cdot 10^{-3}$	$m$	Inner diameter propellant tubing
$T_0$	283	$K$	Ambient temperature in satellite
$h_{vap}$	2256	$kJ/kg$	Heat of vaporization water vapour
$c_{p_l}$	4187	$J/K/kg$	Specific heat of liquid water
$c_{p_v}$	1996	$J/K/kg$	Specific heat of water vapour

Table 4.2: Inputs for the calculations on the operational envelope

Input	Comment	Unit
$V(0)$	The initial volume of nitrogen, input as function of $V_{tube}$	$m^3$
$p(0)$	Initial pressure of nitrogen	$Pa$
$T_c$	Temperature in thruster	$K$

An overview of the operation of the system can be seen in Figure 4.8.

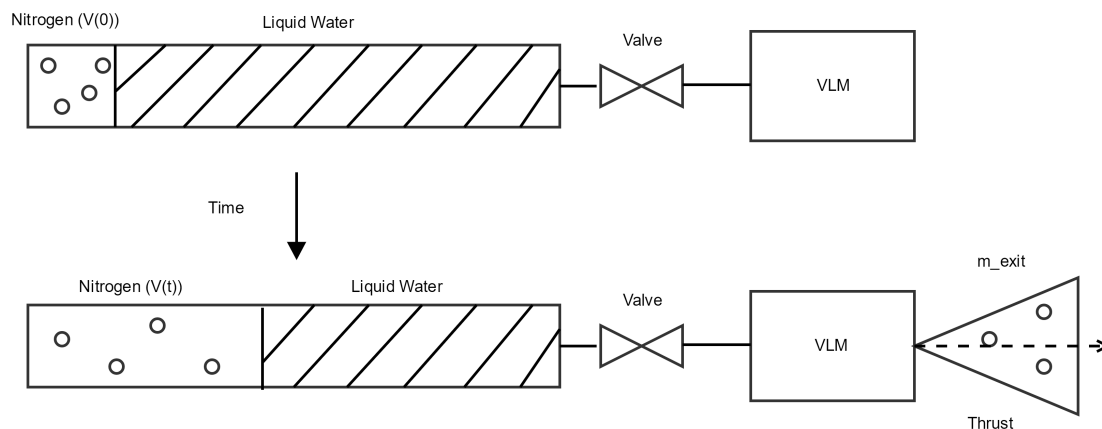


Figure 4.8: An overview of the operations of the system.

Now assuming isothermal expansion within the propellant storage tube and using the ideal gas law for the pressure of the nitrogen results in Equation 4.2. Here  $V_1$  and  $p_1$  are the volume and pressure in state one, while  $V_2$  and  $p_2$  are the volume and pressure in state two.

$$p_1 \cdot V_1 = p_2 \cdot V_2 \quad (4.2)$$

Equation 4.2 can be rewritten as Equation 4.3, where  $V(t)$  is the volume of nitrogen at time  $t$  and  $p(t)$  is the pressure within the tubing at time  $t$ .

$$p(t) = \frac{V(0)}{V(t)} \cdot p(0) \quad (4.3)$$

However, the volume for the nitrogen will increase over time because water will leave the propellant tubing. The mass of the propellant which has left the tubing at time  $t$  is denoted by  $m_{exit}(t)$ . This is seen in Equation 4.4.

$$V(t) = V(0) + \frac{m_{exit}(t)}{\rho_{water}} \quad (4.4)$$

Next the mass flow of water vapour leaving the thruster through the nozzle is calculated by Equation 4.5 and Equation 4.6.

$$\dot{m} = \frac{p_c \cdot A_t}{c^*} \quad (4.5)$$

$$c^* = \frac{\sqrt{R \cdot T_c}}{\Gamma} \quad (4.6)$$

Combining these equations results in Equation 4.7 with  $p_c$  being equal to  $p(t)$ ,  $A_t$  being equal to the area of the throat of the thruster,  $T_c$  equal to the temperature in the thruster,  $R$  is the gas constant of water vapour and  $\Gamma$  the van der Kerckhoven constant for water vapour.

$$\dot{m}(t) = \frac{p(t) \cdot A_t \cdot \Gamma}{\sqrt{R \cdot T_c}} \quad (4.7)$$

Equation 4.7 is the first of the relations between mass flow and pressure for the final calculation.

$$p(t) = \frac{V(0)}{V(0) + \frac{m_{exit}(t)}{\rho_{water}}} \cdot p(0) \quad (4.8)$$

Equation 4.8 is the second relation between mass flow and pressure which is required to plot the pressure change over time. This is obtained by combining Equation 4.3 and Equation 4.4. However, the value for the chamber temperature in the thruster is yet to be selected. Two options will now be analysed to define that. The first is simply by using a constant temperature for the heater.

#### 4.2.1. Option 1: Constant Thruster Temperature

The selection of constant temperature to the thruster can be applied in this case as it will likely be necessary to vary the power input to the thruster anyway due large change in mass flow of the propulsion system over time. By taking the thruster temperature as independent from the pressure and mass flow, the calculation is somewhat simplified. The system is reduced to two equations (4.7 and 4.8) and two unknowns ( $p(t)$  and  $\dot{m}(t)$ ). The value for  $T_c$  is chosen to be 600 K, which is within the range of temperatures used in previous VLM tests within TU Delft[4]. If selecting a higher chamber temperature, the mass flow reduces. However, lower mass flow increases the operation time of the system, which allows for more testing. Furthermore, increasing temperature does not require a large increase power, as will be explained in Equation 4.10, the largest amount of power goes into vaporizing liquid water. Raising the temperature of water vapour costs little power relative to the heat of vaporization required.

The first step to solving Equations 4.7 and 4.8 is calculating the mass leaving the system. The mass of the propellant leaving the system over time is calculated using a for-loop in Matlab. It can be approximated by multiplying a time step  $\Delta t$  with the mass flow  $\dot{m}$  at certain time  $t$  and adding this to the previous value of  $m_{exit}$ , which can be seen in Equation 4.9. For this calculation a time step of 1 ms was used. The initial value for the mass flow is calculated by using Equation 4.7.

$$m_{exit}(i) = m_{exit}(i-1) + \dot{m}(i) \cdot \Delta t \quad (4.9)$$

What follows is graphs of the pressure within the propellant tubing and mass flow over time. To investigate the effect of the variables of initial pressure and initial nitrogen volume, both the pressure and the mass flow graphs were plotted with one initial nitrogen volume and multiple initial pressures. This was then followed by graphs showing one initial pressure and multiple initial nitrogen volumes. Higher initial pressure results in translation of the mass flow curve upwards, while higher initial volume of nitrogen results in a smaller decrease in mass flow over time and a higher final value for the mass flow.

**Algorithm 1** Constant Temperature Pseudocode

```

1: procedure Constant Temperature
2:   time = 0 :  $\Delta t$  : 1200
3:    $p(1) = p_0$ 
4:   calculate  $m(1)$ 
5:    $m_{exit}(1) = 0$ 
6:   loop:
7:   for  $i = 2$ :length(t)
8:      $p(i) = V_0 \cdot p_0 / (V_0 + m_{exit}(i-1)/\rho)$ 
9:      $m(i) = p(i-1) \cdot A_t \cdot \Gamma / \sqrt{R \cdot T_c}$ 
10:     $m_{exit}(i) = m_{exit}(i-1) + \dot{m}(i) \cdot \Delta t$ 
11:  end

```

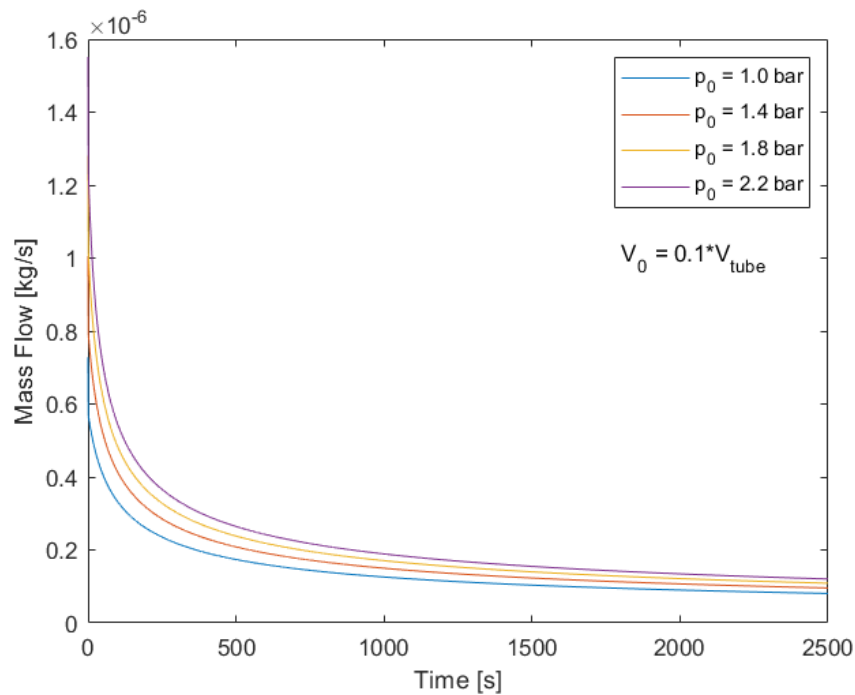


Figure 4.9: Mass flow of the propulsion system over time at different initial pressures with  $V(0) = 0.1 \cdot V_{tube}$  and  $T_c = 600K$

Another important graph for the operational envelope is the power which is required to keep the thruster temperature constant over time. This will vary over time because the mass flow reduces as the system loses pressure over time. The power which needs to be flowing into the propellant over time can be calculated using Equation 4.10 and is shown in Figure 4.14. There are three parts to this equation: the power required to vaporize the liquid when the propellant is at the vaporization temperature, the power required to heat the liquid water to the vaporization temperature and the power required to heat the water vapour to the desired chamber temperature. In Equation 4.10  $h_{vap}$  is the heat of vaporization, while  $T_{vap}$  is the vaporization temperature of the propellant,  $c_{pl}$  is the heat capacity of liquid water and  $c_{pv}$  is the heat capacity of water vapour. It is important to note that the efficiency of heat transfer needs to be found by experiment, which means that this calculation only provides the power that needs to be received by the water and not the input power.

$$\dot{Q} = \dot{m} \cdot (h_{vap} + c_{pl} \cdot (T_{vap} - T_0) + c_{pv} \cdot (T_c - T_{vap})) \quad (4.10)$$

The vaporization temperature changes over time due to the change in pressure of the system. The relationship between the vaporization pressure and the temperature of the fluid is given by the Clausius-Clapeyron relationship, which is defined in Equation 4.11. Variables are defined in Table 4.3.

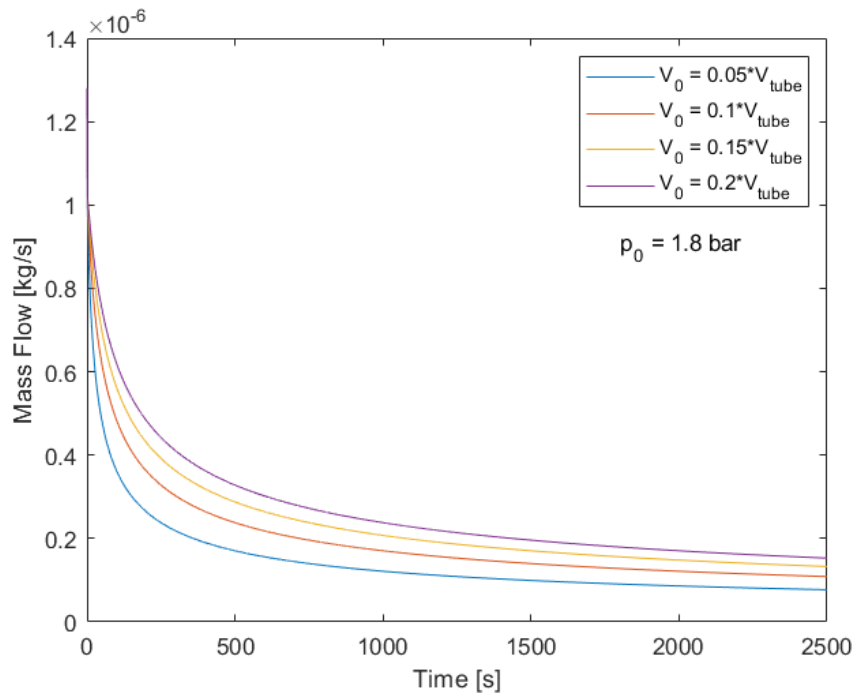


Figure 4.10: Mass flow of the propulsion system over time at different initial volumes of nitrogen with  $p(0) = 1.8\text{bar}$  and  $T_c = 600\text{K}$

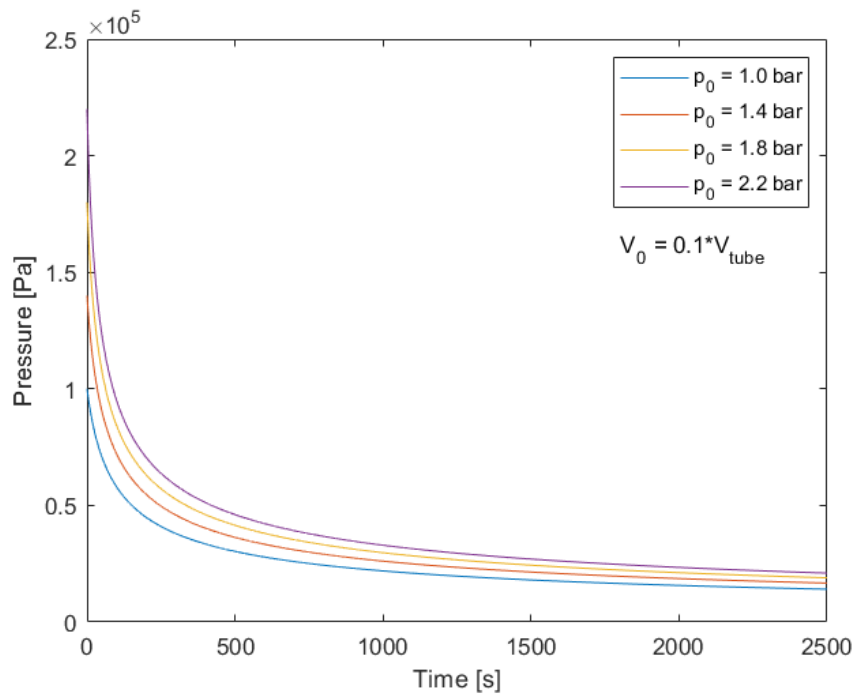


Figure 4.11: Pressure of the propulsion system over time at different initial pressures with  $V(0) = 0.1 \cdot V_{tube}$  and  $T_c = 600\text{K}$

$$\frac{R}{\Delta h_{vap}} \ln\left(\frac{p_1}{p_2}\right) = \frac{1}{T_2} - \frac{1}{T_1} \quad (4.11)$$

Rewriting the general relationship given in Equation 4.11 for the purpose of this report, the variables

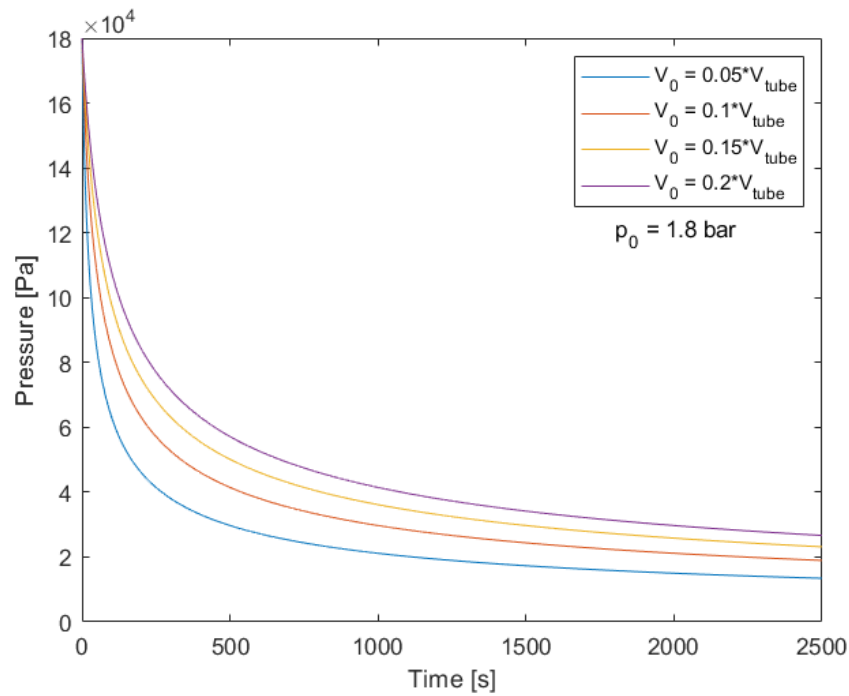


Figure 4.12: Pressure of the propulsion system over time at different initial volumes of nitrogen with  $p(0) = 1.8\text{bar}$  and  $T_c = 600\text{K}$

$p_1$  and  $T_1$  are set to the boiling point of water (373 K) at 1 atm. Variables  $T_2$  and  $p_2$  are the vaporization temperature ( $T_{vap}$ ) and the pressure  $p(t)$  respectively. Finally,  $\Delta h_{vap}$  has the unit of  $J/mol$  in this equation. Values for these constants can be seen in Table 4.3.

Table 4.3: Inputs for the Clausius-Clapeyron relation

Variable	Value	Unit
$T_1$	373	$K$
$p_1$	$1.013 \cdot 10^5$	$Pa$
$R$	8.314	$J/K/mol$
$\Delta h_{vap}$	$40.65 \cdot 10^3$	$J/mol$

Equation 4.11 can then be rewritten to find an expression for  $T_{vap}$ . The equation for the vaporization temperature as a function of the pressure is given by Equation 4.12.

$$T_{vap} = \frac{T_1 \cdot \Delta h_{vap}}{T_1 \cdot R \cdot \ln\left(\frac{p_1}{p}\right) + \Delta h_{vap}} \quad (4.12)$$

Using Equation 4.12 together with Equation 4.10 results in the required power flow into the propellant during operation of the VLM thruster. This can be seen in Figure 4.14.

Finally, there is one more graph of importance to the operational envelope. The mass of the remaining propellant is important to determine the length of thrust time of the VLM thruster such that there is sufficient propellant remaining to test the LPM thruster for 200 seconds. This is done by calculating the initial mass of the propellant in the tubing at time  $t = 0\text{s}$  and subtracting the variable  $m_{exit}(t)$  to give the remaining propellant over time.

$$m_w(0) = (V_{tube}(0) \cdot -V(0)) \cdot \rho_{water} \quad (4.13)$$

$$m_w(t) = m_w(0) - m_{exit}(t) \quad (4.14)$$

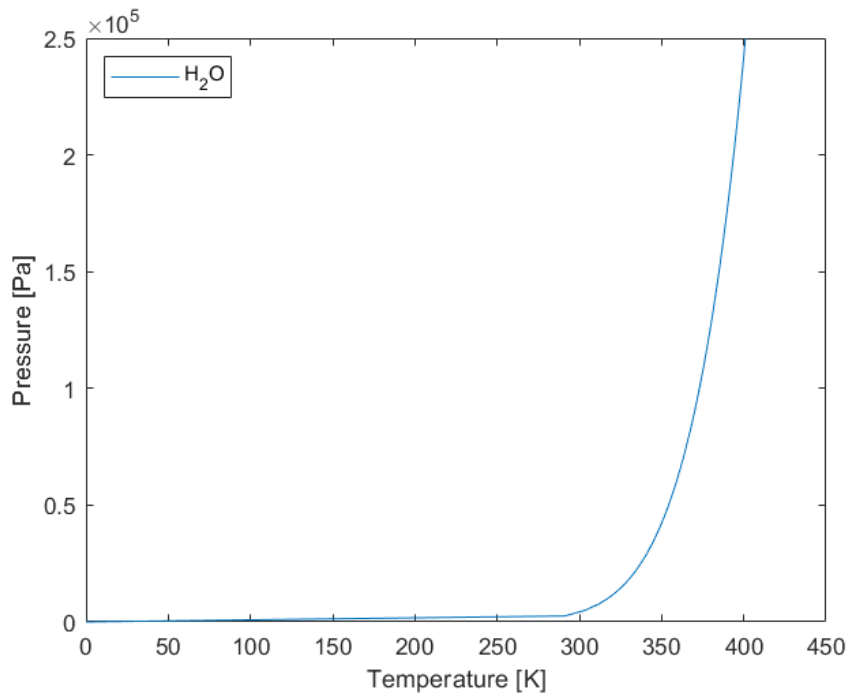


Figure 4.13: Vaporization temperature to pressure graph using the Clausius-Clapeyron relation

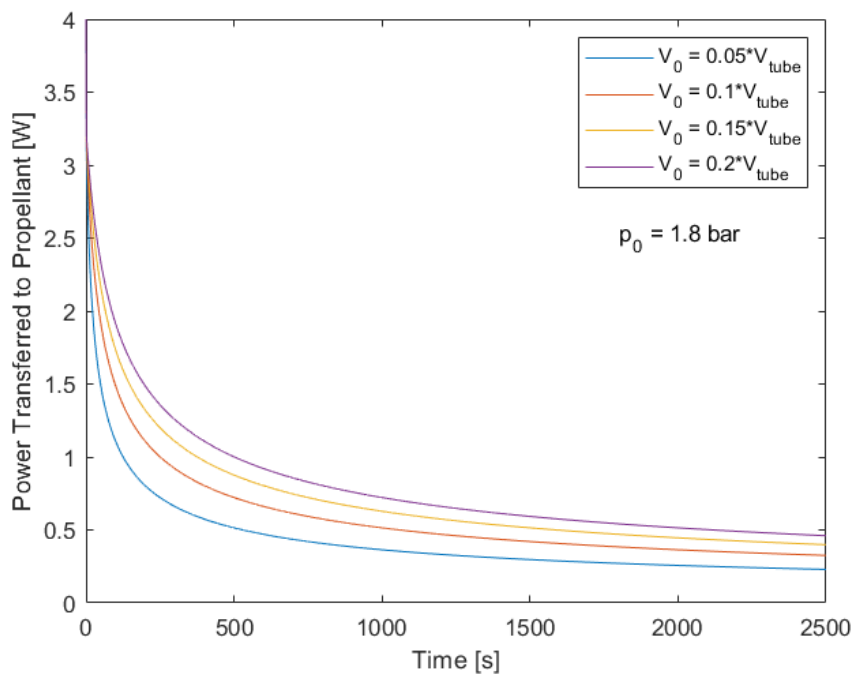


Figure 4.14: Power transfer required into propellant over time at different initial volumes with  $p(0) = 1.8 \text{ bar}$  and  $T_c = 600 \text{ K}$

The plot for Equation 4.14 over time can be seen in Figure 4.15.

#### 4.2.2. Option 2: Provide Minimum Vaporization Temperature

The second option concerning the temperature input for the propulsion system is to provide just enough power to the system to vaporize the propellant at each pressure during operation of the system.

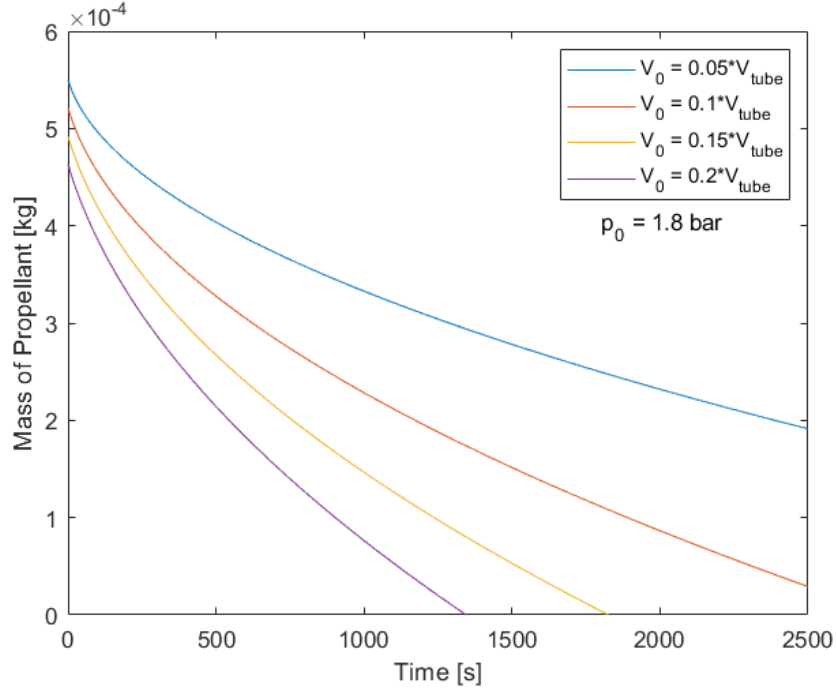


Figure 4.15: Propellant mass over time at different initial volumes with  $p(0) = 1.8 \text{ bar}$  and  $T_c = 600 \text{ K}$

However, this is more complicated as it requires a third equation with  $T_c$  as an unknown. The third equation is found by substituting  $T_{vap}$  by  $T_c$  in Equation 4.12. Since all three are nonlinear, a numerical solution is the only possibility.

This now gives a system of three equations (4.15, 4.16 and 4.17) with three unknowns where the variables are  $T_c$ ,  $p$  and  $\dot{m}$ . This system of equations solves for the pressure, mass flow and temperature over time when the temperature is set exactly to the temperature required for propellant vaporization.

$$p(t) = \frac{V(0)}{V(0) + \frac{m_{exit}(t)}{\rho_{water}}} \cdot p(0) \quad (4.15)$$

$$\dot{m} = \frac{p(t) \cdot A_t \cdot \Gamma}{\sqrt{R \cdot T_c}} \quad (4.16)$$

$$T_c = \frac{T_1 \cdot \Delta h_{vap}}{T_1 \cdot R \cdot \ln\left(\frac{p_1}{p(t)}\right) + \Delta h_{vap}} \quad (4.17)$$

This was done by calculating the initial value of  $T_c$  based on the initial value of  $p_0$  using Equation 4.11. The initial value of  $p_0$  and  $T_c$  allowed for calculation of the initial value for the mass flow at  $t = 0.001 \text{ s}$ . Similarly to the calculation with constant temperature, an iterative technique was used with a small time step  $\Delta t$ . Since the mass leaving the system during the time step  $\Delta t$  is equal to the mass flow multiplied by  $\Delta t$ . What follows from the results of this method is that only a slightly higher mass flow is achieved by varying the temperature to match the vaporization temperature. This makes sense, because Equation 4.16 shows that lower temperature is inversely proportional to the square of the mass flow. The comparison between the two options be seen in Figures 4.16 and 4.17.

The solution can be verified by reading the pressure sensor within the tubing during an experimental test. After reading the pressure sensor, the Clausius-Clapeyron relation can be used to set the temperature to the vaporization pressure. However, changing the temperature will cause the pressure in the system to change, which will require another smaller change in temperature, resulting in an iterative process. A number of tests will be required to fully map the temperatures required for vaporization at the pressure ranges within the system and then the effectiveness of using a variable temperature can be properly assessed. The test plan for the propulsion system will be addressed in Chapter 5.

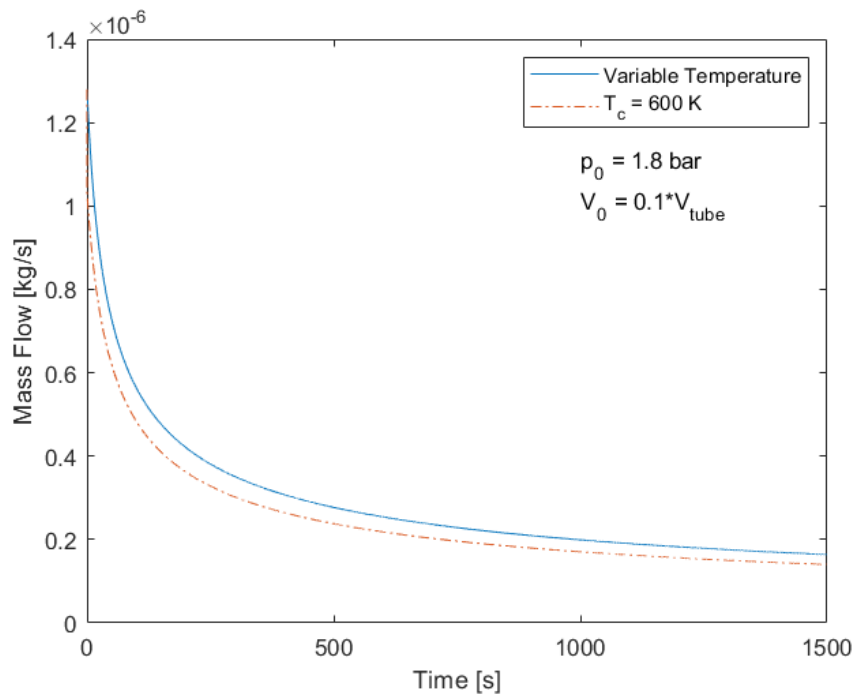


Figure 4.16: Comparison of mass flows over time using a variable temperature input equal to the vaporization temperature and a constant temperature of 600 K

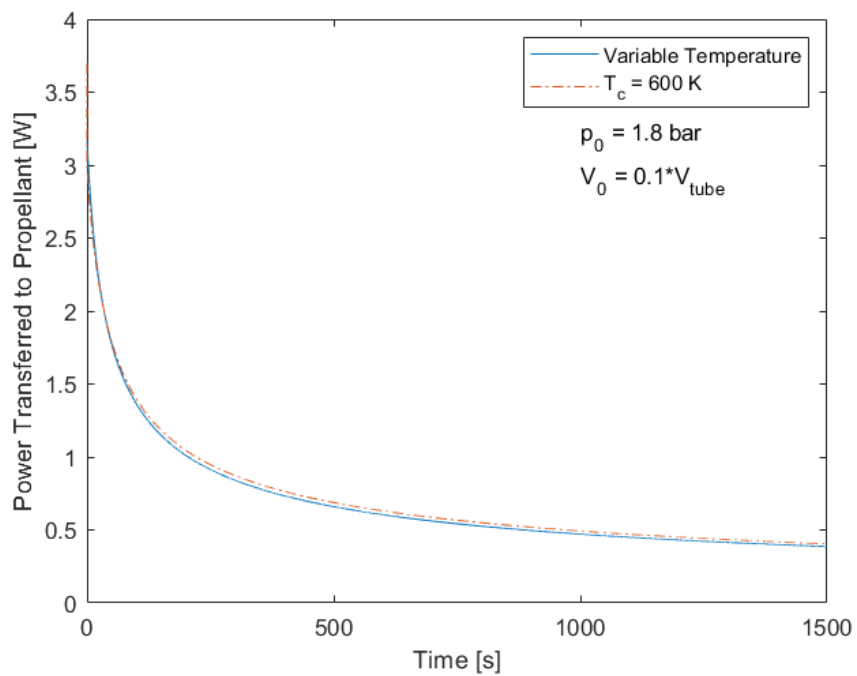


Figure 4.17: Comparison of power transfer required to the propellant over time using a variable temperature input equal to the vaporization temperature and a constant temperature of 600 K

### 4.3. Final Operational Envelope

First a choice must be made on whether to vary the temperature over time to match the vaporization temperature or to keep it constant. By looking at Figures 4.16 and 4.17 it can be seen that using variable temperature set to be as close as possible to the vaporization temperature without going beneath it, the mass flow is slightly higher. The difference between the two methods is small though and the input power must be varied in both cases. To keep the temperature within the system lower and in order to avoid possible overheating of components, the lower variable temperature method is selected to be the input method for the temperature  $T_c$ . The method of selecting the initial variables  $p_0$  and  $V_0$  was done by looking at three graphs. A nice combination needs to be found between high mass flow (which results in higher thrust), the mass of propellant over time (which allows for longer VLM operating time) and low power. By increasing the initial pressure of the nitrogen ( $p_0$ ) the mass flow increases, however the required power level also increases. The mass of the propellant also decreases faster, making the operational time of the VLM shorter. By increasing the initial volume of the nitrogen ( $V_0$ ), the mass flow reduces less over time, the power also reduces less over time and the initial amount of propellant is reduced, which results in shorter operating times for the VLM. The parameter  $p_0$  needs to be set such that the initial power to be transferred into the propellant does not exceed the maximum operating power set by the requirement in **PROP-FUN-100**. However, the efficiency of the heat transfer from the heating unit to the propellant is unknown and needs to be found experimentally. This initial power requirement is independent of  $V_0$  and can therefore be selected first. Without knowing the heating efficiency, an assumption of 60 percent efficiency in heat transfer is made. This gives an initial pressure set at 1.1 bar as this corresponds to a power transfer of 2.11 W, which should adhere to the maximum 4 W requirement.

A higher initial volume  $V_0$  allows higher mass flows and thus higher thrust to be achieved throughout operation of the VLM.  $V_0$  is selected based on the minimum thrust requirement **PROP-PERF-210** of 0.12 mN. At the switching point between the VLM and LPM, the expected thrust seen in Figure 4.24 must exceed 0.12 mN. The other consideration is that there is 0.2 g of propellant remaining to run the LPM testing phase. 0.2 grams of water allows for 200 seconds of testing for the LPM, as previous tests on the LPM show the mass flow for the LPM to be approximately 1 mg/s. Therefore,  $V_0$  and VLM thruster time ( $t_{VLM}$ ) both need to be selected together. By selecting a  $V_0$  of  $0.12V_{tube}$  with  $t_{VLM}$  set to 1200 s both of these requirements are met. Filling the volume of the capillary tube with 12 percent nitrogen should also be achievable in a practical sense. Using these values for initial pressure and nitrogen volume, this corresponds to a switching point between the VLM and LPM where the pressure is equal to 0.201 bar.

Table 4.4: Final values for the operational envelope of the propulsion system

Variable	Value	Unit
$T_c$	Option2: $T_{vap}$	K
$p_0$	$1.1 \cdot 10^5$	Pa
$V_0$	$0.12 \cdot V_{tube}$	$m^3$
$t_{VLM}$	1200	s

Another graph which could be of importance to the operations of the system is the amount of power required at a certain pressure during operation. The microcontroller will read the pressure sensor and will need to determine what power to send to the heater based on the pressure reading. This relationship can be seen in Figure 4.23.

Finally, a very rough estimate on the expected thrust provided by the VLM thruster can be calculated based on the mass flow obtained with this specific operational envelope. Equation 4.18 is used for this calculation. In which the specific impulse at 550 K is found from literature. A specific impulse of 94.9 s at 550 K is taken from Cervone et al. (2017), which is obtained from experiments on the VLM thruster [4]. However, because the average chamber temperature in this case is 342 K, the average specific impulse will be lower. This can be approximated by realising that the specific impulse is proportional to the square root of the chamber temperature. Using this approximation for the specific impulse at 342 K gives an estimated value of 75 seconds, which provides an indication towards the thrust level

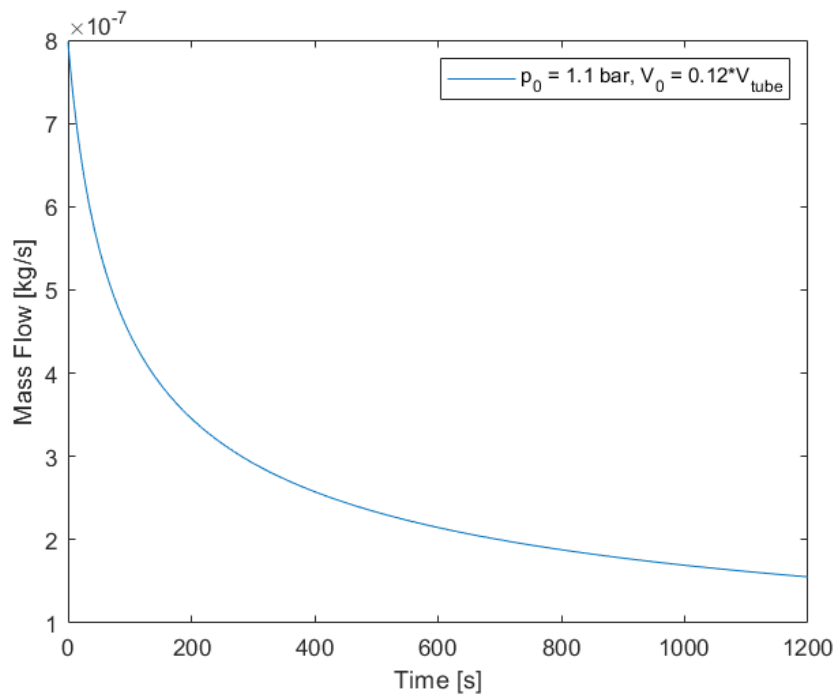


Figure 4.18: Mass flow over time with operational envelope inputs as specified in Table 4.4.

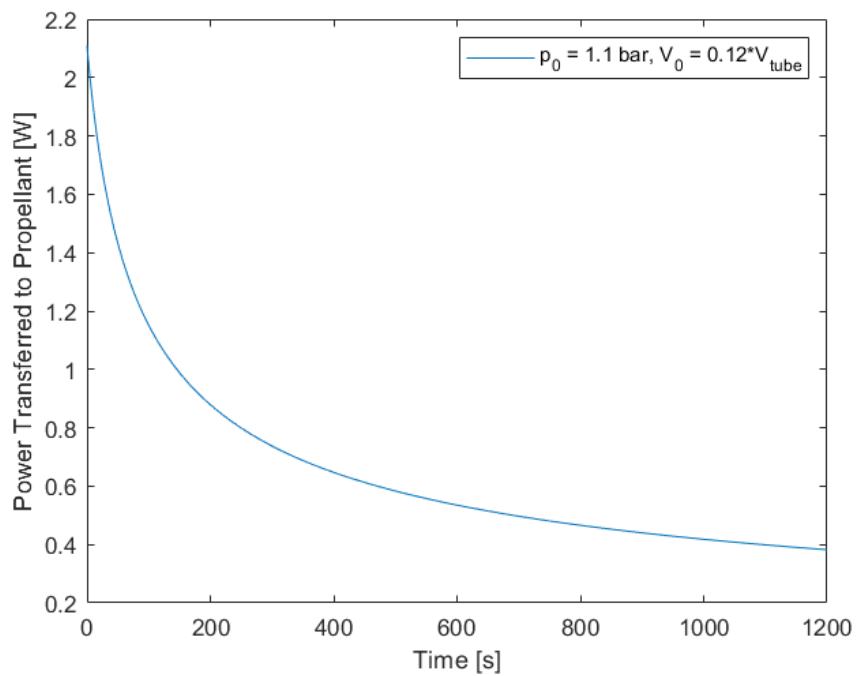


Figure 4.19: Power required to flow into propellant over time with operational envelope inputs as specified in Table 4.4.

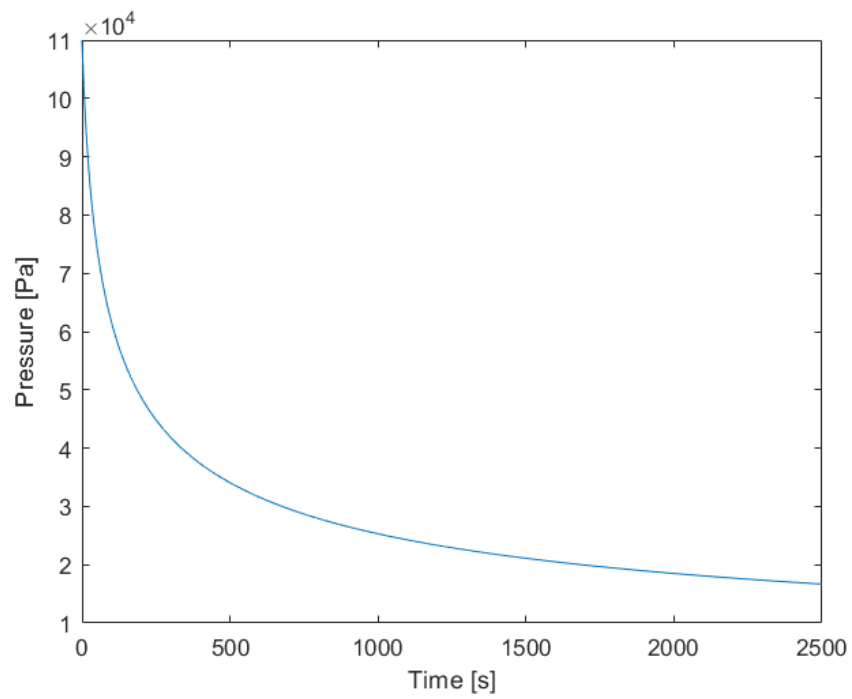


Figure 4.20: Pressure over time with operational envelope inputs as specified in Table 4.4.

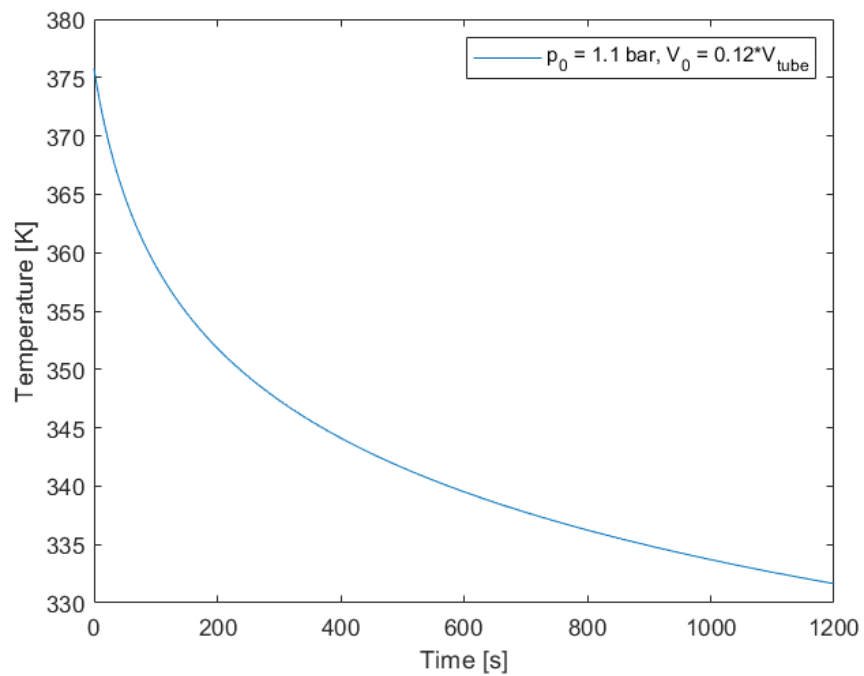


Figure 4.21: Temperature over time with operational envelope inputs as specified in Table 4.4.

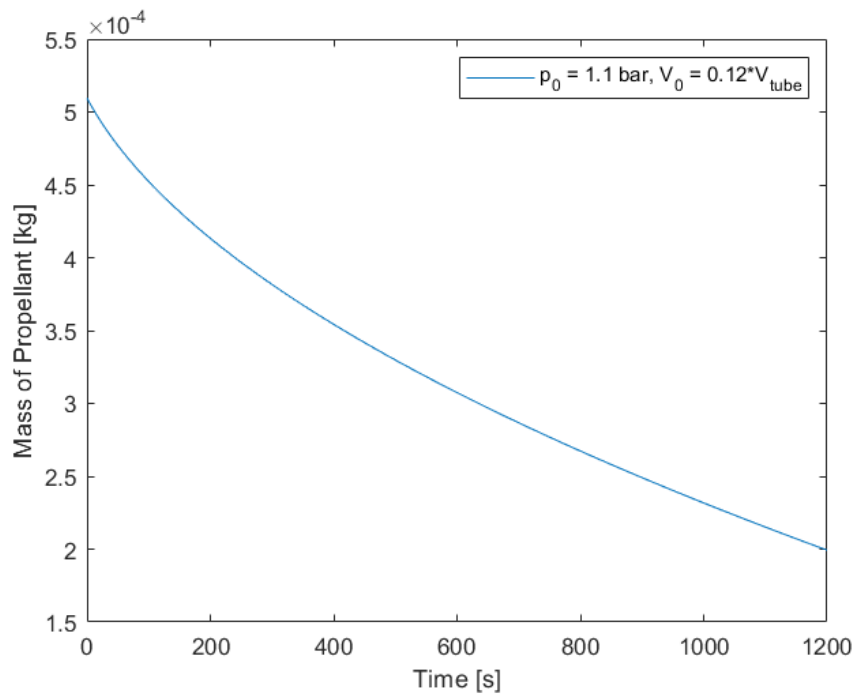


Figure 4.22: Propellant mass over time with operational envelope inputs as specified in Table 4.4.

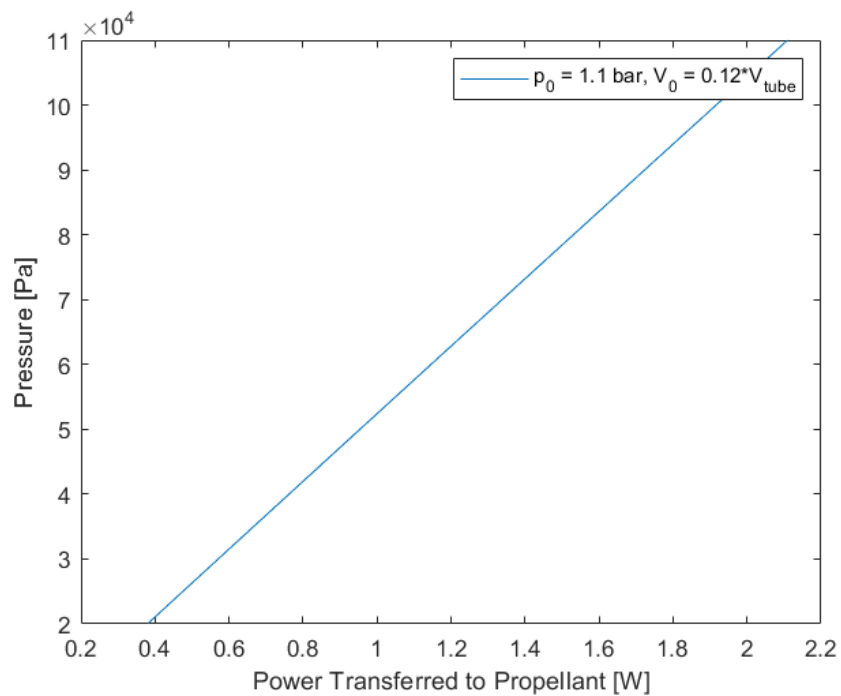


Figure 4.23: The power required to flow into the propellant at each pressure within the system using the operational envelope inputs as specified in Table 4.4.

and profile of the propulsion system.

$$F_T = \dot{m} \cdot I_{sp} \cdot g_0 \quad (4.18)$$

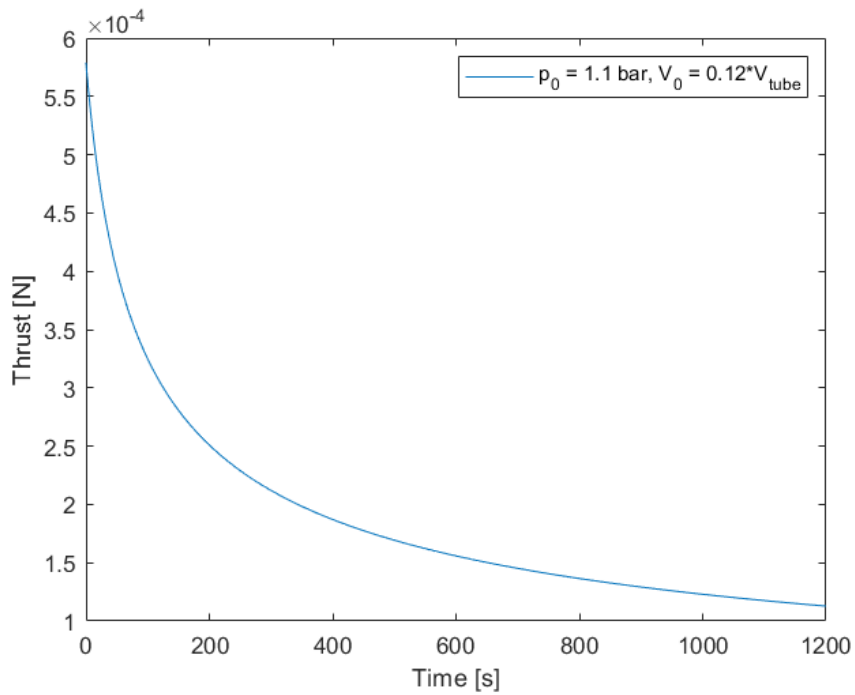


Figure 4.24: Projected thrust over time with operational envelope inputs as specified in Table 4.4.

With the chosen operational envelope described in this section, requirements **PROP-PERF-200**, **PROP-PERF-210** and **PROP-FUN-100** are satisfied. However, choices for the operational envelope concerning **PROP-PERF-200** and **PROP-PERF-210** were made based on a very rough estimate of the thrust provided by the system. The thrust will need to be found experimentally to confirm the chosen operational envelope adheres to the requirements. Similarly for **PROP-FUN-100**, the chosen operational envelope adheres to the requirement under the assumption of 60 percent heater efficiency, which needs to be confirmed experimentally.

# 5

## Design Verification and Testing

### 5.1. Verification of Design

Verifying that the final design does indeed adhere to the requirements set at the start of this report is the final step of this thesis. Each requirement is taken individually and given a method of verification. The four types of requirement verification are: test, analysis, inspection and review of design. All verification tests will be further described in Section 5.4.

Table 5.1: Verification methods of requirements

Identifier	Requirement	Verification
PROP-SYST-100	The total wet mass of the propulsion system at launch shall not be higher than 75 g.	Inspection
PROP-SYST-200	The total size of the propulsion system shall be within 42 mm x 42 mm x 30 mm (including thrusters, valves, electronics board, harness, connectors & propellant storage tube).	Inspection
PROP-SYST-300	The peak power consumption of the propulsion system during ignition or heating shall be not higher than 4 W and duration shall not be longer than <TBD> s per day.	Test
PROP-SYST-400	The maximum amount of propulsion system data that can be stored in the memory storage unit on board the satellite is <TBD> GB.	Inspection
PROP-SYST-500	The critical mission lifetime of the propulsion system shall be equal to at least 3 months.	Analysis
PROP-SYST-600	The time available for the development of the propulsion system is <TBD> months	Review of design
PROP-PERF-100	The first prototype shall be a technology demonstration.	Review of design
PROP-PERF-200	The thrust provided by the propulsion system shall be 3 mN as a maximum.	Test
PROP-PERF-210	The thrust provided by the propulsion system shall be at least 0.12 mN	Test
PROP-PERF-300	The maximum leak rate shall be <TBD> at maximum operating pressure.	Test
PROP-PERF-400	The micro-propulsion system shall operate on a single unregulated supply voltage of 3 [VDC] to 4.1 [VDC].	Review of design, Test
PROP-FUN-100	The micro-propulsion system shall have at least two modes: idle with max. power consumption 15 mW and full thrust with max. power consumption 4 W.	Review of design, Test

Table 5.2: Verification methods of requirements

Identifier	Requirement	Verification
PROP-FUN-200	The thruster shall be able to operate on gaseous $N_2$ , as well as on liquid $H_2O$ .	Review of design, Test
PROP-FUN-300	The feed system shall operate in a normally closed configuration.	Review of design, Test
PROP-FUN-400	The micro-propulsion payload will be turned off if the system is not undergoing any type of demonstration/-operations and also when the propellant storage tank is empty.	Review of design, Test
PROP-FUN-500	The propellant storage shall be left empty when the micro-propulsion payload demonstration is completed.	Test
PROP-FUN-600	The control electronics shall have a Spike and Hold circuit, voltage & current monitoring circuit, Resistor heater circuit, microcontroller, sensor interfacing and overcurrent protection circuit.	Review of design
PROP-FUN-700	The micro-propulsion system shall allow for the mounting of electronic sensing devices for the measurements of propellant temperature and pressure inside the tank, temperature and pressure measurements, IMU measurements (accelerometers & gyroscopes), voltage monitoring/current monitoring/temperature monitoring)	Review of design
PROP-INT-100	The mechanical interface between the propulsion system and the satellite shall be compliant with option 7 from the PQ9 standard connector stacking and shall respect the PQ9 standard in PCB selection and sizing.[27].	Review of design
PROP-INT-200	The thermal interface between the propulsion system and the satellite shall allow for the propulsion system components to stay in a temperature range between $+5 \text{ }^\circ\text{C}$ and $+85 \text{ }^\circ\text{C}$ during all the mission phases when propulsion system operations are required.	Analysis
PROP-INT-300	The propulsion system shall be electrically connected to the satellite power subsystem through the standard RS-485 interface and shall respect the mechanical and electrical interface of connector stacking option 7 from the PQ9 standard document [27].	Review of design
PROP-INT-400	The data exchange interface between the propulsion system and the satellite shall be RS-485 with a data transfer rate of <b>&lt;TBD&gt;</b> bit/s .	Test
PROP-INT-500	The propellant storage system shall allow for filling and draining the propellants at any time when the fully assembled satellite is still accessible to human operators.	Test
PROP-RAMS-200	The internal pressure of all propulsion system components shall not be higher than 10 bar.	Review of design
PROP-RAMS-300	The propulsion system shall not include any pyrotechnic devices.	Review of design
PROP-RAMS-310	Materials used in the thruster shall be compatible with liquid demineralised water in both liquid and vapour state, nitrogen gas and air.	Review of design

Table 5.3: Verification methods of requirements

Identifier	Requirement	Verification
PROP-RAMS-320	Materials used in the propulsion system shall not be toxic, flammable, or in any way potentially hazardous for the operators or the other satellite subsystems.	Review of design
PROP-RAMS-400	A thermal vacuum bake-out of the propulsion system shall be carried out before launch to ensure a proper outgassing of all the components.	Inspection, Test
PROP-RAMS-500	All external parts of the thruster shall be electrically grounded.	Inspection, Test
PROP-RAMS-600	The propulsion system shall have a design factor of safety higher than 1.6 for yield load.	Analysis
PROP-RAMS-700	The propulsion system shall have a design factor of safety higher than 2.0 for the ultimate load.	Analysis
PROP-ERL-100	The payload shall be compatible with a large range of launch opportunities as described in M. Boerci (2017) [28].	Analysis
PROP-ERL-200	The maximum axial and lateral accelerations that the propulsion system shall withstand during the launch are as described in M. Boerci (2017) [28].	Test
PROP-ERL-300	The maximum vibration levels at the point of attachment of the satellite during the launch are as described in M. Boerci (2017) [28].	Test
PROP-ERL-400	The maximum acoustic pressures and loads that the propulsion system shall withstand during the launch are as described in M. Boerci (2017) [28].	Test
PROP-ERL-500	The maximum flight shocks that the propulsion system shall withstand during the launch are as described in M. Boerci (2017) [28].	Test
PROP-ERL-600	The pre-launch thermal environment within the launcher fairing is as described in M. Boerci (2017) [28].	Analysis
PROP-ERL-700	The maximum heating of the nose fairing during the launch is as described in M. Boerci (2017) [28].	Test
PROP-ERL-800	The maximum pressure changes inside the fairing that the propulsion system shall withstand during the launch are as described in M. Boerci (2017) [28].	Test
PROP-ERL-900	The micro-propulsion subsystem shall be compatible with the vacuum and temperature levels of the space environment in Low Earth Orbit.	Test

## 5.2. Risk Analysis

In this section a number of risks for the development and operation of the propulsion system after the conceptual design phase are discussed. This is done by use of a risk matrix, which combines both the likelihood of occurrence and the consequence of the occurrence to provide an indication of the risk. Although some risks have already been mitigated to an extent in the design choices made in Chapters 2 and 3, they could still provide problems in the manufacturing phase of the propulsion system. By identifying these problems at this stage, a targeted testing campaign can be made to efficiently test the system. The list of identified risks can be seen in Table 5.4. In keeping with the standard currently used at TU Delft shown in Palichadath et al. (2018), low probability is defined as a proven flight design and moderate probability is technology based on a working laboratory model. Furthermore, a marginal consequence is seen as a small reduction in technical performance, a critical consequence is seen as mission success being questionable and catastrophic is seen as mission failure [32]. These risks are to be iteratively assessed and modified during the testing phase of the propulsion system.

Table 5.4: Identified risks associated with the further development and manufacturing of the propulsion system (before testing)

#	Risk	Probability	Consequence
1	Leakage at valve connections	Moderate	Marginal
2	Problems during filling of propulsion system	Moderate	Critical
3	Insufficient power available due to low heater efficiency	Low-Moderate	Marginal
4	Pressure sensor failure	Low	Critical
5	Accelerometer failure	Low	Critical
6	Structural failure of components	Moderate	Critical
7	Thermal failure valves	Low	Critical
8	Issues with connections of components to metal plate	Moderate	Critical
9	Insufficient flexibility of propellant tubing during final build	Moderate	Critical
10	VLM thruster chip malfunction	High-Moderate	Critical
11	LPM thruster chip malfunction	High-Moderate	Critical
12	Thruster housing development time	Moderate	Catastrophic
13	Structural interface with Delfi-PQ incompatible	Low	Critical
14	Manufacturing error of components	Moderate	Marginal

The probability of occurrence for valve leakage is determined to be moderate because they have not been thoroughly tested yet in an integrated test setup for this dual VLM-LPM system and the three month mission lifetime is sufficiently long for leakage to occur. Although leakage is unfavourable, the result would be a reduced amount of testing time and lower thrust, which is deemed to be marginal of consequence because it only slightly reduces mission performance. As most of the propellant tubing is located in a storage container, it is unlikely that leakage will sufficiently damage electrical components to endanger the mission. Issues in filling the propulsion system are equally likely to occur due to the untested nature of the fill system. The consequence of the system not being filled correctly is determined to be critical. Risk number three is insufficient power available, however, with the selected initial pressure of 1.1 bar this is unlikely to be an issue. If this does occur, the propellant may not be fully vaporized. As the pressure decreases, this problem will solve itself. Therefore a marginal consequence is decided for risk three. For risks no. 4 and no. 5, the sensors are unlikely to fail as space qualified COTS components have been selected for use, however, if they were to fail in-orbit data from the propulsion system would not be provided and data on thrust would be missing. However, because there are multiple sensors and only a technology demonstration is required, consequences for risk numbers four and five are both deemed to be critical. Since there has yet to be any structural or thermal analysis to be completed on the system, the risk of structural or thermal failure of the components is present, although unlikely. The temperature of the valves is unlikely to exceed the operating temperature of the valves and the structure of the propulsion system only has to survive the launch loads and vibrations. Risk eight describes issues with the connection of the components to the metal plate in the flight model. As the components in the prototype are clamped, the flight model will use glue or soldered brackets to secure all components in place, which is yet to be confirmed. Therefore this has a moderate likelihood of occurrence. Components becoming loose would have a critical consequence as it may damage the system and stop testing. Risk nine is the risk of the flexibility of the tubing in the final design of the system. Although the fit test from Chapter 3 proved the design to be possible, this was without all the connections and components. Therefore the risk of kinks occurring in the propellant tubing is present and should be taken into account. Large kinks occurring or insufficient flexibility of the tubing may cause the flight model to not be able to access a large amount of its propellant. Therefore the consequence of this risk is set to critical. Risks 10 and 11 concern the operation of the VLM- and LPM- thrusters which have shown during previous testing at TU Delft that

they can become blocked or leak. Therefore, the probability of this occurring is set to high-moderate. Since they are an integral part to the system, they are deemed as critical risks, but not catastrophic as failure of one could still allow for the operation of the other. The development time for the thruster housings is also important, since they are yet to be designed and manufactured this could be the cause of long delays in the development process and should be continuously monitored to make sure the flight model is ready for the launch of Delfi-PQ. Due to the importance of monitoring this risk for the flight model of the system, the consequence is set at catastrophic. Risk 13 is the risk of incompatibility with Delfi-PQ, which is deemed to be low due to the adherence of the interface requirements for Delfi-PQ. However, it is risk to be monitored and tested. Therefore the probability is set at low. Finally, risk 14 is the risk of manufacturing mistakes of components which is always possible. However, components which have defects can be identified and will likely only cause a scheduling setback. The consequence for risk 14 is therefore only deemed to be marginal. All of these risks can be sorted into a risk matrix seen in Figure 5.1.

Likelihood	High				
	High-Moderate			10,11	
	Moderate		1,14	2,6,8,9	12
	Low-Moderate		3		
	Low			4,5,7,13	
		Negligable	Marginal	Critical	Catastrophic
		Impact			

Figure 5.1: Risk matrix, showing the danger each risk poses to the development and launch of the system

The conclusion for this risk analysis is that risks 2, 6, 8, 9, 10, 11 and 12 all need careful monitoring and mitigation during future development stages for the propulsion system. Risk 2 can be mitigated by thorough testing of the filling procedure and system. Risk 6 can be mitigated by doing a structural analysis on the system, which is yet to be completed, but falls outside the scope of this thesis. Risk 8 needs to be tested by connecting components to the metal plate of the system. This needs to be done during the assembly phase of the flight model. Risk 9 can be addressed by looking at the behaviour of the system when kinks are present in the propulsion system. Furthermore, methods of carefully bending tubing to avoid kinks should be implemented in the manufacturing process of future propulsion payloads. Risks 10 and 11 require thorough testing of the VLM and LPM thrusters in the clean room. Mitigating this risk all together is difficult, but it can be carefully watched and mitigated through testing. Finally risk 12 can be watched and followed as a mitigation method. A priority should be put on the development of the thruster housings as this is the current bottleneck for the development process.

### 5.3. Prototype Design

The physical interfaces for both the VLM and LPM thrusters do not yet have the dimensions required by the finalised design which is given in Chapter 2. They still need to be redesigned to fit the volume designated in the requirements. However, current thruster interfaces can be used to prove the concept and to provide initial data for the system. Therefore, the prototype of the system will be slightly different to the final design. While the new thruster housings are developed, the layout of the prototype will be kept as similar as possible to the design for the flight model. The positioning of the components will be kept the same, however, due to the larger thruster housings the system will be extended to 60 mm in height (due to the availability of spacer lengths) and the thruster housing will hang partially off the board. The stacking of the boards will only be done using two of the stacking spacers. Furthermore, the electrical interface used by the PQ9 connector will not be used so that there is enough space to clamp the VLM into place. The 3D model for the prototype design can be seen in Figure 5.2 and shows the placement of all major components without the tubing and manifold. A schematic of the final prototype can be seen in Figure 5.3. This prototype will be used in the tests described in Section 5.4.

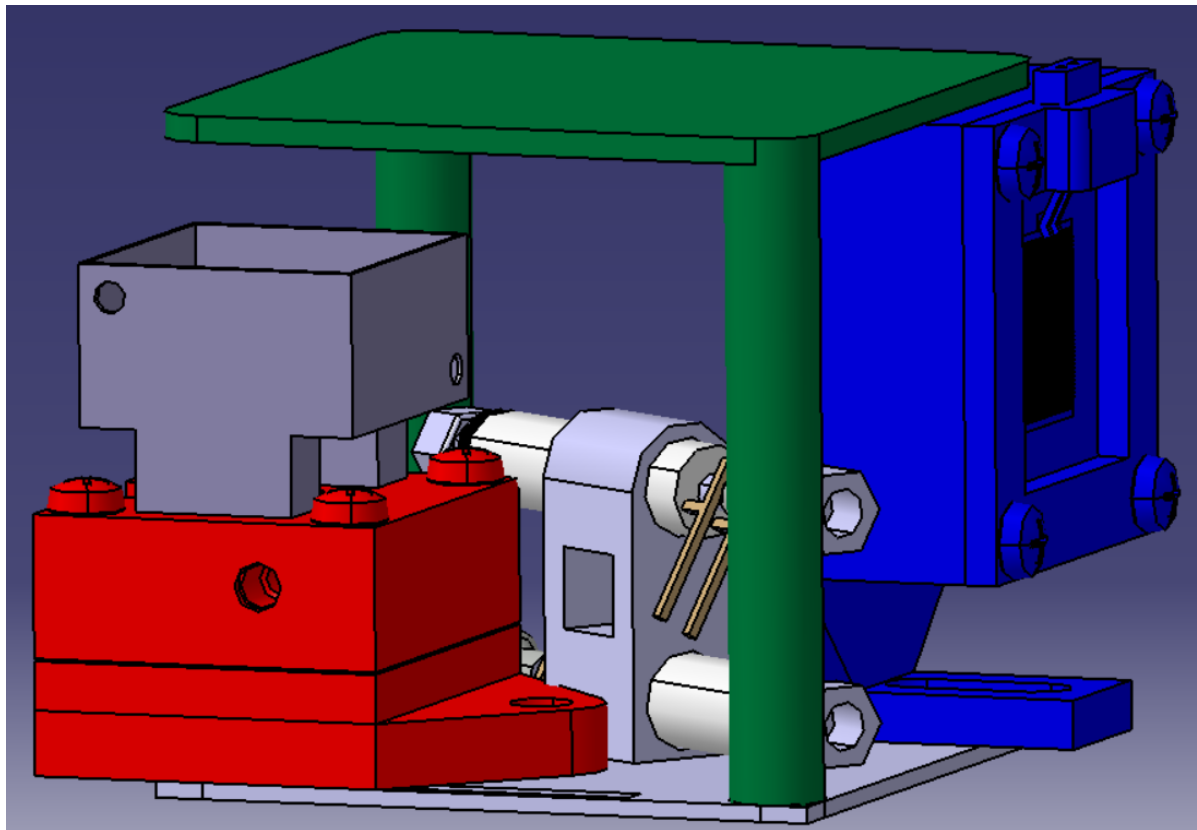


Figure 5.2: CATIAv5 Model showing the locations of the LPM (blue) and VLM (red) thrusters with the current thruster housings.

At the end of this thesis an attempt was made to manufacture this prototype, which can be seen in Figure 5.4. Although most parts were available, the clamping components required to connect the metal plate to the thrusters were absent. Therefore, the thrusters were bolted in place in the corner holes of the metal plate. The result was that the thrusters hung far outside the board and the orientation of Figure 5.2 was not achieved. However, some observations were made during the assembly of this prototype that be useful in future assemblies. Recommendations for future prototype model builds are to:

- Purchase small clamps to connect the metal plate to the thrusters. Alternatively, drill hole through the metal plate to bolt the thrusters in the correct location.
- Size the holes in the metal plate to be smaller than the spacers used for stacking the prototype

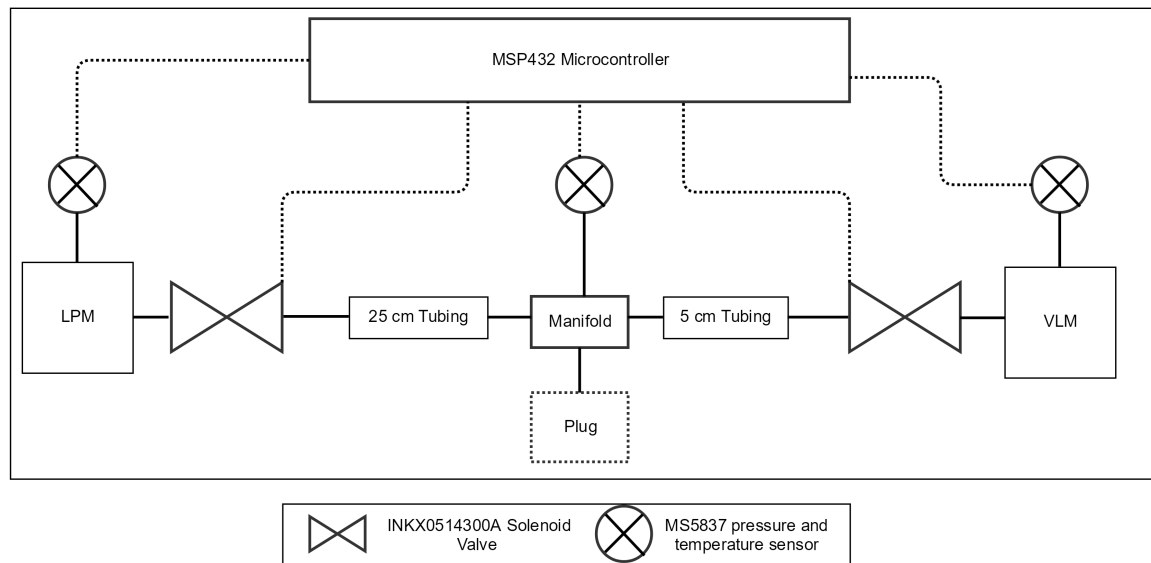


Figure 5.3: Schematic of all the components used in the prototype shown in Figure 5.2

- Reduce the radius of the valve support structure holes to be exactly equal to the valve radius. The valves were loose inside the support structure.
- The prototype was unstable when mounted on the metal plate. It could be worth building the prototype on a CubeSat standard (10 cm x 10 cm) to provide stability during initial testing.
- Use tape over the top of the propellant storage box to keep the propellant tubing coiled up inside.

## 5.4. Proposed Test Campaign

This section will cover the tests required to both verify that the design meets the requirements and propose a test plan for future development of the system. The plan described in this section will provide component, assembly and prototype testing which can be started at the conclusion of this thesis. However, full system testing on a flight model is currently not possible due to the absence of sufficiently small thruster housings for the VLM and LPM. Therefore, requirements concerning the volume and mass of the system can not be verified at this time and should be done in the future using a flight model of the design. It is also important to note that any tests which are not conducted in the vacuum chamber require a pressure input increase of 1 bar if conducted at atmospheric pressure. The test plan will be set up with a consistent structure, asking the following questions:

- Which requirement(s) will be verified?
- When will the test be conducted?
- Where will the test be conducted?
- Who will conduct the test?
- What components will be required for the test?
- How will the test be conducted?
- What is the expected outcome of the conducted test?

Furthermore, four stages of testing will be conducted. The first will be on a component level to test the performance of individual parts such as the thrusters, heaters, control electronics and the valves. The second stage will be the testing of specific assembled parts to check the physical and software

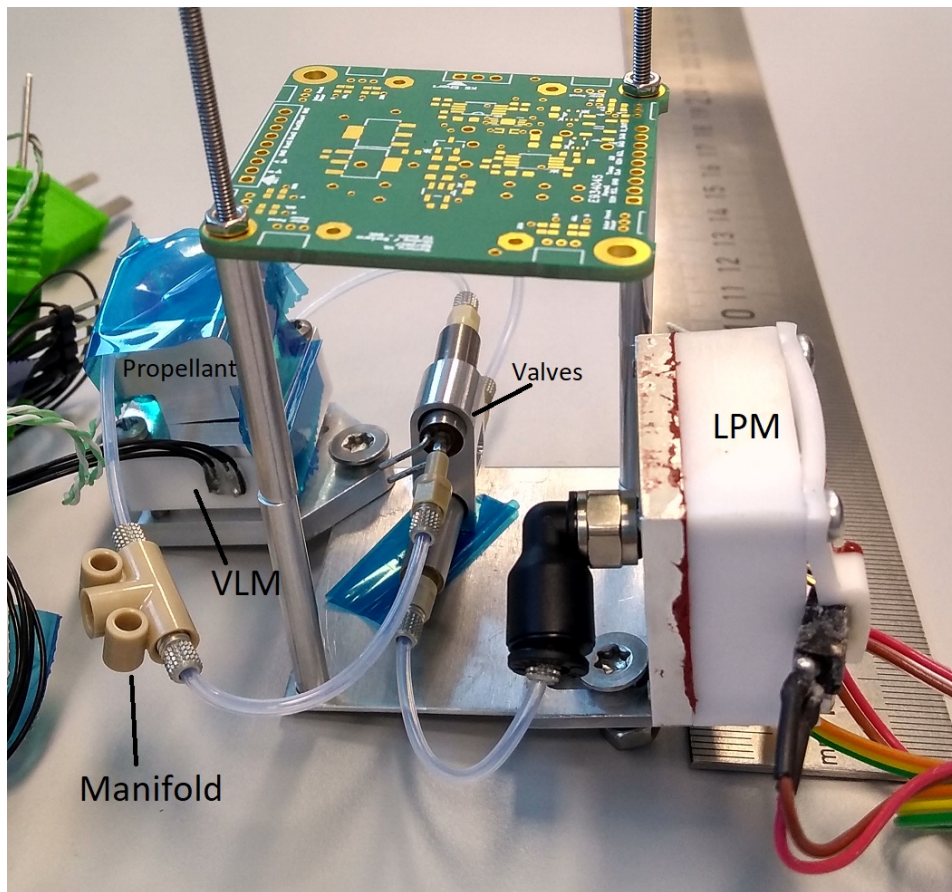


Figure 5.4: Assembly of the prototype completed in the clean room. Pressure sensors and wiring are not attached.

interfaces between them. The third stage will be the testing of the prototype shown in Section 5.3. Results from the operational envelope calculated in Chapter 4 will be tested here together with the expected thrust levels. Finally, stage four will be the testing of the new thruster housings and the flight model design from Chapter 3. A fit test will be required together with a full system test.

#### 5.4.1. Component Testing

Testing at component level is required to check whether components live up to their specifications and operate under the vacuum conditions dictated by space.

##### TEST-COM-01: Valve test

**Which requirement(s):** PROP-FUN-300.

**Why:** This test will be completed to check the specifications of the valve are indeed sufficient in terms of leakage and pressure resistance. Furthermore, pulse width modulation (PWM) throttling may be required by the valve for operation of the LPM in order to reach sufficiently low pressures for operation. All these capabilities need to be tested and confirmed that they can operate in vacuum.

**When:** September 2018.

**Where:** Clean room, vacuum chamber.

**Who:** TBD.

**Components Required:** INKX0514300A Valve, 2x MINSTAC 0.062 Tubing with 0.138-40 UNF interface, propellant (water) feed system, mass flow sensor, microcontroller, wiring.

**How:** Connect the microcontroller to the valve. Then, connect the tubing from the propellant source to the valve. Another piece of tubing with mass flow sensor is located at the other end of the valve. Then turn valve on and measure mass flow sensor. Complete at different time intervals. Initially steps of 1 second, reducing to lowest possible steps allowed by microcontroller to test PWM capabilities.

**Expected Output:** Graph of mass flow over time which should coincide with the signals given by the microcontroller to operate the valve.

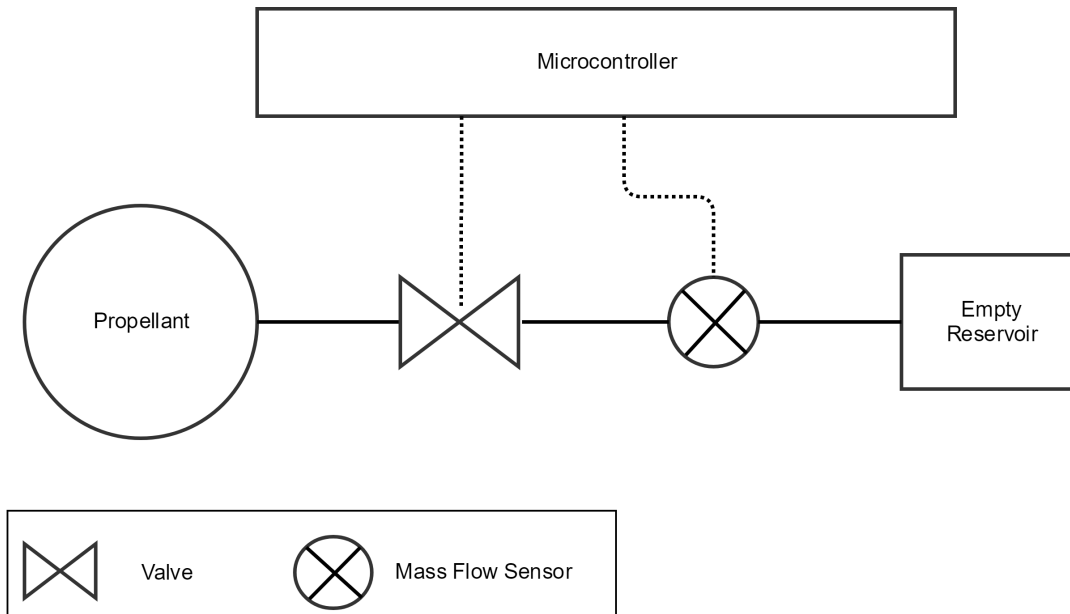


Figure 5.5: Schematic of the test setup for the valve test

### TEST-COM-02: VLM & LPM thruster test

**Which requirement(s):** PROP-PERF-100, PROP-PERF-200, PROP-PERF-210.

**Why:** This test will be done to check the operation of the VLM and LPM thruster chips. Some thrusters become damaged or blocked and need to be confirmed as operational.

**When:** September 2018.

**Where:** Clean room, vacuum chamber.

**Who:** TBD.

**Components Required:** Pressurized propellant (water) feed system, MINSTAC 0.062 Tubing with 0.138-40 UNF interface, VLM thruster, LPM thruster, original VLM thruster housing, original LPM thruster housing, microcontroller, wiring, AE-TB-5m thrust stand [32].

**How:** Connect the pressurized propellant feed system to the VLM thruster using the MINSTAC 0.062 tubing and wire the microcontroller to the VLM thruster. The VLM thruster is then mounted on the AE-TB-5m thrust stand. Pressure is varied from 1.1 bar to 0.2 bar by the supply of propellant. Thrust is measured continuously for a specified amount of time. The test is then repeated at different power inputs, ranging from 0.1 W to 4 W. The LPM thruster is tested similarly but with a pressure supplied in the order of 1000 Pa.

**Expected Output:** With a constant pressure supplied, the thrust values should remain constant. By repeating this test at multiple power levels and pressures, a graph can be generated of the thrust at different power inputs to ensure the thrusters both work at different power levels.

### TEST-COM-03: Heater efficiency test

**Which requirement(s):** PROP-FUN-100, PROP-SYST-300.

**Why:** This test needs to be completed in order to ensure there is sufficient power transfer between the thruster heater and the propellant, otherwise the initial pressure may need to be adjusted based on the heater efficiency obtained in this test. The initial pressure for the nitrogen was set at 1.1 bar in order to allow for the power input to be under the 4 W requirement. This was under the worst case scenario assumption of a heater efficiency of 60 percent. This assumption needs to be verified.

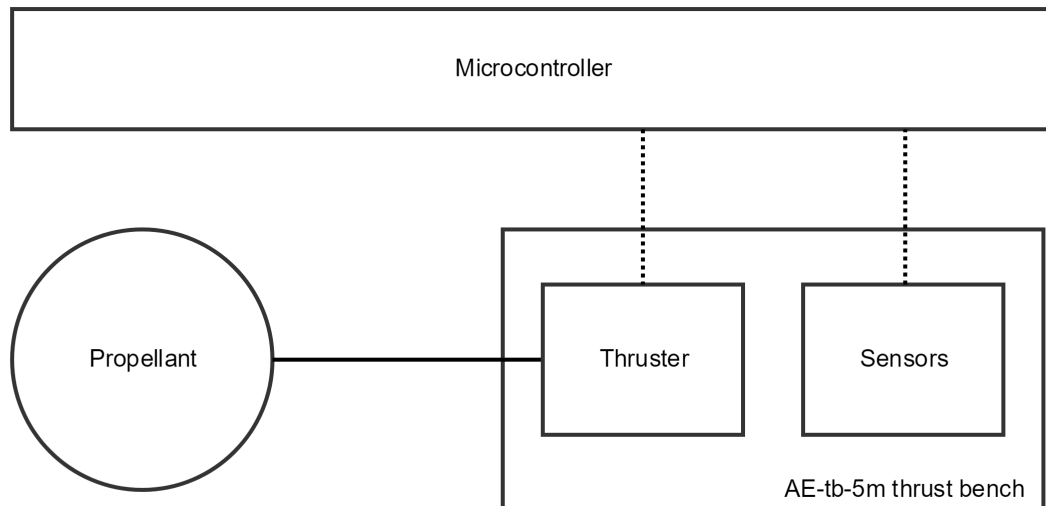


Figure 5.6: Schematic of the test setup for the VLM- and LPM-thruster tests

Following this, the operational envelope may need to be altered. **When:** October 2018.

**Where:** Clean room.

**Who:** TBD.

**Components Required:** Pressurized propellant (water) feed system, MINSTAC 0.062 Tubing with 0.138-40 UNF interface, VLM thruster, microcontroller, wiring, pressure-temperature sensor in thruster.

**How:** Connect the pressurized propellant feed system to the VLM thruster using the MINSTAC 0.062 tubing and wire the microcontroller to the VLM thruster. Measure the input power to the thruster heater, measure the temperature in the thruster and the mass flow of the propellant. This will allow for calculation of the efficiency for the thruster heater. The test setup can be seen in Figure 5.7. To help select input pressures and powers, Figure 4.23 can be used to select input pressures and powers near the curve given by the operational envelope calculations. The operational envelope perhaps may need to be changed based on the initial heater efficiency acquired by this test.

**Expected Output:** The expected output for this test is a range of heater efficiencies at different power inputs and at different pressures which are relevant to the operation of the VLM. Finally a graph can be made of the required power input to the heater at the pressures occurring in the system.

#### 5.4.2. Assembly and Integration Testing

With the testing of components complete, the integration between components needs to be tested to ensure a functional assembly for the system.

##### TEST-INT-01: Fill & Leak test

**Which requirement(s):** PROP-PERF-300, PROP-INT-500.

**Why:** The leak test needs to be completed in order to find the leakage rate which occurs over time within the system. Leakage could result in the loss of a large amount of pressure and propellant, which will reduce the amount of testing which can be completed. If the leakage rate is deemed to be high, perhaps in-orbit testing can be completed immediately after orbit insertion of the satellite to avoid a significant loss of propellant. Furthermore, this test checks whether the filling method proposed in Chapter 3 can be used on the system. If not, a check valve will need to be incorporated into the design and tested as well.

**When:** September 2018.

**Where:** Clean room, vacuum chamber.

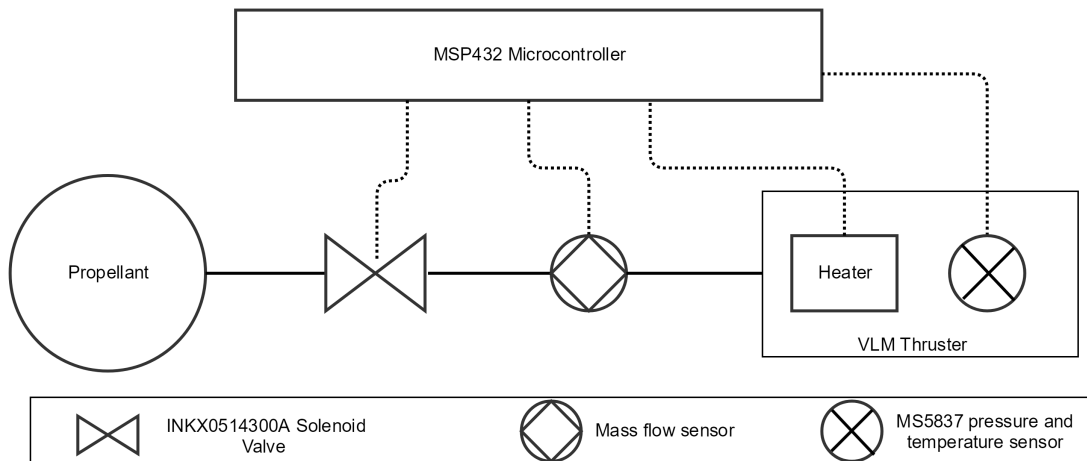


Figure 5.7: Test setup for the heater efficiency test.

**Who:** TBD.

**Components Required:** TMLA3201950Z A2 Line Seal Cap-062 MINSTAC-PEEK (or CCPI2510040S check valve from Lee Company if required), MANIFOLD-3-.062 MINSTAC-PEEK Lee Company, INKX0514300A Valve x2, 25 cm MINSTAC 0.062 Tubing with 0.138-40 UNF interface Lee Company, 5cm Tubing with 0.138-40 UNF interface, fill valve, Pressurized propellant (water) feed system, microcontroller, wiring, pressure sensor in propellant tubing.

**How:** Connect both tubing parts to the manifold and the other ends to the valves. Then, connect the pressurized propellant feed system to the manifold directly using tubing. Fill and overpressurize the system to 1.2 bar. Disconnect the propellant feed system and plug the manifold. If this proven to be unfeasible, the use of a check valve will be required. Once filled, the propulsion system should be placed in the vacuum chamber. Both valves are left in closed state and a timer is started. The pressure is measured at the start and at the end (when the timer reaches 1 hour). This will allow for calculation of the leakage rate. This test is to be conducted at multiple pressures between the range of 1.1 bar and 0.2 bar to find the leakage rate at different pressures.

**Expected Output:** The expected output is verification that the method of overpressurizing and plugging is sufficient for use on the system and problems in the filling process are identified. Furthermore, a graph of the leakage rate at different pressures is the expected output for the leak test.

### TEST-INT-02: Electrical & Software Test

**Which requirement(s):** PROP-SYST-300, PROP-SYST-400, PROP-PERF-400, PROP-FUN-100, PROP-INT-100, PROP-INT-400.

**Why:** The electrical and software tests need to be completed to make sure that the RS-485 interface is functional during operation. The Electric Power System (EPS) will supply an unregulated voltage, which means that the voltage and frequency output of the MSP432 microcontroller to its components needs to be tested. Furthermore, all commands run through the MSP432 which makes verification of the microcontroller a high priority. Interfaces between sensors and the MSP432 microcontroller also need to be tested.

**When:** November 2018.

**Where:** Clean room.

**Who:** TBD.

**Components Required:** MS432 microcontroller, MANIFOLD-3-.062 MINSTAC-PEEK Lee Company, TMLA3201950Z A2 Line Seal Cap-062 MINSTAC-PEEK (or CCPI2510040S check valve from Lee Company, if required), INKX0514300A Valve, 25 cm MINSTAC 0.062 Tubing with 0.138-40 UNF interface from Lee Company, 5cm Tubing with 0.138-40 UNF interface from the Lee Company, pressurized pro-

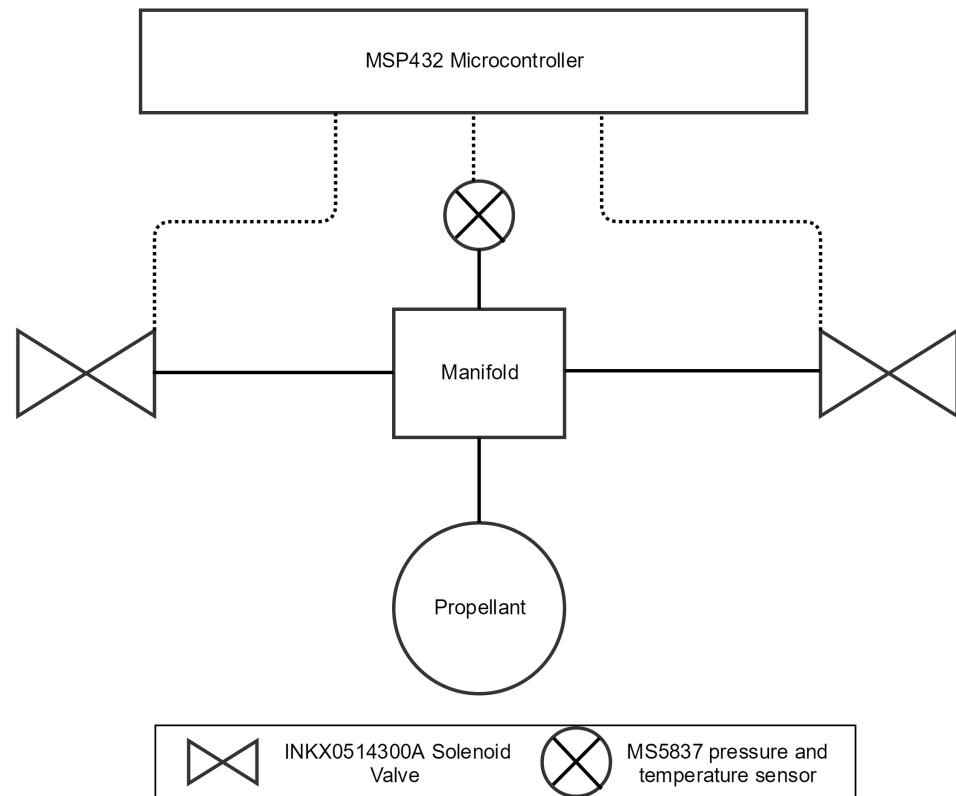


Figure 5.8: Test setup for fill and leak test by method of overpressurizing and plugging the manifold after inserting the propellant

pellant (water) feed system, microcontroller, wiring, pressure sensor in propellant tubing.

**How:** Connect all previously mentioned components to the microcontroller and test the operation of each component using the MSP432 microcontroller. Measure voltage, current and frequency of each component received during the test.

**Expected Output:** The expected output is the confirmation that the RS485 interface together with the MSP432 microcontroller can sufficiently convert and redirect voltage to all required components and can fulfil all requirements for the nominal operation of the propulsion system.

### 5.4.3. Prototype Testing

Now that assembly testing is complete, the prototype shown in Section 5.3 can be tested to provide initial data on the performance characteristics of the system. A diagram for the test setup of the prototype is given in Figure 5.9 and shows all of the components and their physical and software interfaces. This section of testing is used to verify the results obtained in the operational envelope from Chapter 4.

#### TEST-PRO-01: Vaporization test

**Which requirement(s):** PROP-FUN-100.

**Why:** If the temperature in the thruster goes below a certain threshold, the propellant no longer vaporizes and the VLM thruster will operate at very low specific impulse. By getting as close as possible to the vaporization point, the temperature is kept at a minimum which is beneficial for the rest of the components. Knowing the exact power at which vaporization occurs at which pressure is therefore important.

**When:** December 2018.

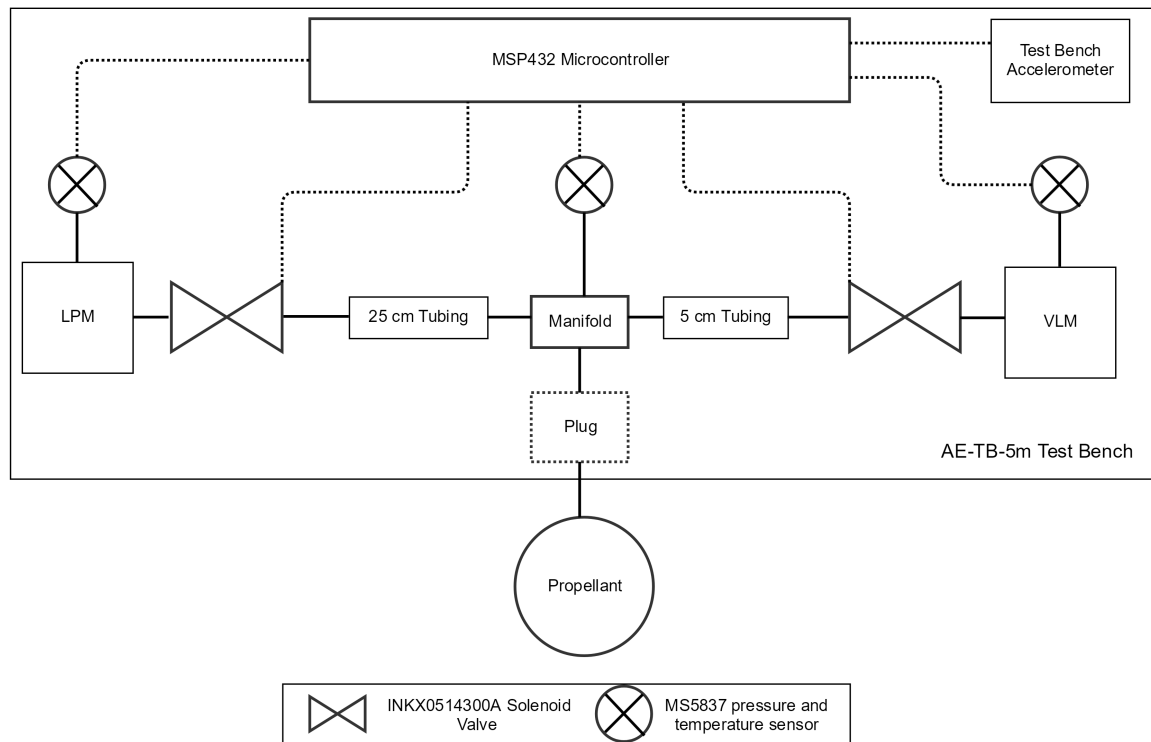


Figure 5.9: General test setup for the prototype testing phase

**Where:** Clean room.

**Who:** TBD.

**Components Required:** Propulsion system prototype, MS432 microcontroller, wiring, MANIFOLD-3-.062 MINSTAC-PEEK Lee Company, TMLA3201950Z A2 Line Seal Cap-062 MINSTAC-PEEK from Lee Company (or CCPI2510040S check valve from Lee Company, if required), pressurized propellant (water) feed system, AE-TB-5m thrust stand

**How:** Connect all components with one another and mount the prototype on the AE-TB-5m thrust stand. Then use the thruster efficiency found in previous test and check if the Clausius-Clapeyron relation is a good estimation for the vaporization pressure. Fill the system at 1.1 bar (if in vacuum chamber) and continuously measure pressure and thrust, while changing the input power to set the temperature equal to the temperature given by the Clausius-Clapeyron relation at a given pressure. If the thrust suddenly decreases to very low values due to a drop in specific impulse, then the vaporization point has been passed and the point should be noted.

**Expected Output:** The expected output is an experimental relation between power input and the vaporization temperature required for pressures. This way, the pressure sensor can be read by the microcontroller and the system can immediately determine the power required to input to the thruster to achieve vaporization.

#### TEST-PRO-02: Pressure profile test

**Which requirement(s):** PROP-SYST-200, PROP-SYST-210.

**Why:** The pressure profile of the system over time can be used to verify the calculations made for the operational envelope in Chapter 4. By verifying the pressure profile over time, the chosen initial pressure and initial volume of nitrogen can be confirmed to be acceptable for the propulsion system.

**When:** January 2019.

**Where:** Clean room.

**Who:** TBD.

**Components Required:** Propulsion system prototype, MS432 microcontroller, wiring, MANIFOLD-3-

.062 MINSTAC-PEEK Lee Company, TMLA3201950Z A2 Line Seal Cap-062 MINSTAC-PEEK (or CCPI2510040S check valve from Lee Company, if required), pressurized propellant (water) feed system, pressure sensor in tubing.

**How:** Connect the prototype to the propellant feed system and all components to the microcontroller. Fill the system to the initial pressure and nitrogen volume (1.1 bar and  $0.12 * V_{tube}$  respectively) when conducted in vacuum. Run the testing mode for the VLM shown in Figure 4.5 if already available, otherwise manually open the valve and measure pressure every 10 ms for the time period mentioned in the operational envelope (1200 s).

**Expected Output:** The expected output is an experimental graph of the pressure over time. This is likely to be different to the operational envelope due to the assumptions stated in Section 4.2.

### TEST-PRO-03: Mass flow profile test

**Which requirement(s):** PROP-SYST-200, PROP-SYST-210.

**Why:** The mass flow profile of the system over time can be used to verify the calculations made for the operational envelope in Chapter 4. By verifying the mass flow profile over time, the chosen initial pressure and initial volume of nitrogen can be confirmed to be acceptable for the propulsion system. The mass flow is of direct influence to the thrust that is achieved by the system, but also the amount of propellant remaining in the system. Therefore, the mass flow directly influences the thrusting time for the VLM.

**When:** January 2019.

**Where:** Clean room.

**Who:** TBD.

**Components Required:** Propulsion system prototype, MS432 microcontroller, wiring, MANIFOLD-3-.062 MINSTAC-PEEK Lee Company, TMLA3201950Z A2 Line Seal Cap-062 MINSTAC-PEEK (or CCPI2510040S check valve from Lee Company, if required), pressurized propellant (water) feed system, mass flow sensor.

**How:** Connect the prototype to the propellant feed system and all components to the microcontroller. Fill the system to the initial pressure and nitrogen volume (1.1 bar and  $0.12 * V_{tube}$  respectively) when conducted in vacuum. Run the testing mode for the VLM shown in Figure 4.5 if already available, otherwise manually open the valve and measure mass flow every 10 ms for the time period mentioned in the operational envelope (1200 s).

**Expected Output:** The expected output is an experimental graph of the mass flow over time. This is likely to be different to the operational envelope due to the assumptions made.

### TEST-PRO-04: Thrust profile test

**Which requirement(s):** PROP-SYST-200, PROP-SYST-210.

**Why:** The thrust test will show that the propulsion system will always provide a thrust between 0.12 mN and 3 mN according to the requirements set in Chapter 2. By having experimental values for the thrust and mass flow, it becomes possible to calculate the specific impulse of the system.

**When:** February 2019.

**Where:** Clean room.

**Who:** TBD.

**Components Required:** Propulsion system prototype, MS432 microcontroller, wiring, MANIFOLD-3-.062 MINSTAC-PEEK Lee Company, TMLA3201950Z A2 Line Seal Cap-062 MINSTAC-PEEK (or CCPI2510040S check valve from Lee Company, if required), pressurized propellant (water) feed system, AE-TB-5m thrust stand.

**How:** Connect the prototype to the propellant feed system and all components to the microcontroller. Mount the system on the thrust bench and fill the prototype to the initial pressure and nitrogen volume (1.1 bar and  $0.12 * V_{tube}$  respectively) when conducted in vacuum. Run the testing mode for the VLM shown in Figure 4.5 if already available, otherwise manually open the VLM valve and measure the thrust every 10 ms for the time period mentioned in the operational envelope (1200 s). After this is completed, stop the heating for the VLM thruster and close the VLM valve. Then pre-heat the LPM

thruster and open the LPM-valve. Measure the thrust every 10 ms until all propellant is depleted and no thrust is measured anymore. This test should be conducted in both atmospheric conditions and in vacuum conditions.

**Expected Output:** The expected output is an experimental graph of the thrust over time. Together with the previous data from the mass flow experiment, this will lead to a first estimate of the specific impulse of the system.

#### 5.4.4. Flight Model Testing

By the time the testing campaign of the prototype is finished, the new designs for the thruster housings should be complete. This will allow for the assembly of a flight model which can fit in the 42 mm x 42 mm x 30 mm volume required. Final testing for the system can then be done on this flight model.

##### TEST-FLT-01: Thruster housing test

**Why:** This test will be done to check the operation of the updated VLM and LPM thruster housings. With the design of a new thruster housing comes the possibility of leakage or blockage, which requires a new thruster test similar to the one described in TEST-COM-02.

**When:** February 2019.

**Where:** Clean room.

**Who:** TBD.

**Components Required:** Pressurized propellant (water) feed system, MINSTAC 0.062 Tubing with 0.138-40 UNF interface, updated VLM thruster, updated LPM thruster, microcontroller, wiring, AE-TB-5m thrust stand [32].

**How:** Connect the pressurized propellant feed system to the updated VLM thruster using the MINSTAC 0.062 tubing and wire the microcontroller to the updated VLM thruster. The updated VLM thruster is then mounted on the AE-TB-5m thrust stand. Pressure is kept constant by the propellant supply. Thrust is measured continuously for a specified amount of time. The test is then repeated at different power inputs, ranging from 0.1 W to 4 W. The LPM thruster is tested similarly but with a pressure supplied in the order of 1000 Pa.

**Expected Output:** With a constant pressure supplied, the thrust values should remain constant. By repeating this test at multiple power levels and pressures, a graph can be generated of the thrust at different power inputs to ensure the thrusters both work at different power levels.

##### TEST-FLT-02: Fit test

**Which requirement(s):** PROP-SYST-100, PROP-SYST-200, PROP-FUN-700.

**Why:** With updated thruster housings, all components can be placed as shown in the conceptual and detailed designs given in Chapters 2 and 3. Although a fit test was performed using a 3D-printed mock up model, this did not allow for the correct interfaces between the tubing and the thrusters or the wiring interfaces between the components and the PCB. Furthermore, the manifold was not included in this fit test. Therefore a new fit test on the flight model needs to be done to check whether the design complies with requirement PROP-SYST-200 for the volume of the system.

**When:** February 2019.

**Where:** Clean room.

**Who:** TBD.

**Components Required:** Updated thruster housing VLM, updated thruster housing LPM, MS432 microcontroller, TMLA3201950Z A2 Line Seal Cap-062 MINSTAC-PEEK (or CCPI2510040S check valve from Lee Company, if required), 2x INKX0514300A Valve, 25 cm MINSTAC 0.062 Tubing with 0.138-40 UNF interface from Lee Company, 5cm Tubing with 0.138-40 UNF interface from the Lee Company, pressurized propellant (water) feed system, microcontroller, wiring, pressure sensor in propellant tubing, PCB, metal plate, valve support structure.

**How:** Place all components in the correct location and connect all wiring from the valves, thrusters and pressure sensors to the PCB and microcontroller. Place all components in the locations shown by

the design in Chapter 3. Connect the two tubing pieces to the manifold and the thrusters. Connect the chosen filling method to the manifold. All components may have an overhang of maximum 2.4 mm off the PCB board. This is the distance to the structural hull of the satellite. Then check that all components adhere to the requirements set by PROP-SYST-200 using measurement equipment.

**Expected Output:** The expected output is confirmation that all components fit inside the designated volume. Difficulties are most likely to occur for the manifold and the filling locations which have not been verified yet due to the unavailability of interfaces between tubing and other components.

### TEST-FLT-03: Integration with Delfi-PQ test

**Which requirement(s):** PROP-INT-300, PROP-INT-500,

**Why:** Although the structural and the software interfaces are designed with Delfi-PQ in mind, they both need to be checked whether they are compatible with Delfi-PQ.

**When:** February 2019.

**Where:** Clean room.

**Who:** TBD.

**Components Required:** Updated thruster housing VLM, updated thruster housing LPM, MS432 microcontroller, TMLA3201950Z A2 Line Seal Cap-062 MINSTAC-PEEK (or CCPI2510040S check valve from Lee Company, if required), 2x INKX0514300A Valve, 25 cm MINSTAC 0.062 Tubing with 0.138-40 UNF interface from Lee Company, 5cm Tubing with 0.138-40 UNF interface from the Lee Company, pressurized propellant (water) feed system, microcontroller, wiring, pressure sensor in propellant tubing, PCB, metal plate, valve support structure and structural interface with Delfi-PQ.

**How:** Connect the flight model to the structural interface and then connect the structure to Delfi-PQ. Test whether access to the propellant is available. Furthermore, check whether the exit holes for the VLM and LPM thrusters are in the correct location. After that, the communication with the OBC and the MSP432 microcontroller needs to be tested. Especially the activation of the different modes needs to be programmed and tested.

**Expected Output:** The expected output is the confirmation that the physical interface is correctly designed for use on Delfi-PQ. The communication between the OBC and the microcontroller should be deemed reliable after testing.

### TEST-FLT-04: Full System Test

**Why:** After the flight model has been successfully manufactured and the software for the flight modes has been written, a full system test can be done in the vacuum chamber. All the flight modes should be tested using the hardware to ensure there are no bugs prior to flight. While the modes are tested a measurement for the thrust of the flight system can be made.

**When:** March 2019.

**Where:** Clean room.

**Who:** TBD.

**Components Required:** Updated thruster housing VLM, updated thruster housing LPM, MS432 microcontroller, TMLA3201950Z A2 Line Seal Cap-062 MINSTAC-PEEK (or CCPI2510040S check valve from Lee Company, if required), 2x INKX0514300A Valve, 25 cm MINSTAC 0.062 Tubing with 0.138-40 UNF interface from Lee Company, 5 cm Tubing with 0.138-40 UNF interface from the Lee Company, pressurized propellant (water) feed system, microcontroller, wiring, pressure sensor in propellant tubing, PCB, metal plate, valve support structure, AE-TB-5m thrust stand.

**How:** Mount the flight model on the AE-TB-5m thrust stand. Fill the flight model to the initial pressure and nitrogen volume ( $1.1 \text{ bar}$  and  $0.12 * V_{tube}$  respectively) in the vacuum chamber. Send commands to the microcontroller to test the following modes of the system:

- Start-up Mode
- Idle Mode
- VLM Testing Mode

- LPM Testing Mode
- Abort Mode
- End-of-life Mode

During the VLM and LPM testing modes thrust measurements are to be made every 10 ms. Operations of the different modes are to be compared to the flow diagrams from the operational envelope in Section 4.1 to check for correct operation.

**Expected Output:** The expected output is confirmation of the different flight modes for the propulsion system as well as the thrust provided by the system during operation of the VLM and LPM thrusters.

Two additional tests which need to be completed before launch of the system which include a vibration test (TEST-FLT-05) and a shock test (TEST-FLT-06) to ensure that the system complies with launch requirements. These tests require external testing facilities and integration of the payload into the Delfi-PQ satellite and are therefore not yet included in this test plan.

## 5.5. Validation

Although the design can be verified thoroughly by means of testing in the clean room, validation of the system is difficult before launch. This is primarily due to the limited number and availability of data from previous CubeSat propulsion missions[32]. Therefore validation of the system will only be possible until the mission has already begun. This will be done by reading the IMU measurements and calculating the thrust provided by both the VLM and LPM thrusters. Also by measuring pressure and temperature levels during operation, an estimate can be made for the mass flow profile. An overview of the in-orbit measurements to be made can be seen in Table 5.5. Measurement 1 can validate the calculations completed in Section 4.2 of this report concerning the operational envelope. Measurements 1, 3 and 4 in this table can be used to calculate an estimate for the mass flow of the system. Since there was no sufficiently small mass flow sensor available, this is the best option to provide some form of validation to the massflow calculations in Section 4.2. Furthermore, by using measurements 2 and 5 together with the moment of inertia of Delfi-PQ, the force exerted by the propulsion system can be found. This gives the value for the thrust of both the VLM and LPM thrusters. Combining results from the mass flow calculated from in-orbit pressure and temperature measurements together with the in-orbit thrust measurements by the IMU, the specific impulse can be found for the VLM thruster.

Table 5.5: Table of in-orbit measurements to be made

	<b>In-orbit measurement</b>	<b>Sensor</b>
#1	Pressure within propellant tubing	MS5837-30BA
#2	Rotational acceleration	BMX055 IMU
#3	VLM thruster temperature & pressure	MS5837-30BA
#4	LPM thruster temperature & pressure	MS5837-30BA
#5	Acceleration	BMX055 IMU

The main requirement for the propulsion system was to provide a technology demonstration for both the VLM and LPM thrusters. Validation of this requirement would occur by measuring thrust produced by both thrusters, but could also be completed by measuring pressure changes in the propellant tubing and thrusters.



# 6

## Conclusion

This report presented a design for the in-orbit technology demonstration of VLM- and LPM- micro-resistojets currently under development at TU Delft. At this stage of the prototype development, there are no indications that the design presented in this report is unsuitable for testing the micro-thrusters in the picosatellite called Delfi-PQ. However, this can not be confirmed until the thruster housing components for the thruster chips are fully developed and a prototype has undergone the testing campaign presented in Chapter 5. By designing a system in adherence to the requirements and developing a test plan for the technology demonstration payload, all the subquestions listed under research questions Q1 and Q2 mentioned in Section 1.2 are deemed to be answered in satisfactory way. Research question 1.1, which concerned component selection, was answered by using a functional analysis and requirement generation process which led to the required components for the propulsion system. Next, research question 1.2 was answered by modelling the components in CATIA software to generate several concepts. Once a concept was selected using a numerical trade-off, question 1.3 was answered by an in-depth analysis into the behaviour of the system. This was modelled using Matlab and resulted in the selection of values for initial pressure, thrusting time and pressurant volume. Finally, research question 2 was answered by writing a verification plan for each of the system requirements. This was followed by a test plan for the system, which can be started following the completion of this thesis.

The required technology demonstrator was selected to be a propulsion system which could test two separate thrusting methods in one payload. What resulted was the selection of a system with a shared propellant tank in the form of a coiled capillary tube between two valves, each of which lead to a thruster. The propellant was determined to be liquid water while the pressurant was selected to be gaseous nitrogen. During operation of the system, thrusting of the VLM occurs first and reduces the pressure over time, until the LPM is activated which benefits from the lower pressure inside the capillary tubing. A functional analysis of the Delfi-PQ mission led to the generation of requirements for the propulsion system. The killer requirement for the design of the propulsion payload was the restriction set on the volume of the satellite due to Delfi-PQ's PocketQube platform. This meant that the design was centred around efficient use of the volume available and primarily around the placement of the two solenoid valves. The use of CAD software provided an efficient option to developing different concepts. What resulted was a compact design with two stacked valves placed diagonally within the 42 mm x 42 mm x 30 mm volume. The remaining components were selected and placed to adhere to the remaining requirements and continuous communication with Delfi-PQ team members was required. Finally, a fit test was successfully completed using 3D printed components to verify whether the propulsion system adhered to the volume requirement.

After the successful conceptual design of the system, the maximum available length of the propellant tubing was found to be 30 cm. Together with the 4 W restriction on peak power to the propulsion system, this allowed for calculation of the operational envelope which contains the initial pressure and nitrogen volume. What resulted was an estimation of pressure, mass flow and thrust profiles over time. The initial pressure was set at 1.1 bar and the initial volume of nitrogen at 12 percent of the 30 cm capillary tubing. Thrust time of the VLM is calculated to be 1200 s and the thrust time of the LPM is

set to be 200 s.

Verification of the results obtained from the calculation from the operational envelope fall outside the scope of this report. However, both the verification process and the design of the prototype given within the final chapter of this report provide a framework for future work on this design. The test plan developed in the final chapter suggests four levels of testing: Component, assembly, prototype and flight model. All of which give detailed tests to prove the feasibility of the design and allow for launch on Delfi-PQ in 2019.

A detailed plan for future steps in the development of the propulsion system been given in Chapter 5. One of the largest risks for the future development of the system are at this moment the method of filling the system will propellant, which may be difficult to execute. Although the selection of the conceptual design was based on volume-saving options, the limited volume available may cause the formation of kinks in the propellant capillary tubing to become an issue. Therefore, a consistent method for bending capillary tubing without causing kinks will be important. The recommendations for future development of this system are therefore to carefully monitor the risks mentioned in Section 5.2 of this report, with specific attention to the method of filling, capillary tubing connections and thruster housing development for the flight model.

The micropropulsion payload demonstrator developed in this report is the first step to in-orbit testing of VLM- and LPM-technology at TU Delft and of importance to provide validation to the technology. Although the testing phase of the system may uncover issues in the design, there are currently no indications that the system has major design flaws and this will be the first of many advanced technology demonstration payloads to fly on Delfi-PQ.

# Bibliography

- [1] A. Poghosyan and A. Golkar, *Cubesat evolution: Analyzing cubesat capabilities for conducting science missions*, Progress in Aerospace Sciences, Elsevier, vol. 88, pp.59–83 (2017).
- [2] A. Cervone, M. A, and B. Zandbergen, *Conceptual design of a low-pressure micro-resistojet based on a sublimating solid propellant*, Acta Astronautica 108, Elsevier, pp. 30-39 (2015).
- [3] P. Kundu, T. K. Bhattacharyya, and S. Das, *Design, fabrication and performance evaluation of a vaporizing liquid microthruster*, Journal of Micromechanics and MicroEngineering, IOP Publishing, Vol. 22, 025016 (25 Jan 2012).
- [4] A. Cervone, B. Zandbergen, and D. Guerreri, *Green micro-resistojet research at delft university of technology: new options for cubesat propulsion*, CEAS Space Journal, Springer, vol 9, Issue 1, pp. 111-125 (2017).
- [5] J. Piattoni, M. Balucani, B. Betti, G. Candini, R. Crescenzi, F. Nasuti, M. Onofri, F. Piergentili, and F. Santoni, *Mems cold gas microthruster on ursa maior cubesat*, (23 - 27 September, 2013).
- [6] D. Guerreri, M. Silva, A. Cervone, and E. Gill, *Selection and characterization of green propellants for micro-resistojets*, Journal of Heat Transfer, ASME, vol. 139 (Oct. 2017).
- [7] The-Lee-Company, *062 minstac - the lee company, 2018 [webpage, online]*, <http://www.theleeco.com/products/electro-fluidic-systems/minstac-tubing-components/tube-fittings/062-minstac/>, [accessed on: 15-06-2018] ().
- [8] The-Lee-Company, *Inkx0514300a a5, 2016 [pdf, online]*, <http://www.theleecocad.com/PDF.nsf/2355f3df133a527185256c9300562a42/b359ed7c99f6028525804f00684722/\protect\TU\textdollarFILE/INKX0514300A%20A5.pdf>, [accessed on: 18-06-2018] ().
- [9] The-Lee-Company, *Tmma320395oz a3, 2016 [pdf, online]*, <http://www.theleecocad.com/PDF.nsf/2355f3df133a527185256c9300562a42/d9dae1b2f2896a2b852580590046feb4/\protect\TU\textdollarFILE/TMMA3203950Z%20A3.pdf>, [accessed on: 05-07-2018] ().
- [10] The-Lee-Company, *Check valve-.062 minstac, 2017 [pdf, online]*, <http://www.theleecocad.com/PDF.nsf/2355f3df133a527185256c9300562a42/22c2e3978d031771852580cf005c58a8/\protect\TU\textdollarFILE/TKLA3201112H%20B5.pdf>, [accessed on: 25-07-2018] ().
- [11] Tensor-Solutions, *Pressure sensor ms5387-30ba-736494.pdf, 201 [webpage, online]*, <https://www.mouser.com/ds/2/418/MS5837-30BA-736494.pdf>, [accessed on: 30-08-2018].
- [12] Bosch, *Bmx055, 201 [webpage, online]*, [https://www.bosch-sensortec.com/bst/products/all\\_products/bmx055](https://www.bosch-sensortec.com/bst/products/all_products/bmx055), [accessed on: 25-07-2018].
- [13] R. A. Deepak and R. J. Twiggs, *Thinking out of the box: Space science beyond the cubesat*, Journal of Small Satellites JoSS **1**, 3 (2012).
- [14] R. A. Deepak and R. J. Twiggs, *Rise of the cubesat*, Science Magazine, AAAS, 19th December, Vol 346 Issue 6216 pp. 1449 (2014).
- [15] E. Kulu, *World's largest database of nanosatellites, more than 1600 nanosats and cubesats, 2017*, [online], accessed through: <http://nanosats.eu>, [accessed on: 22-03-2017].

- [16] E. Gill and P. S. (2016), *Ae4-s10: Microsat engineering*, [PDF], accessed at: [https://blackboard.tudelft.nl/webapps/blackboard/execute/content/file?cmd=view&content\\_id=\\_2919927\\_1&course\\_id=\\_57127\\_1&framesetWrapped=true](https://blackboard.tudelft.nl/webapps/blackboard/execute/content/file?cmd=view&content_id=_2919927_1&course_id=_57127_1&framesetWrapped=true) (2016).
- [17] K. Lemmer, *Propulsion for cubesats*, Acta Astronautica, Elsevier, vol. 134, p. 231-243 (2017).
- [18] P. Mikellides, P. Turchi, R. Leiweke, C. Schmahl, and I. Mikellides, *Theoretical studies of a pulsed plasma microthruster [online]*, Electric Rocket Propulsion Society, 1997, accessed through: [http://erps.spacegrant.org/uploads/images/images/iepc\\_articledownload\\_1988-2007/1997index/7037.pdf](http://erps.spacegrant.org/uploads/images/images/iepc_articledownload_1988-2007/1997index/7037.pdf) [accessed on: 22-03-2017].
- [19] A. Ketsdever and et al., *Free molecule microresistojet: Nanosatellite propulsion, 2005 [pdf, online]*, accessed through: <http://citeseerx.ist.psu.edu/viewdoc/download?doi=10.1.1.934.8636&rep=rep1&type=pdf>, [accessed on: 22-03-2017].
- [20] BUSEK, *Busek micro resistojet, 2013 [ppt, online]*, [http://www.busek.com/index\\_html\\_files/70008518B.pdf](http://www.busek.com/index_html_files/70008518B.pdf), [accessed on: 22-03-2017].
- [21] V. Buzas, *Lituanicasat-2, september 2016*, [online], accessed through: <http://uniseceurope.eu/missions/lituanicasat-2/> [accessed on: 05-04-2017].
- [22] H. Nguyen, J. Köhler, and L. Stenmark, *The merits of cold gas micropropulsion*, 53rd International Astronautical Congress, Houston, Texas, IAC-02-S.2.07 (10-19 October 2002).
- [23] M. Tajmar and C. Scharlemann, *Development of electric and chemical thrusters*, International Journal of Aerospace Engineering, Hindawi Publishing Corporation, Volume 2011, Article ID 361215 (29 March 2011).
- [24] R. Poyck, A. Cervone, B. Zandbergen, H. van Zeijl, I. Krusharev, and Q. Bellini, *A water-fed micro-resistojet for the delfi formation flying mission*, IAF 65th International Astronautical Congress, Toronto, Canada (29 Sep - 3 Oct, 2014).
- [25] J. M. Pearl, W. F. Louisos, and D. L. Hitt, *Thrust calculation for low-reynolds-number micronozzles*, Journal of Micromechanics and Microengineering vol. 16 R13–R39 (2006).
- [26] V. Pallichadath, *Propulsion subsystem requirements for the delfi-pq satellites*, internal document, TU Delft (2018).
- [27] J. Bouwmeester, *Pq9 & cs14 electrical and mechanical subsystem interface standard for pocketubes and cubesats*, internal document, TU Delft (2018).
- [28] M. Boerci, *Launcher loads for small satellites*, internal document, TU Delft (2017).
- [29] The-Lee-Company, *Line seal cap-062 minstac peek, 2008 [pdf, online]*, <http://www.theleecocad.com/PDF.nsf/2355f3df133a527185256c9300562a42/97742693fcb28e5f852574120049007d/\protect\TU\textdollarFILE/TMLA3201950ZA2.pdf>, [accessed on: 25-07-2018] ().
- [30] V. Pallichadath, *Propulsion subsystem mass, volume & power budgets*, internal document, TU Delft (Feb 2018).
- [31] The-Lee-Company, *Electro-fluidic systems technical handbook*, Release 8, Component Catalog with engineering reference material (2013).
- [32] V. Pallichadath, M. Silva, D. Guerrieri, A. Cervone, and S. Radu, *Integration and miniaturization challenges in the design of micro-propulsion systems for picosatellite platforms*, Spacepropulsion 2018 by 3AF, Seville Spain: 3AF (2018).



## Concept Trade-off Survey

This chapter of the appendix contains the survey conducted within micropropulsion team at TU Delft. An opinion on the weighting of criteria was received by experts and incorporated into the selection process of the conceptual design. The reasoning behind this, was that the surveys would provide an element of objectivity by averaging the weights received from eight experts.

Name:

Date:

This document concerns the trade-off criteria for the micro-resistojet technology demonstrator payload. Two different designs with some variations in propellant tank placement and shape have been selected for the final trade-off. For this trade-off, the following trade-off criteria have been identified and still need to be weighed. To try and create as much objectivity as possible in the trade-off, I would much appreciate your opinion on the weights for these criteria ranging from 1 to 10. Any comments or suggestions on the criteria are also very welcome. Thanks in advance!

Trade-off Criteria	Weight (1-10)	Comments on criteria
Simplicity (in manufacturing, testing and design)		
Proximity of thermal components near valves		
Volume of propellant storage		
Proximity of thermal components near propellant storage (to avoid propellant freezing in orbit)		

# B

## Matlab Code: Operational Envelope

This chapter of the appendix gives the Matlab code used for calculations in the operational envelope chapter of this report. Three different codes are provided: two for the constant temperature calculations and one used to determine the final operational envelope.

### B.1. Operational Envelope: Constant Temperature and Multiple Initial Pressures

```
clc
clear all

h = 2256e3; %J/kg
c_l = 4187; %J/K/kg liquid water
c_v = 1996; %J/K/kg water vapour
T_0 = 283;%K
A = 4.5e-9; %m^2
Gamma = 0.6712;
R = 461.67; %?
rho = 997; %kg/m^3
l = 0.30; %m
d = 1.57e-3; %m

V_tube = (l*pi()*d^2)/4; %m^3

%Inputs:
p_0 = [1.0e5 1.4e5 1.8e5 2.2e5];

V_0 = 0.1*V_tube; %m^3
delt = 0.1;
t = [0:delt:2500];

p_vap0=1e5;
T_vap0=373;
h_vap = 40e3;
R_vap = 8.341;
T_c0 = h_vap*T_vap0./(T_vap0*R_vap*log(p_vap0./p_0)+h_vap);
m_0 = p_0*A*Gamma./(\sqrt(R*T_c0));

m = zeros(length(p_0), length(t));
p = zeros(length(p_0), length(t));
```

```

T_c = zeros(length(p_0), length(t));
temp = zeros(length(p_0), length(t));
m(:,1)=m_0;
p(:,1)=p_0;
T_c=600;
temp(:,1) = 0;
for jj = 1:(length(p_0))
for ii = 2:(length(t))
    p(jj, ii) = V_0*p_0(jj)/(V_0+ temp(jj, ii -1));
    m(jj, ii) = p(jj, ii -1)*A*Gamma./(sqrt(R*T_c));
    temp(jj, ii) = temp(jj, ii -1)+ m(jj, ii)*delt/rho;
end
end

```

```
T_vap = h_vap*T_vap0./(T_vap0*R_vap*log(p_vap0./p)+h_vap);
```

```

figure(1)
plot(t,p)
xlabel('Time [s]')
ylabel('Pressure [Pa]')
legend('p_0=1.0_bar', 'p_0=1.4_bar', 'p_0=1.8_bar', 'p_0=2.2_bar')
text(1800, 1.6e5, 'V_0=0.1*V_{tube}')

```

```

figure(2)
plot(t,m)
xlabel('Time [s]')
ylabel('Mass Flow [kg/s]')
legend('p_0=1.0_bar', 'p_0=1.4_bar', 'p_0=1.8_bar', 'p_0=2.2_bar')
text(1800, 1e-6, 'V_0=0.1*V_{tube}')

```

```

%figure(3)
%plot(t, T_c)
%xlabel('Time [s]')
%ylabel('Temperature [K]')

```

```
Q = m.*(h+(T_vap-T_0)*c_l+(T_c-T_vap)*c_v);
```

```

figure(3)
plot(t,Q)
xlabel('Time [s]')
ylabel('Power Transferred to Propellant [W]')
legend('p_0=1.0_bar', 'p_0=1.4_bar', 'p_0=1.8_bar', 'p_0=2.2_bar')
text(1800, 3, 'V_0=0.1*V_{tube}')

```

```

%figure(5)
%plot(Q,p)
%xlabel('Power Transferred to Propellant [W]')
%ylabel('Pressure [Pa]')

```

```

V_t = V_0.*(p_0./p); % Volume of nitrogen over time
mass = (V_tube-V_t)*rho; % Mass of propellant left in tubing

```

```

figure(4)
plot(t, mass)
xlabel('Time [s]')
ylabel('Mass of Propellant [kg]')

```

```

legend('p_0=1.0_bar', 'p_0=1.4_bar', 'p_0=1.8_bar', 'p_0=2.2_bar')
text(1800, 4e-4, 'V_0=0.1*V_{tube}')
ylim([0 0.6e-3])

```

```

I_sp = 95;
g_0 = 9.81;
F_t = m*I_sp*g_0;

```

```

figure(5)
plot(t, F_t)
xlabel('Time[s]')
ylabel('Thrust[N]')

```

## B.2. Operational Envelope: Constant Temperature and Multiple Initial Nitrogen Volumes

```

clc
clear all

```

```

h = 2256e3; %J/kg
c_l = 4187; %J/K/kg liquid
c_v = 1996; % J/K/kg vapour
T_0 = 283;%K
A = 4.5e-9; %m^2
Gamma = 0.6712;
R = 461.67; %?
rho = 997; %kg/m^3
l = 0.30; %m
d = 1.57e-3; %m

```

```

V_tube = (l*pi()*d^2)/4; %m^3

```

```

%Inputs:

```

```

p_0 = 1.8e5;

```

```

V_0 = [0.05*V_tube 0.1*V_tube 0.15*V_tube 0.2*V_tube]; %m^3
delt = 0.1;
t = [0:delt:2500];

```

```

p_vap0=1e5;
T_vap0=373;
h_vap = 40e3;
R_vap = 8.341;
T_c0 = h_vap*T_vap0./(T_vap0*R_vap*log(p_vap0./p_0)+h_vap);
m_0 = p_0*A*Gamma./(sqrt(R*T_c0));

```

```

m = zeros(length(V_0), length(t));
p = zeros(length(V_0), length(t));
T_c = zeros(length(V_0), length(t));
temp = zeros(length(V_0), length(t));
m(:,1)=m_0;
p(:,1)=p_0;
T_c=600;
temp(:,1) = 0;
for jj = 1:(length(V_0))
for ii = 2:(length(t))

```

```

    p(jj, ii) = V_0(jj)*p_0/(V_0(jj)+ temp(jj, ii - 1));
    m(jj, ii) = p(jj, ii - 1)*A*Gamma./ (sqrt(R*T_c));
    temp(jj, ii) = temp(jj, ii - 1) + m(jj, ii)*delt/rho;
end
end

T_vap = h_vap*T_vap0./ (T_vap0*R_vap*log(p_vap0./p)+h_vap);

figure(1)
plot(t, p)
xlabel('Time [s]')
ylabel('Pressure [Pa]')
legend('V_0=0.05*V_{tube}', 'V_0=0.1*V_{tube}', 'V_0=0.15*V_{tube}', 'V_0=0.2*V_{tube}')
text(1800, 1.2e5, 'p_0=1.8 bar')

figure(2)
plot(t, m)
xlabel('Time [s]')
ylabel('Mass Flow [kg/s]')
legend('V_0=0.05*V_{tube}', 'V_0=0.1*V_{tube}', 'V_0=0.15*V_{tube}', 'V_0=0.2*V_{tube}')
text(1800, 0.9e-6, 'p_0=1.8 bar')

Q = m.*(h+(T_vap-T_0)*c_l+(T_c-T_vap)*c_v);

figure(3)
plot(t, Q)
xlabel('Time [s]')
ylabel('Power Transferred to Propellant [W]')
legend('V_0=0.05*V_{tube}', 'V_0=0.1*V_{tube}', 'V_0=0.15*V_{tube}', 'V_0=0.2*V_{tube}')
text(1800, 2.5, 'p_0=1.8 bar')

V_t = V_0.*(p_0./p); % Volume of nitrogen over time
mass = (V_tube-V_t)*rho; % Mass of propellant left in tubing

figure(4)
plot(t, mass)
xlabel('Time [s]')
ylabel('Mass of Propellant [kg]')
legend('V_0=0.05*V_{tube}', 'V_0=0.1*V_{tube}', 'V_0=0.15*V_{tube}', 'V_0=0.2*V_{tube}')
text(1800, 4e-4, 'p_0=1.8 bar')
ylim([0 0.6e-3])

I_sp = 95;
g_0 = 9.81;
F_t = m*I_sp*g_0;

figure(5)
plot(t, F_t)
xlabel('Time [s]')
ylabel('Thrust [N]')
legend('V_0=0.05*V_{tube}', 'V_0=0.1*V_{tube}', 'V_0=0.15*V_{tube}', 'V_0=0.2*V_{tube}')

```

### B.3. Operational Envelope: Variable Temperature and Final Values

```
clc
```

```

clear all
%Q = 1; %W
h = 2256e3; %J/kg
c = 4187; %J/K/kg liquid
T_0 = 283;%K
A = 4.5e-9; %m^2
Gamma = 0.6712;
R = 461.67; %?
rho = 997; %kg/m^3
l = 0.30; %m
d = 1.57e-3; %m

V_tube = (l*pi()*d^2)/4; %m^3

%Inputs:
p_0 = 1.1e5; %Pa
V_0 = 0.12*V_tube; %m^3
delt = 0.001;
t = [0:delt:1200];

p_vap0=1e5;
T_vap0=373;
h_vap = 40e3;
R_vap = 8.341;
T_c0 = h_vap*T_vap0/(T_vap0*R_vap*log(p_vap0./p_0)+h_vap);
m_0 = p_0*A*Gamma./(sqrt(R*T_c0));

m = zeros(1, length(t));
p = zeros(1, length(t));
T_c = zeros(1, length(t));
m(1)=m_0;
p(1)=p_0;
T_c(1)=T_c0;
temp(1) = 0;

for ii = 2:(length(t))
    p(ii) = V_0*p_0/(V_0+ temp(ii -1));
    m(ii) = p(ii -1)*A*Gamma./(sqrt(R*T_c(ii -1)));
    T_c(ii) = h_vap*T_vap0/(T_vap0*R_vap*log(p_vap0./p(ii -1))+h_vap);
    temp(ii) = temp(ii -1)+ m(ii -1)*delt/rho;
end

figure(1)
plot(t,p)
xlabel('Time_ [s] ')
ylabel('Pressure_ [Pa] ')
legend('p_0=_1.1_bar ,_V_0=_0.12*V_{tube} ')

figure(2)
plot(t,m)
xlabel('Time_ [s] ')
ylabel('Mass_Flow_ [kg/s] ')
legend('p_0=_1.1_bar ,_V_0=_0.12*V_{tube} ')

figure(3)
plot(t,T_c)

```

```

xlabel( 'Timeu[s] ' )
ylabel( 'Temperatureu[K] ' )
legend( 'p0u=1.1ubar ,uV0u=0.12*V_{tube} ' )

Q = m.*(Tc-T0)*c+h*m;

figure(4)
plot(t,Q)
xlabel( 'Timeu[s] ' )
ylabel( 'PoweruTransferredutouPropellantu[W] ' )
legend( 'p0u=1.1ubar ,uV0u=0.12*V_{tube} ' )

figure(5)
plot(Q,p)
xlabel( 'PoweruTransferredutouPropellantu[W] ' )
ylabel( 'Pressureu[Pa] ' )
legend( 'p0u=1.1ubar ,uV0u=0.12*V_{tube} ' )

Vt = V0'.*(p0./p); % Volume of nitrogen over time
mass = (Vtube-Vt)*rho; % Mass of propellant left in tubing

figure(6)
plot(t,mass)
xlabel( 'Timeu[s] ' )
ylabel( 'MassuofuPropellantu[kg] ' )
legend( 'p0u=1.1ubar ,uV0u=0.12*V_{tube} ' )

Isp = 74;
g0 = 9.81;
Ft = m*Isp*g0;

figure(7)
plot(t,Ft)
xlabel( 'Timeu[s] ' )
ylabel( 'Thrustu[N] ' )
legend( 'p0u=1.1ubar ,uV0u=0.12*V_{tube} ' )

%Test plan section
Eff = 0.6;
Qinput = Q/ Eff;
pinput = 1e5+p;

%figure(8)
%plot(Qinput,pinput)
%xlabel('Power Input [W]')
%ylabel('Pressure [Pa]')
%text(2.5,1.2e5,'Efficiency = 60%')

```